A SYSTEMATIC STUDY OF SELECTED *KROYERIA* SPECIES FROM THE SOUTH AFRICAN COAST

by

PETER JABU MOKUMO

DISSERTATION

Submitted in fulfilment of the requirements for the degree

MASTER OF SCIENCE

in

ZOOLOGY

in the

FACULTY OF SCIENCE AND AGRICULTURE

SCHOOL OF MOLECULAR AND LIFE SCIENCES

at the

UNIVERSITY OF LIMPOPO

SUPERVISOR: Prof. S.M. DIPPENAAR

2014

DECLARATION

I declare that the dissertation hereby submitted to the University of Limpopo, for the degree of Masters of Science in Zoology has not previously been submitted by me for a degree at this or any other university; that it is my work in design and execution, and that all material contained herein has been duly acknowledged.

…….. …….

MOKUMO P.J. (Mr) Date

ACKNOWLEDGEMENTS

I acknowledge my Father-God, my Lord Jesus and the Great Mighty Holy Spirit who help me to face the challenges of life with a smile.

I acknowledge the National Research Foundation (NRF) for funding this research.

I also aclnowledge the KwaZulu-Natal Sharks Board (KZNSB) and the Department of Agriculture, Forestry and Fishery (DAFF) Marine Dynamics for helping with the sampling.

I would like to thank Prof. S.M. Dippenaar ("Dipps") for sharing with me "the gospel of Copepods". I am a believer. I appreciate the time she spent on this work. I would also like to thank Tshepo "Sporo-genious" Mangena who has been my mentor in genetics, Modjadji "Madame Rain-Queen" Lebepe who has stirred a passion for copepod morphology in me. I also thank Bea "The Boss" Jordaan for entrusting me with responsibilities in the museum and for helping with copepod collections. I also thank Dr J-S Ho and Prof Rony Huys for lectures and training during the 2nd International Workshop on Symbiotic Copepoda (IWOSC) at the University of Limpopo.

I express my gratitude to S. Wintner for her talk on the KwaZulu Natal Sharks Board that provided me with understanding of how sharks are caught. I extend my gratitude to interns and staff at Inqaba biotech, especially the CEO and founder, Oliver Preisig who allowed me to stay in his house during the 2 weeks I spent at Inqaba; Christiaan Labuschagne and Hamilton Ganes who helped me with sequencing and using CLC workbench. I also express my gratitude to Charles Wairuri who helped me with Whole Genome Amplification.

I express my sincere gratitude to Prof. W.J. Luus-Powell who recruited me for post-graduate studies while I was still doing my first year of undergrad, Prof. A. Addo-Bediakko who sees what other do not see in me. I also express my sincere thanks to Dr Tshefiwa Mandiwana-Neudani for her motherly support and to Dr "Matla" Matla for wonderful chatting times.

I also thank my friends Tshepiso "Promise" Ramalepe who encouraged me in my writing and has checked my work for errors, Irene Walter who travelled the country

with me and my angel in white, “Zowe”, who has borne me like an eagle on her wings of strength.

I thank alI the post-graduate students and staff members at the Department of Biodiversity for all the help and company they provided me with during this research. I also would like to thank the Biodiverity Student Society for making me a leader and providing me with an opportunity to mentor hundreds of students.

I sincerely appreciate my late great grandfather, Dr E.W. Kenyon who sets my spirit on fire through the legacy of books he authored especially “Sign posts on the road to success”.

I dedicate this dissertation to my parents Peter and Sarah Mokumo “who love me” and have made me rich in this lifetime. Likewise I extend dedication to my younger sister Maggie “The attorney general” and my cousins Gobrey, Paul, Matome and Ruby for their support and love. Lastly, I dedicate this work to my wonderful aunt Mavis Makgoba and my uncle Samson Makgoba who has been my role model for all my life.

TABLE OF CONTENTS

ABSTRACT

One of the 11 families of the siphonostomatoids found parasitic on elasmobranchs is the Kroyeriidae which has three accepted genera namely *Kroyeria*, *Kroeyerina* and *Prokroyeria*. Parasites from this family are found living on the gills (*Kroyeria* spp. and *Prokroyeria* sp.) or in the nasal fossae (*Kroeyerina* spp.) of Chondrichthyes. There are currently 21 nominal species in the genus *Kroyeria*.

Kroyeria specimens were collected from the gill filaments of their elasmobranch hosts which were caught: (1) in the nets of the KwaZulu-Natal Sharks Board (KZNSB) installed along the east coast of South Africa, (2) by commercial fishermen off the west coast at Gansbaai as well as (3) during the demersal trawls of Department of Agriculture, Forestry and Fishery (DAFF) off the south and west coasts. Collected specimens were fixed and preserved in 70% ethanol. Morphological features were drawn where necessary to illustrate differences from previously described features. Host-parasite relationships of the different species were determined by calculating prevalence, mean abundance and mean intensity on their hosts as well as estimating the pattern of dispersion by calculating the coefficient of dispersion. DNA was extracted from selected identified samples. A partial fragment of the COI gene was amplified via PCR using the forward and reverse universal primers LCO 1490 and HCO 2198, or those with additional M13 tails, LCO 1490_t1 and HCO 2198_t1. Additionally, the complete 18S rDNA gene of some species was amplified using the forward and reverse primers as follows: 18Sf and 1282r for the first fragment, 554f and 614r for the second fragment and 1150f and 18sr for the third fragment. Phylogenetic relationships among different *Kroyeria* species were estimated by employing neighbor joining (NJ), parsimony (MP) and maximum likelihood (ML) in PAUP*. The use of real-time PCR and melt curve analysis to distinguish among different *Kroyeria* species based on their different melt temperatures of a part of the COI gene was also attempted.

Eleven *Kroyeria* species were found on the gill filaments of elasmobranchs belonging to the families Carcharhinidae, Sphyrnidae and Triakidae off the coasts of South Africa. These include *K. carchariaeglauci* from *C. leucas*; *K. decepta* from *C. obscurus*; *K. deetsi* from *C. brevipinna*; *K. dispar* from *G. cuvier; K. elongata* from *R. acutus*; *K. lineata* from *M. palumbes*; *K. longicauda* from *C. limbatus*; *K. papillipes*

from *G*. *cuvier*; *K*. *procerobscena* from both *C*. *leucas* and *C*. *amboinensis*; *K. sphyrnae* from both *Sphyna lewini* and *S*. *zygaena* and *a* new *Kroyeria* sp. from *G. galeus*. This is the first record of *K. lineata* from the south coast of South Africa and is also as a new host record for *Mustelus palumbes*. Three *Kroyeria* species have previously been reported from *G. galeus*, namely *K. brasiliense, K. lineata* and *K. rhophemophaga*. The new *Kroyeria* sp. is most similar to *K*. *rhophemophaga* which in turn shares morphological features with *K. triakos*. However, the *Kroyeria* sp. can be distinguished from both *K. rhophemophaga* and *K. triakos* in the armature of the legs.

Most *Kroyeria* species are relatively host specific, infecting a single host or related group of host species. During this study two species, *K. dispar* and *K. papillipes* were collected from *G. cuvier*, while *K. procerobscena* and *K. sphyrnae* were each collected from two host species. *Kroyeria* sp. and *K. dispar* displayed very high prevalence values, 95.7% and 94.1% respectively, in contrast to the other *Kroyeria* species which have lower values (6.3–68.6%). Additionally, when compared to other siphonostomatoid species such as *Nemesis lamna*, *Kroyeria* species have relatively low prevalence values. *Kroyeria* species generally have low parasite loads (between 4 and 33 copepods per infected host), except for *K. dispar* which has a high mean intensity of 74 copepods per infected host. The mean abundance of *Kroyeria* species is also generally low (between 0 and 23 per examined host), with *K. dispar* (69 individuals per examined host) being an exception. Furthermore *Kroyeria* species generally display an aggregative pattern of distribution which is common in most copepod species indicating that individuals have social interactions.

A preliminary estimation of the phylogenetic relationships among seven *Kroyeria* species revealed topologies with unresolved polytomies. The 18S rDNA gene did not make any significant changes on the topology, except that it produced very minimal resolution in one of the groupings. Therefore, COI is found to be a gene of choice that can be used in estimating molecular phylogenetics and population genetics of siphonostomatoids as it provides useful sequence divergence within individuals of the same species as well as among congeneric species due to its fast evolving rate. However, in this study, single species did not form monophyletic groupings.

The 18S rDNA gene is found to be very conservative, providing no sequence divergence within individuals of the same species and very little divergence among conspecifics due to its low mutation rate and is therefore more useful at genus and family levels.

With polytomies in the estimated phylogenetic relationships, haplotype networks were used to compare the distribution of different haplotypes among the different species. Haplotype sharing did occur between species e.g. for COI, H1 is shared by *K. lineata*, *Kroyeria sp.* and *K. sphyrnae*. This haplotype sharing by different species is unexpected and could be due to specimen misidentification before DNA extraction. Specimen misidentification is common for *Kroyeria* species because some of them are not easy to identify. The haplotype network results confirmed the relationships shown by the phylogenetic trees, dividing *Kroyeria* species into three different groupings.

Real-time PCR and melt curve analysis have the potential to distinguish among *Kroyeria* species. However, the quality of the extracted DNA is an important factor in producing successful amplifications and determining the T_m. Therefore it is necessary to ensure that the extracted DNA has the ideal concentration of 50 ng/μl and is free of Taq polymerase inhibitors such as phenol, RNA and guanine residuals from the extraction process.

LIST OF TABLES

LIST OF FIGURES

CHAPTER 1

GENERAL INTRODUCTION

1.1. Arthropoda Siebold, 1848

The phylum Arthropoda von Siebold, 1848 is the largest and most diverse of all phyla in the animal kingdom. In this phylum about 1 100 000 species (more than 75% of the currently known living species) have been reported (Hickman *et al*. 2008). Arthropods are found everywhere on the biosphere and have evolved to adapt to all kinds of habitats and lifestyles (Shao & Barker 2007). They are subdivided into four main groups: insects, myriapods (millipedes and centipedes), chelicerates (spiders and scorpions) and crustaceans (Van Hook & Patel 2008). Most of them are free-living while some are parasitic (Bush *et al*. 2001).

1.2. Crustacea Brünnich, 1772

The sub-phylum Crustacea Brünnich, 1772 differs from other arthropod groups in that it is the only group that possesses two pairs of antennae. Crustaceans also possess a pair of mandibles and two pairs of maxillae on the head, as well as a pair of appendages on every somite of their bodies (Hickman *et al*. 2008). Most crustaceans are found in aquatic environments, especially marine environments. Terrestrial species are also present, although the majority of them require water as a necessity for breeding (Bush *et al*. 2001; Van Hook & Patel 2008). Crustaceans are currently divided into six classes, namely: Cephalocarida Sanders, 1955; Remipedia Yager, 1981; Branchiopoda Latreille, 1817; Ostracoda Latreille, 1802; Maxillopoda Dahl, 1956 (copepods) and Malacostraca Latreille, 1802 (Martin & Davis 2001; WoRMS 2014), with parasitic species only found in the last two classes. Approximately 3 000 of the 50 000 (about 6%) known crustacean species are parasitic (Bush *et al*. 2001). Three main sub-classes that represent most of the parasitic crustaceans affecting commercial aquaculture have been identified i.e. Branchiura Thorell, 1864; Isopoda Latreille, 1817 and Copepoda Milne-Edwards, 1840. The Branchiura and Isopoda species are relatively large in comparison to the small to microscopic Copepoda species. However, members of the sub-class Copepoda are the most common parasitic crustaceans (Jithendran *et al*. 2008).

1.3. Copepoda Milne-Edwards, 1840

The name copepod can be literally translated as “oar-footed” (Huys & Boxshall 1991). Copepods are the most diverse group of crustaceans found in all types of aquatic environments, i.e. brackish, marine and freshwater environments (Boxshall & Defaye 2008; Bron *et al*. 2011). Their habitats also include marine sediments, subterranean habitats, deep-sea vents, ephemeral streams, rock hollows, natural caves and springs amongst others (Reid 2001), with a vertical range from a depth of 10 000 metres in the Philippine Trench to an altitude of 5 500 metres in the Himalayas (Huys & Boxshall 1991; Boxshall & Halsey 2004). They are the most dominant metazoan invertebrates in the world and have various morphological appearances (Morales-Ramirez & Suarez-Morales 2009). Their adult forms range in size from < 0.1 mm to 23 cm (Bron *et al*. 2011). Huys & Boxshall (1991), regarded them as the “insects of the sea”, when taking into account their size, diversity and abundance. There are about 14 582 accepted species of copepods worldwide (Walter & Boxshall 2014) and only 405 species have been found in Sub-Sahara African waters (Boxshall & Defaye 2008).

Copepods belonging to the orders Calanoida Sars, 1903 and Cyclopoida Burmeister, 1835 are ecologically important because of their numerical abundance, biomass predominance as well as being a part of marine plankton which forms a critical primary link in the food chain (Huys & Boxshall 1991; Bucklin *et al*. 2003). Commercially exploited fishes like anchovy, cod, flounder, herring and salmon feed directly on copepods (Bron *et al*. 2011). In addition, copepods are also important pests in aquaculture (Piasecki *et al*. 2004; Morales-Serna *et al*. 2014), for instance, *Caligus elongatus (*Nordmann, 1832), has been reported to be responsible for economic losses in salmon farming (Øines & Schram 2008; Dojiri & Ho 2013) and *Lepeoptheirus salmonis* (Krøyer, 1837) can cost a Canadian farmer a fortune to control (Mustafa *et al*. 2000). In 2004, it was estimated that the annual global economic loss caused by sea lice (caligid copepods) in salmon farming was over 100 million US dollars (Johnson *et al*. 2004). Five years later, the estimated economic loss costs were reported to be over 430 million US dollars per annum (Costello 2009). In Asian countries like China, Japan and Korea, more copepods species affecting aquaculture have been reported than in Western countries (Ho 2001). These copepods not only affect fish species, but also other aquaculture

organisms like the hard clam, *Meretrix meretrix* Linnaeus, 1758 and wakame (sea weed), *Undaria pinnatifida* (Harvey) Suringar, 1873 (Ho & Zheng 1994). Furthermore, copepods are also vectors of human parasites like the guineaworm, *Dracunculus medinensis* (Linnaeus, 1758) (Bimi 2007; Boxshall & Defaye 2008) and the broad fish tapeworm, *Diphyllobothrium latum* (Linnaeus, 1758) (Piasecki *et al*. 2004).

A large proportion of copepods (one-third of all known copepods) are symbiotic in nature, i.e. they co-exist together with other organisms in parasitic and/or commensalistic relationships, as no mutualism has been reported in copepods yet. Symbiotic copepods account for more than 35% of all copepods known to date and are found in the five major orders of Copepoda, namely Calanoida, Harpacticoida Sars, 1903, Cyclopoida, Poecilostomatoida Burmeister, 1835 and Siphonostomatoida Thorell, 1859 (Ho 2001; Boxshall 2014). They form symbiotic relationships with animals ranging from sponges, to the most complex, i.e. mammals e.g. cetaceans (Bush *et al*. 2001; Ho 2001). Symbiotic copepods are morphologically the most diverse of all the crustaceans (Jithendran *et al*. 2008) and are believed to have evolved from free-living forms (Ho 2001).

1.4. Parasitic copepods

Parasitic copepods have various adaptations which reflect the diversity of hosts they infect. They are ectoparasites, mesoparasites and endoparasites of aquatic organisms. In parasitic copepods, some appendages have been modified to suit their mode of life, e.g. the swimming legs can display changes associated with a loss of function or change of function. Other changes involve the appendages like antennules, antennae, mandibles, maxillules, maxillae and maxillipeds (Kabata 1979). In addition, sexual dimorphism is exhibited in parasitic copepods with males being smaller than females (Pillai 1985). Most parasitic copepods of fish are included in the orders Poecilostomatoida and Siphonostomatoida (Kabata 1979).

1.5. Order Siphonostomatoida Thorell, 1859

Copepods belonging to the order Siphonostomatoida have a tube mouth or syphon formed by the fusion of the labrum and labium. All members of this order are parasites or live in association with other animals (Kabata 1979) and are largely

marine, although a few of them are freshwater fish parasites (Huys & Boxshall 1991; Boxshall & Jaume 2000).

Siphonostomatoida consists of 39 families (Martin & Davis 2001; Boxshall 2014) of which 17 are symbiotic on vertebrates (mostly fish and mammals) (Ho 2001; Boxshall 2014) having the loss of the mandibular palp as the synapomorphy that makes them monophyletic (Huys & Boxshall 1991). Eleven of the 17 families are found existing in symbiotic relationships with elasmobranchs (Benz 1994; Boxshall 2014). In 2005, only 9% of the known symbiotic siphonostomatoid copepods were reported from southern African waters, these included eight families, 19 genera and 35 species (Dippenaar 2005). Two years later, there was an increase in the number of siphonostomatoids reported (11 families, 27 genera and over 58 species) from southern African waters (Dippenaar & Jordaan 2007).

The gill filaments and gill arches of elasmobranchs serve as excellent sites for anchoring because they are sources of nutrients for ectoparasites (Bush *et al*. 2001). Examples of ectoparasitic siphonostomatoids which attach on the gills include species of *Eudactylina* van Beneden, 1853; *Lamproglena* Von Nordmann, 1832 and *Nemesis* Risso, 1826 amongst many others (Kabata 1979; Huys & Boxshall 1991; Deets 1994). Some ectoparasitic species such as *Caligus* Müller, 1785 and *Nesippus* Heller, 1865 are cosmopolitan in terms of a wide range of host species they infect and do not only attach to the external body surfaces or gill arches, but are found in the mouth and nasal passages (Kabata 1979), while more site and host specific ones like *Anthosoma crassum* Abildgaard, 1794 are found located in the jaws of Lamniform sharks (Kabata 1979; Benz *et al*. 2002). The members of a few siphonostomatoid families are mesoparasites, such as most members of the family Pennellidae Burmeister, 1835 e.g. *Peroderma* Heller, 1868 found deep within the muscles of its host (Kabata 1979; Huys & Boxshall 1991); members of the family Lernaeopodidae Milne-Edwards, 1840 (Kabata 1979), e.g. *Schistobrachia jordaanae* Dippenaar, Olivier & Benz, 2004 found with the maxillae embedded underneath the gill filaments of the diamond ray, *Gymnura natalensis* (Gilchrist & Thomson, 1911) (Dippenaar *et al*. 2004) as well as all the known members of the family Sphyriidae Wilson, 1919 (Kabata 1979), e.g. *Driocephalus cerebrinoxious* (Diebakate, Raibaut and Kabata, 1997), which is found inhabiting the nasal capsules of the west African shark, *Leptocharias smithii* (Müller and Henle, 1839) and may penetrate the host's

olfactory lobe of the brain (Diebakate *et al*. 1997). Endoparasitic copepods include species of the family Philichthyidae Vogt, 1877 (Poecilostomatoida) which are highly modified endoparasites of marine actinopterygian fishes, found occupying spaces associated with the sensory canals of the lateral line system and skull bones (Madinabeitia & Iwasaki 2013; Madinabeitia *et al*. 2013).

1.6. Family Kroyeriidae Kabata, 1979

One of the 11 families of the siphonostomatoids found parasitic on elasmobranchs is the Kroyeriidae. This family has three accepted genera (Deets 1987), namely *Kroyeria* van Beneden, 1853; *Kroeyerina* Wilson, 1935 and *Prokroyeria* Deets, 1987. Parasites from the family Kroyeriidae are found living on the gills (*Kroyeria* spp. and *Prokroyeria* sp.) or in the nasal fossae (*Kroeyerina* spp.) of Chondrichthyes Huxley, 1880, mainly sharks (Deets & Ho 1988; Benz 1994; Thatcher & Júnior 2006). The family Kroyeriidae is characterised by three leg-bearing free distinct somites between the cephalothorax and the genital complex, a cephalothorax that has a caligiform dorsal shield and four pairs of biramous, trimerite swimming legs and a fifth vestigial leg in females (a sixth vestigial leg observed in males) (Kabata 1979; Deets 1994).

1.7. Representatives of *Kroyeria*

The genus *Kroyeria* consisted of 20 valid species (Thatcher & Júnior 2006). Izawa (2008) validated *K*. *sublineata* Yamaguti and Yamasu, 1959 which was relegated to be a synonym of *K. lineata* van Beneden, 1853 by Kabata (1979) to make up a total of 21 species. The confusion in the identification of some species resulted from the fact that *Kroyeria* species are not easily identified because their morphology is superficially conservative (Deets 1994; Izawa 2008). Currently, only nine of the 21 species have been recorded from South African waters (Dippenaar & Jordaan 2007).

According to Deets (1994), most *Kroyeria* species are host specific on carcharhiniform sharks of the families Carcharhinidae Jordan & Evermann, 1896 and Triakidae Gray, 1851 with a few species having been reported from the family Sphyrnidae Gill, 1872. In fact, *Kroyeria* is only second to *Eudactylina* as the most species-rich genus of all parasitic copepods that inhabit the gills of Chondrichthyes. They are found attached primarily to the secondary lamellae and secondarily to the underlying excurrent water channels of the gills by using the chelate antennae as primary attachment organs aided by the dorsal stylets, interdorsal stylets and

maxillipeds which serve as secondary attachment organs (Deets 1994; Dippenaar *et al*. 2000). Exceptionally, the female of *Kroyeria caseyi* Benz and Deets, 1986 is the only known mesoparasite in the genus *Kroyeria* and is found embedded into the interbranchial septa of the host species whereas all the females and males of the other species are ectoparasites (Deets 1994). Additionally, *Kroyeria* species display sexual dimorphism with males being smaller than females mainly because of the long, tubular genital complex of the female (Benz 1994).

1.8. The host species

Elasmobranchs (sharks and rays) together with the Holocephali (chaemeras) belong to the class Chondrichthyes, comprised only of cartilaginous fishes. A characteristic of this class is an entirely cartilaginous skeleton that is hardened by calcification. Elasmobranchs have upper jaws that are not fused to the skull, teeth that are separated and 5-7 pairs of gill openings (Smith & Heemstra 1986). There are about 210 chondricthyan species (18% of all chondricthyan species known worldwide) in southern African waters (Compagno 1999).

Sharks of the family Carcharhinidae (Requiem sharks) are found globally, in all warm and temperate seas, and consist of about 12 genera containing 56 species, 23 of which are found in South African waters (Compagno 1999; Heemstra & Heemstra 2004; Compagno *et al*. 2005; Froese & Pauly 2014). Similarly, the family Triakidae (Hound sharks) is found globally, in all warm and temperate seas and consists of nine genera containing 46 species (Froese & Pauly 2014), seven of which are found in South African waters (Compagno 1999; Compagno *et al*. 2005). The family Sphyrnidae (Hammerhead sharks) is also found globally, mainly in warm waters but occasionally in brackish waters and consists of two genera containing 10 species (Froese & Pauly 2014), three of which are found in South African waters (Compagno 1999; Compagno *et al*. 2005).

1.9. Taxonomy and systematics

The classification of biodiversity is an essential basic task for biologists (Freeman & Herron 2007). The study that is aimed at discovering, describing, identifying, naming and classifying both living and extinct species is known as taxonomy (Pearson *et al*. 2011) whereas systematics is defined as “the reconstruction and study of phylogenies” (Raven & Johnson 2002). Traditionally, both taxonomy and systematics

have been based on grouping organisms that are similar in their morphology (Giribet 2010). Traditional taxonomy and systematics do not only provide a large amount of information on the morphology of species, but also on the biology, habitat preference, host association and distribution of the identified species (Löbl 2014).

The light and stereo microscopes have been used as instruments to identify and classify marine zooplankton (of which copepods form the majority) traditionally, based on morphological features (Lindeque *et al*. 2004; Pan *et al*. 2008; Rajthilak *et al*. 2010). However, to use these instruments necessary skills, experience and dedication are required as well as knowledge about the studied organisms (Pan *et al*. 2008). Unfortunately, the number of expert professional taxonomists who have the skills, experience and knowledge to identify and distinguish species is rapidly decreasing (Tautz *et al*. 2003; Šlapeta 2013; Löbl 2014). It has also been mentioned that classification of organisms based on their morphology has several disadvantages, i.e. different nutritional regimes can produce morphological differences within the same species e.g. colouration, especially in birds and fish. Cryptic species or sibling species (i.e. those species that are similar in morphology and are not easily distinguished by more traditional techniques (Knowlton 2000)), also complicate morphological classification. Another limitation of this classification system is that where only small numbers of biological material is available, this classification cannot be used because the material would not be enough to make accurate descriptions of the species concerned (Pereira *et al.* 2008). According to Bucklin *et al*. (2003), there is a decrease in the number of copepod systematists who can identify species belonging to difficult groups, which can lead to misidentification of these species. However, advances in molecular technology provide tools to assist in classification of organisms (Pereira *et al.* 2008), copepods in particular (Rajthilak *et al*. 2010).

A DNA based taxonomy has some advantages over classical taxonomy, since DNA is extremely stable and is found in all nucleated cells (Pereira *et al.* 2008). In addition, an increasing number of taxonomists and systematists are beginning to question phylogenies based on morphology and are moving towards molecular phylogenetics (Wyngaard *et al*. 2010). However, DNA based taxonomy has limitations when it comes to dealing with sister species that have very recently diverged from a common ancestor. The limitations are due to shared alleles and

occasional transference of organelles between the sister species (Tautz *et al*. 2003). Therefore a combined approach, where both morphological and molecular data are used has been applied in this study.

1.10. Molecular techniques

1.10.1. DNA quantification

An important factor in using DNA samples efficiently in molecular techniques is the accuracy and precision of the DNA concentration quantification. The lack of accuracy in DNA quantification may result in unnecessary DNA consumption, while low DNA concentration may result in low quality sequencing. Therefore, high variability in PCR products can be a result of imprecise DNA quantification (Haque *et al*. 2003).

1.10.2. Polymerase Chain Reaction (PCR)

The development of the Polymerase Chain Reaction (PCR) made it possible for biologists to study individual genes (Woo *et al*. 2000). PCR is an *in vitro* molecular technique that uses the enzymatic synthesis of DNA to amplify a relatively short segment of DNA multiple times (Saiki *et al*. 1988). During the PCR process three distinct phases can be recognized namely, the exponential, linear and plateau phases. In the exponential phase, there is an exponential increase in the quantity of amplified DNA because there is no reagent limitation. There is a linear increase in the linear phase due to progressive limitations in PCR reagents. The plateau phase is characterized by no change in the amount of products, because there is reagent depletion (Yuan *et al*. 2006). These phases give the PCR product accumulation a sigmoidal amplification curve (D'haene *et al*. 2010). Each cycle of PCR generates 2^n copies of DNA, where n is the number of cycles. However, this exponential amplification has a limit, when the PCR reaches the plateau phase of DNA accumulation (Miesfeld 1996).

1.10.3. Real-time PCR

Real-time PCR, also known as quantitative PCR (qPCR), is a molecular technique that is based on conventional PCR and is widely used in clinical, forensic, food safety and environmental studies (Sivaganesan *et al*. 2010). It also has applications in microarray verification, cancer quantification, transgenic copy number determination and drug therapy studies (Yuan *et al*. 2006). It is a method of choice because it has a wide dynamic range of quantification (7-8 log decades), high

technical sensitivity (< 5 copies) and high precision. In addition, it is rapid and reproducible, has high throughput and requires no post PCR processing such as DNA sequencing (Klein 2002).

Real-time PCR detects amplified products while the reaction is in progress, i.e. without terminating the reaction and running the products out on a gel (Rebouças *et al*. 2013). The simplest and most cost effective way is by using DNA intercalating dyes which increase fluorescence after binding to the newly synthesized amplicon. These dyes are advantageous in that there is no need to design specific complementary probes, only the forward and reverse primers are needed (Li *et al*. 2010). A disadvantage of these intercalating dyes is that they are non-specific, i.e. they bind to all newly synthesized double-stranded DNA (including primer dimers and non-specific products), and this can lead to error in interpreting the results (Naumenko *et al*. 2008; Li *et al*. 2010). Furthermore these dyes can lead to product inhibition, enzyme instability and a decrease of reaction components in time (Ramakers *et al*. 2002).

1.10.4. Melt curve analysis

Specific real-time PCR products can be identified by doing melting curve analysis after the amplification. This is because the shape and position of the melting curve is determined by the Guanine-Cytosine (GC) content, double-stranded DNA (dsDNA) length and sequence and thus each PCR amplification product has a distinct melting temperature (T_m). The curve is a useful tool that can be used to distinguish PCR products based on differences in melting temperatures (Ririe *et al*. 1996). Therefore primer dimers and non-specific products can be distinguished from authentic amplicons (Li *et al*. 2010). Moreover, melting curve analysis also uses the non-specific DNA-binding intercalating dye chemistry. Following qPCR, the amplified product is incrementally heated until the dsDNA dissociates into single strands with decreasing fluorescence which is plotted against the increasing temperature to produce a melt curve. The melt curve is further converted into a melt peak which can easily be interpreted (Winder *et al*. 2011). The simplicity, rapidness, cost effectiveness as well as the reliability of this assay makes it suitable to answer research questions (Guion *et al*. 2008).

Melt curve analysis has been used successfully to distinguish among different *Leishmania* Ross, 1903 species (Nicolas *et al*. 2002), three weevil and four tick species (Winder *et al*. 2011) as well as distinguishing between two blacktip sharks, *Carcharhinus limbatus* (Valenciennes, in Müller & Henle, 1839) and *Carcharhinus tilstoni* (Whitley,1950), which are not easily distinguished morphologically (Morgan *et al*. 2011). It has also been used to rapidly identify maternal lineages in the common carp, *Cyprinus carpio* Linnaeus, 1758 based on mtDNA haplotypes (Haynes *et al.* 2009).

1.11. Genetic markers

The phylogenetic relationships of metazoans at different taxonomic levels have been analysed using mitochondrial DNA amplified by PCR, including those of 34 species of calanoid copepods (Machida *et al*. 2004). Larvae of two species of sea lice, i.e. *Lepeophtheirus salmonis* and *Caligus elongatus* have also been specifically detected using real-time PCR Taqman® MGB (Minor groove binder) probe-based assays (McBeath *et al*. 2006). Furthermore, the mitochondrial gene, cytochrome oxidase I (COI) has been reported as being successful in discriminating closely allied species in the animal kingdom except in the phylum Cnidaria (Pan *et al*. 2008), thus the COI gene is used as a marker of choice for evolutionary relationships in metazoans (Folmer *et al*. 1994). Therefore, it was also used as a molecular marker to recognize different cryptic species in symbiotic Siphonostomatoida (Dippenaar *et al*. 2010). An advantage of mitochondrial DNA is that it is maternally inherited without any recombination. Furthermore, it is easily retrieved from low quantity or degraded DNA samples and is more abundant in each cell than nuclear DNA (Pereira *et al.* 2008).

The COI gene is the largest mitochondria-encoded cytochrome oxidase subunit and is among the largest protein-coding genes in the mitochondrial genome of metazoans. It forms part of the mitochondrial respiratory chain as a terminal catalyst (Lunt *et al*. 1996). It has also been commonly used in evolutionary studies, population dynamics and systematics because of its relatively high sequence variation (Harvey *et al*. 2003; Hurst & Jiggins 2005). Additionally, sequences of the COI gene are used in DNA barcoding for taxonomic identification and biodiversity assessment (Hurst & Jiggins 2005; Hajibabaei *et al*. 2007; Löbl 2014).

The 18S rDNA gene is found in all eukaryotes. This gene has been used as an effective marker in the barcoding of Nematodes (Floyd *et al*. 2005). Additionally, it has been used in the detection of zebra mussel larvae in different environments (Frischer *et al.* 2002). The 18S rDNA gene has variable as well as highly conserved regions, for example Gonzalez and Schmickel (1986) found that there is a 0.1% rate in the divergence of sequences between the human and mouse genes over a period of 80 million years since mammalian radiation.

1.12. Purpose of the study

1.12.1. Aim: To distinguish *Kroyeria* species collected from different elasmobranch hosts caught off the coasts of South Africa.

1.12.2. Objectives:

- To identify *Kroyeria* species using described morphological characteristics.
- To determine the host-parasite relationships of the different species by calculating their prevalence, mean abundance and mean intensity on their hosts.
- To estimate the pattern of dispersion of the *Kroyeria* species among their hosts by calculating the coefficient of dispersion ($s^2/\bar{x}$).
- To estimate phylogenetic relationships among different *Kroyeria* species using a fragment of the COI and the complete18S rDNA genes.
- To distinguish among different *Kroyeria* species using their sequence divergences.
- To distinguish among different *Kroyeria* species based on their different melt temperatures of a fragment of the COI gene.

CHAPTER 2

MATERIAL AND METHODS

2.1. Taxon sampling

Kroyeria specimens were collected from the gill filaments of their elasmobranch hosts which were caught: (1) in the nets of the KwaZulu-Natal Sharks Board (KZNSB) installed along the east coast of South Africa, (2) by commercial fishermen off the west coast at Gansbaai as well as (3) during the demersal trawls of Department of Agriculture, Forestry and Fishery (DAFF) off the south and west coasts. The nets utilised by KZNSB have a length of 214 m, a depth of 6 m and a mesh size of 51 cm. They are placed in two parallel rows about 400 m offshore, in water depths of 10–14 m and are cleared at first light each day. Species that are found caught by the nets are released if still alive or transported to KZNSB headquarters where they are stored in deep freezers for later use by researchers. The use of drumlines is also deployed by KZNSB (S. Wintner, pers. comm.). Collected copepods were counted, fixed and preserved in 70% ethanol. The identity of the host species was confirmed by well-trained staff members of the various organizations and FishBase (Froese & Pauly 2014) was utilised to confirm the accepted scientific names. Several individuals of different *Kroyeria* spp. were selected for molecular work depending on the number of available collected specimens (Table 2.1).

Table 2.1 *Kroyeria* species specimens used for DNA extraction, the host names and locations where they were caught as well as the number of specimens used for the DNA extractions of each species.

Kroyeria species	Host name	South African coasts where hosts were caught	Number of *Kroyeria* specimens used for DNA extraction
K. dispar	*Galeocerdo cuvier* (Péron & Leseur, 1822)	East coast (Indian Ocean)	14
K. carchariaeglauci	*Carcharhinus leucas* (Valenciennes, 1839)	East coast (Indian Ocean)	13
K. decepta	*Carcharhinus obscurus* Leseur, 1818	East coast (Indian Ocean)	5
K. deetsi	*Carcharhinus brevipinna* (Müller & Henle, 1839)	East coast (Indian Ocean)	10
K. *elongata*	*Rhizoprioonodon acutus* (Rüppel, 1837)	East coast (Indian Ocean)	5
K. lineata	*Mustelus palumbes* Smith, 1957	South coast (Indian Ocean)	10
K. longicauda	*Carcharhinus limbatus* (Valenciennes, in Müller & Henle, 1839)	East coast (Indian Ocean)	15
K. papillipes	*Galeocerdo cuvier* (Péron & Leseur, 1822)	East coast (Indian Ocean)	2
K. procerobscena	*Carcharhinus leucas* (Valenciennes, 1839)	East coast (Indian Ocean)	3
K. sphyrnae	*Sphyrna zygaena* (Griffith & Smith in Cuvier, 1834)	East coast (Indian Ocean)	10
K. sphyrnae	*Sphyna lewini* (Linnaeus, 1758)	East coast (Indian Ocean)	10
Kroyeria. sp	*Galeorhinus galeus* (Linnaeus, 1785)	West coast (Atlantic Ocean)	5

2.2. Data collection

2.2.1. Morphological features

The identity of collected *Kroyeria* specimens was confirmed using morphological characteristics as described and illustrated by Deets (1994), Dippenaar *et al*. (2000), Thatcher & Júnior (2006) and Izawa (2008) to distinguish among the species of *Kroyeria*. Both the light and stereo microscopes were used to identify collected *Kroyeria* specimens stained with a small amount of lignin pink dissolved in 70% EtOH, using the wooden slide technique (Humes & Gooding 1964). Some copepods were dissected using fine needle probes and where necessary, morphological features were drawn with the aid of drawing tubes and measured using a stage micrometer to illustrate differences from described features (Chapter 3). The terminology of the morphological descriptions is based on Kabata (1979) and Huys and Boxshall (1991) while the classification of Chondrichthyes is according to Compagno (1999).

2.2.2. Host-parasite relationships

To determine the host-parasite relationships of the collected species, the prevalence (the number of specific host species infected with one or more individuals of a specific *Kroyeria* species divided by the number of specific host species examined for that *Kroyeria* species; i.e. the percentage of infected hosts), mean abundance (the total number of individuals of a particular *Kroyeria* species in a sample of a particular host species divided by the total number of hosts of that species examined; i.e. number of individuals per examined host) and mean intensity (the total number of *Kroyeria* individuals of a particular species found in a sample divided by the number of hosts infected with that *Kroyeria* species; i.e. number of individuals per infected host) of the copepods on their hosts were calculated according to Bush *et al*. (1997) (Chapter 3). Additionally, the pattern of dispersion of *Kroyeria* species on their hosts was estimated by calculating the coefficient of dispersion ($(s^2/\bar{x})$ where s^2 is the variance and $\bar{x}$ is the sample mean) in accordance with Bush *et al*. (2001).

2.2.3. DNA extraction

The selected identified samples (Table 2.1) were prepared for DNA extraction by being cleaned with brushes to remove traces of host tissue and were left at room temperature until all the ethanol on the body had evaporated. DNA was extracted using the QIAGEN DNeasy® blood and tissue kit following the manufacturer's protocols with the following initial changes: overnight incubation at 50°C and heating up the elution buffer to 70°C before use. For the second batch of extractions, the above procedure was still followed with the elusion buffer substituted with double distilled water (ddH_2O) heated to 70°C before use and the incubation time of the DNeasy membrane at room temperature increased to 5 min. The extracted DNA was stored in a freezer at -20°C.

2.2.4. DNA quantification

The extracted DNA was concentrated by reducing the elution volume from 100 μl to 50 μl by heating at 37°C. DNA concentration was then measured using the Qubit® 2.0 Fluorometer (Invitrogen™) and NanoDrop™ 2000 spectrophotometer (ThermoScientific) according to the manufacturers' recommended protocols (Chapter 4).

2.2.5. Whole genome amplification

Whole genome amplification (WGA) was performed for 24 selected samples (Chapter 4) that had very low DNA concentrations (< 10 ng/μl) by using REPLI-g® mini kit (QIAGEN) following the manufacturer's protocol. The aim was to increase the DNA concentration of the samples, as indicated on the kit.

2.2.6. Gradient annealing temperature determination for COI

Eight annealing temperatures (45°C, 45.7°C, 47.1°C, 49°C, 51.2°C, 53°C, 54.3°C and 55°C) were tested on DNA samples extracted previously from a *Nemesis lamna* specimen to determine the optimum annealing temperature (T_A) for the cytochrome oxidase I (COI) universal primers HCO 1490 and LCO 2198 (Table 2.2). A fragment of the mitochondrial COI gene was amplified via PCR using a mastermix containing 2.5 μM of each of the forward and reverse primers HCO 1490 and LCO 2198, respectively (Table 2.2), 84 μl of SsoFast™ EvaGreen® Supermix (including $MgCl_2$, dNTPs, Sso7d fusion polymerase, EvaGreen dye and stabilisers) (Bio-Rad Laboratories, Inc.) and 49.4 μl of ddH_2O. Four microlitres of DNA template were

added to 16 μl of the mastermix to make up a total reaction volume of 20 μl. The reaction was performed in a MiniOpticon^{TM} Real-Time PCR Detection System (Bio-Rad Laboratories, Inc.) with the following thermal cycling conditions: initial denaturation at 98°C (2 min), 40 cycles of denaturation at 95°C (30 sec), annealing at different temperatures (indicated above) for 20 seconds and extension at 72°C (30 sec) respectively. The amplification was concluded by the final extension at 72°C (4 min).

Table 2.2 The universal primers used in PCR amplification of the partial mitochondrial gene (COI) and the complete nuclear gene18S, their sequences and expected sizes of the amplified products.

Name of primer	Sequence	Gene size	Reference
LCO 2198	5'-GGTCAACAAATCATAAAGATATTGG-3'	670 bp	Folmer *et al*. 1994
HCO 1490	5'-TAAACTTCAGGGTGACCAAAAAATCA-3'	670 bp	Folmer *et al*. 1994
LCO 2198_t1	5'-TGTAAAACGACGGCCAGTGGTCAACAAATCATAAAGATATTGG-3'	670 bp	Messing 1983
HCO 1490_t1	5'-CAGGAAACAGCTATGACTAAACTTCAGGGTGACCAAAAAATCA-3'	670 bp	Messing 1983
18Sf	5'-TACCTGGTTGATCCTGCCAG-3'	600 bp	Huys *et al*. 2007
1282r	5'-TCACTCCACCAACTAAGAACGGC-3'	600 bp	Huys *et al*. 2007
554f	5'-AAGTCTGGTGCCAGCAGCCGC-3'	600 bp	Huys *et al*. 2007
614r	5'-TCCAACTACGAGCTTTTTTAACC-3'	600 bp	Huys *et al*. 2007
1150fp2	5'-ATTGACGGAAGGGCACCACCAG-3'	600 bp	Huys *et al*. 2007
18Sr	5'-TAATGATCCTTCCGCAGGTTCAC-3'	600 bp	Huys *et al*. 2007

2.2.7. Polymerase Chain Reaction (PCR)

Initially, a fragment of the mitochondrial COI gene was amplified via PCR (Chapter 4) using a mastermix containing 10 μM each of the forward and reverse universal primers LCO 1490 and HCO 2198, or those with additional M13 tails, LCO 1490_t1

and HCO 2198_t1 (Table 2.2.) respectively, 5 units of Supertherm Taq DNA polymerase (Southern Cross Biotechnology), 10X PCR buffer, 25 mM $MgCl_2$, 2.5 mM of each of the following dNTPs: dATP, dCTP, dGTP and dTTP; and ddH_2O. Four microlitres of DNA template was added to 21 μl of the mastermix to make up a total reaction volume of 25 μl. Later, the reaction setup was changed to using a mastermix containing 10 μM each of the forward and reverse universal primers LCO 1490 and HCO 2198 or LCO 1490_t1 and HCO 2198_t1 (Table 2.2) respectively, ddH_2O and a DreamTaq™ Green PCR mastermix (2X) (ThermoScientific) consisting of DreamTaq™ green buffer, DreamTaq™ DNA polymerase, 4 mM $MgCl_2$ and 0.4 mM of each of the dNTPs: dATP, dCTP, dGTP and dTTP (Inqaba biotech™).

The reaction was performed in a MiniOpticon™ Real-Time PCR Detection System (Bio-Rad Laboratories, Inc.) with the following thermal cycling conditions: initial denaturation at 94°C (3 min), 44 cycles of denaturation at 94°C (45 sec), annealing at 45.7°C (45 sec) and extension at 69°C (45 sec) respectively and a final extension at 69°C (15 min). The protocol was later varied to: initial denaturation at 95°C (5 min), 44 cycles of denaturation at 95°C (30 sec), annealing at either 43°C (45 sec), 45°C (45 sec) or 50°C (1 min) respectively, extension at 72°C (1 min) and a final extension at 72°C (10 min).

The complete 18S ribosomal DNA (rDNA) gene was amplified by separately amplifying three overlapping fragments (600 bp each) via PCR using a mastermix containing 10 μM each of the forward and reverse universal primers as follows: 18Sf and 1282r for the first fragment, 554f and 614r for the second fragment and 1150f and 18sr for the third fragment (Table 2.2.), ddH_2O and a DreamTaq™ Green PCR mastermix (2X) (ThermoScientific) constituted by DreamTaq™ green buffer, DreamTaq™ DNA polymerase, 4 mM $MgCl_2$ and 0.4 mM of each of the dNTPs. Four microlitres of DNA template was added to 16 μl of the mastermix to make up a total reaction volume of 20 μl.

Amplification for the first fragment had the following thermal cycling conditions: initial denaturation at 95°C (15 min), 44 cycles of denaturation at 94°C (1 min), annealing at 55°C (1 min) and extension at 72°C (2 min) and a final extension at 72°C (10 min) according to Huys *et al*. (2007). The annealing temperature was later varied to: 52°C (1 min). Amplification for the second and third fragments followed the same protocol

with the annealing temperature being 59°C (1 min) and 57°C (1 min) respectively. The annealing temperature for the second fragment was later changed to: 56°C (1 min).

2.2.8. Agarose gel electrophoresis

Agarose gel (1.5%) was prepared by dissolving 0.7 g agarose in 45 ml of 1X Tris Acetate EDTA (TAE) buffer. Two microlitres of Ethidium bromide (10 mg/ml) were added to the melted agarose mixture. Five microlitres of each PCR product was mixed with two microlitres of loading dye [10 mM Tris-HCL (pH 7.6), 0.15% orange G, 0.03% xylene cyanol FF, 60% glycerol and 60 mM EDTA], loaded onto the agarose gel and run for about 10 minutes at 150 V. The gel bands were visualized under UV light (Chapter 4).

2.3. DNA sequencing and phylogenetic analyses

2.3.1. DNA sequencing

PCR products were sent to Inqaba biotech^{TM} for purification and were sequenced in both directions. The same primers used for PCR were also used for sequencing (Table 2.2). A BLAST (Basic Local Alignment Search Tool) search was done for PCR products that were successfully sequenced to compare them against sequences previously deposited in GenBank.

2.3.2. Sequence alignment

The forward and reverse sequences were analysed and evaluated using both CLC Main Workbench 6.7.1 (CLC Bio, Katrinnebjerg, Denmark) and BioEdit 7.0.0 (Hall 1999). Nucleotide ambiguities were checked by eye and edited manually to ensure correct sequences for further applications. The contig sequences that were generated from these programs and *Kroyeria* sequences included in Genbank (COI sequences: *K. decepta*, accession no. FJ447365.1; *K. dispar*, accession no. FJ447361.1; *K. longicauda*, accession no. FJ447364.1; *K. papillipes*, accession no. FJ447362.1 and *K. sphyrnae*, accession no. FJ447363.1) and (18S sequences: *K. dispar*, accession no. FJ447424; *K. papillipes*, accession no. FJ447425; *K. sphyrnae*, accession no. FJ447426; *K. longicauda*, accession no. FJ447427 and *Kroyeria* species, accession no. DQ538499) were aligned in ClustalX 2.0.12 (Thompson *et al*. 1997). For the final data set of COI sequences, *K*. *deetsi* and *K*. *procerobscena* were excluded as their sequences were much shorter after being

trimmed. To accommodate shorter sequences for 18S, all the sequences were pruned to 1668 bp. The nucleotides for the coding COI sequences were translated to amino acids in MacClade 4.0 (Madison & Madison 2000) to detect the presence of pseudogenes in this part of the gene.

2.3.3. Phylogenetic analyses

The phylogenetic relationships among *Kroyeria* species were estimated in PAUP* 4.0b10 (Swofford 2002) using neighbor-joining (NJ) (Saitou & Nei 1987), maximum likelihood (ML) (Felsenstein 1981) and parsimony (MP) (Camin & Sokal 1965).

2.3.3.1. COI

A branch-and-bound tree search was performed for MP with 1000 random additional replicates and the initial upper bound being computed via stepwise option. 50% majority rule tree was constructed from the multiple most parsimonious trees. A branch-and-bound search was also performed for ML, with the search parameters being estimated from the results obtained for the NJ tree. The Rogers-Swofford method was selected as the starting branch for non-clock models, with all characters equally weighted. The initial upper bound was computed via stepwise option with 1000 random additional replicates. All the phylogenies were rooted using the outgroup method, with *Kroeyerina elongata* selected as the outgroup species as it closely related to *Kroyeria* species. The bootstrap analysis (Felsenstein 1985) for both MP and ML trees were calculated using a branch-and-bound search and 1000 replicates. The genetic divergence among COI sequences was estimated in MEGA 5.0.5 (Tamura *et al*. 2011) (Chapter 4).

2.3.3.2. 18S rDNA

A partition homogeneity test (IDL) was implemented in PAUP to test whether the different 18S sequences were homogenous (rate heterogeneity) and thus if midpoint rooting was justified. The test was conducted by performing a branch and bound search computed via stepwise option with homogeneity replicates automatically increased by 1000.

An exhaustive tree search was performed for MP with 1000 random additional replicates. An exhaustive search was also performed for ML, with the search parameters being estimated from the results obtained for the NJ tree. The Rogers-

Swofford method was selected as the starting branch for non-clock models, with all characters equally weighted. Midpoint rooting (MPR) (Farris 1972) was used to root all the phylogenies since a suitable outgroup species, e.g. *Kroeyerina* sp. could not be amplified. Since MPR does not allow bootstrap analyses on the branches of the trees generated, the phylogenies have no bootstrap values. The genetic divergence among 18S sequences was estimated in MEGA 5.0.5 (Tamura *et al*. 2011) (Chapter 4).

2.3.4. Network analyses

Haplotype diversities (Nei 1987) of the mtDNA and rDNA were done using DnaSP version 5.10 (Librado & Rozas 2009) and median-joining networks were constructed using Network version 4.6 (Polzin & Daneschmand 2003) (Chapter 4).

2.3.5. Real-time PCR (qPCR)

A fragment of the mitochondrial COI gene was amplified via qPCR (Chapter 4) using a mastermix containing 2 μM of each of the forward and reverse universal primers LCO 1490 and HCO 2198 (Table 2.2), respectively, 84 μl of SsoFast^{TM} EvaGreen® Supermix (including $MgCl_2$, dNTPs, Sso7d fusion polymerase, EvaGreen dye and stabilisers) (Bio-Rad Laboratories, Inc.) and 49.4 μl of ddH_2O. Four microlitres of DNA template was added to 16 μl of the mastermix to make up a total reaction volume of 20 μl. The reaction was performed in a MiniOpticon^{TM} Real-Time PCR Detection System (Bio-Rad Laboratories, Inc.) following initial denaturation at 98°C (2 min), 44 cycles of denaturation at 95°C (30 sec), annealing at 45.7°C (20 sec) and extension at 72°C (30 sec) respectively. The amplification was concluded by the final extension at 72°C (5 min).

2.3.6. Melt curve analysis

A melt curve analysis was performed after amplification using the same MiniOpticon^{TM} (Bio-Rad Laboratories, Inc.). The DNA samples were heated rapidly to 95°C (10 sec) for denaturation, then cooled to 45°C (5 sec) to re-anneal where after they were heated slowly (0.5°C every 5 sec) to 95°C and the fluorescence measured continuously (at every 0.1°C change). The melt curves were converted to melt peaks by plotting the negative derivative of fluorescence over time vs temperature (Chapter 4).

2.3.7. GC content calculation

The GC content of the *Kroyeria* sequences were calculated using default parameters in uMelt^{SM} v2.02 (http://dna.utah.edu/umelt/umelt.html) (Dwight *et al*. 2011) to estimate their predicted T_m.

CHAPTER 3

MORPHOLOGICAL IDENTIFICATION OF *KROYERIA* SPECIES AND THEIR PARASITE-HOST RELATIONSHIPS ON DIFFERENT ELASMOBRANCH HOSTS

3.1. Introduction

There are 21 nominal species in the genus *Kroyeria* van Beneden, 1853 (Deets 1994; Dippenaar *et al*. 2000; Thatcher & Júnior 2006; Izawa 2008), namely *K. branchiocetes* Deets, 1994; *K*. *brasiliense* Thatcher & Júnior, 2006; *K*. *carchariaeglauci* (Hesse,1879); *K*. *caseyi* Benz & Deets, 1986; *K*. *cresseyi* Deets, 1994; *K*. *decepta* Deets, 1994; *K*. *deetsi* Dippenaar, Benz & Olivier, 2000; *K*. *dispar* Wilson, 1935; *K*. *echinata* Rangnekar, 1956; *K*. *elongata* Pillai, 1967; *K*. *gemursa* Cressey, 1967; *K*. *lineata* van Beneden, 1853; *K*. *longicauda* Cressey, 1970; *K*. *minuta* Pillai, 1976; *K*. *papillipes* Wilson, 1932; *K*. *procerobscena* Deets, 1994; *K*. *rhophemophaga* Deets, 1994; *K*. *spatulata* Pearse, 1948; *K*. *sphyrnae* Rangnekar, 1957; *K*. *sublineata* Yamaguti & Yamasu, 1959 and *K*. *triakos* Fukui, 1965.

Species of the genus *Kroyeria* are primarily characterised by the dorsal shield (resembling the one observed in the primitive *Dissonus* Wilson, 1906 species) of the cephalothorax with posterior sinuses (Kabata 1979) and dorsal stylets (reminiscent of similar structures observed in *Jusheyus* Deets & Benz, 1987 and *Eudactylinopsis* Pillai, 1968) arising dorsolaterally along the posterior margin of the cephalothorax (Kabata 1979; Deets 1994) and articulated via a ball and socket joint (Benz 1994). Other distinguishing features include a small one to three segmented abdomen; elongate, tubular genital complex forming more than 50% of the body length (in females); caudal rami with six distal setae; indistinctly seven or eight segmented antennule; chelate antenna (similar to the one observed in the family Pennellidae and the genus *Pseudohatschekia* Yamaguti, 1939) with four segments, the third segment having a groove that holds the claw of the fourth segment; two-part mandible with seven to ten teeth; unmodified, biramous and trimerite arrangements in legs one to four and a vestigial fifth leg represented by four setae (Kabata 1979; Benz 1994; Deets 1994; Dippenaar & Olivier 1999; Dippenaar *et al*. 2000; Dippenaar *et al*. 2001; Thatcher & Júnior 2006; Izawa 2008).

Due to the homogeneity in morphological characteristics, it is not an easy task to identify some species belonging to the genus *Kroyeria* (Deets 1994; Izawa 2008).

For instance, *K. carchariaeglauci* and *K. decepta* have unobvious morphological differences (Deets 1994) while *K. deetsi* is superficially similar to *K. brasiliense* (Thatcher & Júnior 2006). Furthermore, the superficial morphological similarities of *Kroyeria* species caused Pillai (1967) to regard *K. elongata* as a synonym of *K. spatulata* while Kabata (1979) considered *K. sublineata* as a synonym of *K. lineata*. However, both *K. elongata* and *K. sublineata* have been proven to be valid species (Deets 1994; Izawa 2008) (see Table 3.1). Concerning *K. sublineata*, Izawa (2008) argued that Kabata (1979) overlooked the difference in the chaetotaxy of the legs, especially the number of setae on the third exopodal segments of legs 1–4, which is the main distinguishing feature between *K. sublineata* and *K. lineata*. Additionally, *K. elongata* has a dorsal stylet that terminates as a projection that curves inwardly contrasting to the bifid dorsal stylet seen in *K. spatulata* (Deets 1994; Izawa 2008). Moreover, three *Kroyeria* species, *K. acanthiasvulgaris* Hesse, 1879, *K. galeivulgaris* Hesse, 1884 and *K. scyllicaniculae* Hesse, 1879, are treated as *species inquirenda* because they have been insufficiently described and cannot be compared with any known species (Deets 1994; Walter & Boxshall 2014). However, detailed morphological differences can be used to distinguish *Kroyeria* species (Table 3.1).

According to Deets (1994), *Kroyeria* species display host specificity as a general rule. However, *Kroyeria* species and their host species, the Carcharhiniformes, display morphological conservativeness and this has led to misidentification of *Kroyeria* species and reported wide host distribution (Deets 1994).

Table 3.1 A review of *Kroyeria* species, their distinguishing features, reported hosts and their geographical locations (Deets 1994; Dippenaar *et al*. 2000; Thatcher & Júnior 2006 and Izawa 2008).

Kroyeria species	Distinguishing characteristics	Host species	Geographical range
Kroyeria branchiocetes Deets, 1994	Similar in appearance to *K. cresseyi*, *K. lineata*, *K. rhophemophaga* and *K. triakos* in that the antenna has a claw with only two slender setae. However, differs from these species in that it	*Carcharhinus amblyrhynchos* (Bleeker, 1856) (Deets 1994).	Red sea (Deets 1994).

	possesses endopodal denticulations on the second and third segments of all the swimming legs (Deets 1994).		
Kroyeria brasiliense Thatcher & Júnior, 2006	Similar to *K. deetsi* but differs from it in the following: larger maxillipeds which project well beyond the lateral margins of the cephalothorax; shorter, two-segmented abdomen in contrast to the long, slender, three-segmented abdomen in *K. deetsi*; rounded second and third endopodal segments of equal length and are devoid of denticles, in contrast to the length of the third endopodal segments which are twice or more than twice as long as those of the corresponding second endopodal segments (Dippenaar *et al*. 2000; Thatcher & Júnior 2006).	*Galeorhinus galeus* (Linnaeus, 1758) (Thatcher & Júnior 2006).	Atlantic Ocean near Rio Grande, Brazil (Thatcher & Júnior 2006).
Kroyeria carchariaeglauci Hesse, 1879	Characterized by the combination of bifid dorsal stylets; caudal rami with stout, pyriform, pinnate setae adjacent to	*Prionace glauca* (Linneaus, 1758); *Carcharhinus falciformis* (Müller and Henle, 1839);	Eastern North Atlantic, Mediterranean, Japanese waters, Chile, Western North Atlantic, Tunisian waters,

	the two elongate pinnate setae in females as well as the relative length to width ratio of the caudal ramus of the male (Deets 1994).	*Carcharhinus longimanus* (Poey, 1861); *Carcharhinus plumbeus* Nardo, 1827; *Carcharhinus leucas* (Müller and Henle, 1839) (Deets 1994; Dippenaar 2005; Dippenaar & Jordaan 2007). Questionable records have been provided from *Eulamia sp*., *Mustelus asterias* Cloquet, 1819, *Mustelus mustelus* (Linnaeus, 1758) and *Squalus blainville* (Risso, 1827) (Deets 1994).	Eastern North Pacific, Mexico, Channel Islands, Southern California Bight, Madagascar (Deets 1994;), East coast of South Africa (Dippenaar 2005; Dippenaar & Jordaan 2007).
Kroyeria caseyi Benz and Deets, 1986	Largest and only known mesoparasitic *Kroyeria* species. It is characterized by a genital complex that is extremely elongate, forming 95% of the entire body; maxilla with very elongate claw; antenna aperture with reduced seta; inflated abdomen with only one segment; caudal rami lacking the typical medial fringe of setules but bearing stout naked setae (Deets 1994).	*Carcharhinus signatus* (Poey, 1868) (Deets 1994).	Western North Atlantic (Deets 1994).
Kroyeria cresseyi Deets,	Similar to *K. branchiocetes*, *K. lineata*, *K. rhophemophaga* and	*Triakis semifasciata* Girard, 1855 (Deets	Inshore waters off El Segundo, Seal Beach and Palos Verde,

1994	*K. triakos* by possessing antennae with the claw having only two slender setae. However, differs from *K. branchiocetes* and *K. lineata* because the claw and the corpus of the antennae lack the large membranous expansion distally. It differs from *K. triakos* by having the terminal segment of the third exopod possessing only four pinnate setae, one lateral slender seta with serrated membrane and one lateral semi-pinnate seta (*K. triakos* has five pinnate setae and one slender naked seta). Contrary to *K. rhophemophaga* which has a subquadrangular cephalothorax, *K. cresseyi* has an orbicular cephalothorax. Additionally, *K. cresseyi* has a bifid dorsal stylet as opposed to the other species that are similar to it (Deets 1994).	1994).	California (Deets 1994).
Kroyeria decepta Deets, 1994	Very similar to *K. carchariaeglauci*, but differs by possessing pinnate setae (naked in *K. carcharhiaeglauci*) on endopod of maxillule,	*Carcharhinus obscurus* (Lesueur, 1818) (Deets 1994; Dippenaar & Jordaan 2007).	West coast of Florida, tropical Northeastern Pacific (Deets 1994), East coast of South Africa (Dippenaar &

	pectinate lateral membranes (thin and smooth in *K. carcharhiaeglauci*) on second and third segments of exopod of leg 1 and teeth of alternating sizes on the mandible (uniform size in *K. carcharhiaeglauci*). *K. decepta* is bigger than *K. carcharhiaeglauci* in size (Deets 1994).		Jordaan 2007).
Kroyeria deetsi Dippenaar, Benz & Olivier, 2000	Characterized by the third endopodal segments of legs 1–4 which are about twice (leg 1, 2 and 4) or more than twice (leg 3) as long as the corresponding second endopod segments (Dippenaar *et al*. 2000).	*Carcharhinus brevipinna* (Müller and Henle, 1839) (Dippenaar *et al*. 2000).	East coast of South Africa (Dippenaar *et al*. 2000; Dippenaar 2005).
Kroyeria dispar Wilson, 1935	Characterized by the unusually wide cephalothorax; lack of endopodal denticulations; two elongate, pinnate setae on the medial margin of endopods of legs 1 and 2; maxillule with spinulated endopod and maxilliped having peculiar cuticular flaps on myxal area (Deets 1994).	*Galeocerdo cuvier* (Péron & Lesueur, 1822) (Deets 1994; Dippenaar & Olivier 1999).	West coast of Florida (Deets 1994), East coast of South Africa (Dippenaar & Olivier 1999; Dippenaar 2005).
Kroyeria	Dorsal stylets short and	*Sphyrna zygaena*	Indian Ocean (Deets

echinata Rangnekar, 1956	stout, resembling those of *K. dispar* and *K. papillipes*, but smaller. The presence of endopodal denticulations on the second endopodal segment of all the legs is the same in both *K. echinata* and *K. papillipes*, but all the endopods of *K. dispar* lack denticulations. *K. papillipes* differs from *K. echinata* by having an orbicular cephalothorax and different armature on the caudal rami as well as on the legs (Deets 1994).	(Linnaeus, 1758) (Deets 1994).	1994).
Kroyeria elongata Pillai, 1967	Very elongated claw and corpus of antenna (Deets 1994).	*Rhizoprionodon acutus* (Rüppell, 1837) and *Carcharhinus sorrah* (Müller and Henle, 1839) (Deets 1994).	Indian Ocean (Deets 1994).
Kroyeria gemursa Cressey, 1967	The distal region of the last segment of abdomen is laterally bulging and heavily sclerotized; antenna with thickened claw and extension of the corpus thickened resulting in reduced aperture; labrum with large patches of spinules on distolateral surfaces; second and third segments of leg 1 and 2 with numerous (25–33)	*Sphyrna mokarran* Rüppell, 1837 (Deets 1994; Dippenaar 2005; Dippenaar & Jordaan 2007).	Madagascar, Indian Ocean, West coast of Florida, (Deets 1994; Dippenaar 2005), East coast of South Africa (Dippenaar 2007).

	endopodal denticulations (Deets 1994).		
Kroyeria lineata van Beneden, 1853	Endopods devoid of endopodal denticulations, proximal region of the claw of the antenna bearing only two prominent setae, the only *Kroyeria* species with distal membranous extensions near the tip of the claw of the maxilla (Deets 1994).	*Galeorhinus galeus* (Linneaus, 1758), *Mustelus mustelus* (Linneaus, 1758), *Mustelus asterias* Cloquet, 1821 and *Mustelus punctulatus* Risso, 1827. Other records which are questionable come from hosts like *Sphyrna zygaena* (Linnaeus, 1758), *Carcharhinus limbatus* (Müller and Henle, 1839), *Negaprion brevirostris* (Poey, 1868) and *Prionace glauca* (Linneaus, 1758) (Deets 1994).	Adriatic Sea, North Sea, Mediterranean off Tunisia, Japan (Deets 1994).
Kroyeria longicauda Cressey, 1970	Characterized by a deeply incised, bifid dorsal stylet with lateral tine; caudal rami with lateral cuticular flange and the small number of unusually large endopodal denticulations (Deets 1994).	*Carcharhinus limbatus (*Müller & Henle, 1839), *Carcharhinus brevipinna* (Müller and Henle, 1839) (Deets 1994).	Florida, Mozambique Channel (Deets 1994; Dippenaar 2005), East coast of South Africa (Dippenaar & Jordaan 2007).
Kroyeria minuta Pillai, 1968	Characterized by small size; dorsal stylets that are long and bifid, extending to the posterior margin of the fourth	*Rhizoprionodon acutus* (Rüppell, 1837) (Pillai 1968).	India (Pillai 1968).

	thoracic segment; serrated medial margin; lateral margin of coxa of the second leg with atypical patch of spinules; third segment of exopod of leg 2 with six pinnate setae (Deets 1994).		
Kroyeria papillipes Wilson, 1932	Distinguished by being the only known *Kroyeria* species having all six setae on the caudal rami being elongate and pinnate (Deets 1994).	*Galeocerdo cuvier* (Péron & Lesueur, 1822) (Deets 1994; Dippenaar & Jordaan 2007).	West coast of Florida (Deets 1994), East coast of South Africa (Dippenaar & Jordaan 2007).
Kroyeria procerobscena Deets, 1994	Unusually long genital complex which forms 80% of the entire body length; the proximal region of the bifid dorsal stylet with a unique lateral tine; caudal rami with two elongate, proximally inflated medially-pinched pinnate setae (Deets 1994).	*Carcharhinus leucas* (Müller and Henle, 1839) and *Carcharhinus amboinensis* (Müller & Henle, 1839) (Deets 1994; Dippenaar 2005; Dippenaar & Jordaan 2007).	Mozambique Channel, (Deets 1994; Dippenaar 2005), East coast of South Africa (Dippenaar & Jordaan 2007).
Kroyeria rhophemophaga Deets, 1994	Similar *to K. branchiocetes*, *K. lineata*, *K. cresseyi* and *K. triakos* by possessing antennae with the claw bearing only two slender elongate setae, rather than three.	*Galeorhinus galeus* (Linnaeus, 1758) (Deets 1994).	New Zealand, Eastern Atlantic, Eastern North Pacific (Deets 1994).

	However, differs from *K. branchiocetes* and *K. lineata* because the claw and the corpus of the antennae lack the large membranous expansion distally. It differs from *K. triakos* by having the terminal segment of the third exopod possessing only four pinnate setae and two lateral slender setae. Contrary to *K. cresseyi which* has an orbicular cephalothorax, *K. rhophemophaga* has a subquadrangular cephalothorax (Deets 1994).		
Kroyeria spatulata Pearse, 1948	Characterized by the presence of unique sinuous, pectinate membranes, located medial to the short, spiniform setae on all segments of the exopod of leg 4 and wrapping down the lateral margins of the second and terminal segments (Deets 1994).	*Rhizoprionodon terraenovae* (Richardson, 1836), *Carcharias littoralis* (Rafinesque, 1810), *Carcharhinus limbatus* (Müller & Henle, 1839), *Rhizoprionodon acutus* (Rüppell, 1837), *Negaprion brevirostris* (Poey, 1868) and *Carcharhinus leucas* (Müller and Henle, 1839). Reports of *K. spatulata* on the *Carcharhinus brevipinna* (Müller and Henle, 1839) and	North Carolina, Bahamas, Gulf of Mexico, Indian Ocean, West coast of Florida (Deets 1994).

		Carcharhinus sorrah (Müller and Henle, 1839) are errors (Deets 1994).	
Kroyeria sphyrnae Rangnekar, 1957	Characterized by long, acute, lissome dorsal stylets, seven-toothed mandible formula, relatively short interpodal stylets which barely reach the distal margin of the basipods of legs 2–4 (Deets 1994).	*Sphyrna zygaena* (Linnaeus, 1758) and *Sphyrna lewini* (Griffith and Smith, 1834) (Deets 1994; Dippenaar *et al*. 2001). Additionally, reports of *Kroyeria sphyrnae* on *Chiloscyllium punctatum* Müller and Henle, 1838 and *Carcharhinus acronotus* (Poey, 1860) are questionable (Deets 1994).	India, Australia, West coast of Florida, Hawaiian Islands, Southern Sea of Cortez, Mexico, Eastern North Pacific, Indian Ocean (Deets 1994; Dippenaar 2005), East coast of South Africa (Dippenaar, *et al*. 2001; Dippenaar & Jordaan 2007).
Kroyeria sublineata Yamaguti and Yamasu, 1959	Resembles *K. lineata* in appearance but differs from it in the chaetotaxy of the legs. The number of setae and spines on the terminal segments of exopods of legs 1–4 in *K. sublineata* is 6,6,6,6 but 6,7,7,7 in *K. lineata* (Izawa 2008).	*Mustelus manazo* Bleeker, 1855 and *Mustelus griseus* Pietschmann, 1908 (Deets 1994; Izawa 2008).	Inland Sea of Japan Tanabe Bay (Deets 1994; Izawa 2008).
Kroyeria triakos Fukui, 1965	The only *Kroyeria* species with the terminal exopodal segment of leg 3 bearing five elongate, pinnate setae. Additionally, the first and	*Triakis scyllium* Müller and Henle, 1839 (Deets 1994).	Japan (Deets 1994).

	second segments of the fourth exopod lack typical lateral setae (Deets 1994).		

3.2. Aim and Objectives

3.2.1. Aim: To distinguish *Kroyeria* species collected from different elasmobranch hosts caught off the coasts of South Africa based on their morphological characteristics and to determine their host-parasite relationships.

3.2.2. Objectives:

- To identify *Kroyeria* species using described morphological characteristics.
- To determine the host-parasite relationships of the different species by calculating their prevalence, mean abundance and mean intensity on their hosts.
- To estimate the pattern of dispersion of the *Kroyeria* species among their hosts by calculating the coefficient of dispersion ($s^2/\bar{x}$).

3.3. Material and methods

Material and methods are as described in Chapter 2.

3.4. Results

Kroyeria species that were collected from elasmobranchs off the coasts of South Africa were verified using morphological characteristics as described by Deets (1994), Dippenaar *et al*. (2000), Thatcher & Júnior (2006) and Izawa (2008). These included *K*. *carchariaeglauci* from *C. leucas*; *K*. *decepta* from *C*. *obscurus*; *K*. *deetsi* from *C*. *brevipinna*; *K*. *dispar* from *G. cuvier; K*. *elongata* from *R. acutus*; *K*. *lineata* from *M. palumbes*; *K*. *longicauda* from *C*. *limbatus*; *K*. *papillipes* from *G*. *cuvier*; *K*. *procerobscena* from both *C*. *leucas* and *C*. *amboinensis*; *K. sphyrnae* from both *S. lewini* and *S*. *zygaena* and *Kroyeria* sp. from *G. galeus* (see Table 3.2). The *Kroyeria* species collected from the gills of *G. galeus* could not easily be identified using the previous descriptions. It superficially resembled *K. branchiocetes* and *K. elongata* by

the presence of a cuticular distolateral flange on the terminal part of the dorsal stylet. However, it differed from both species by the length of the dorsal stylets. Additionally these specimens strongly resembled *K. rhophemophaga* by the shape of the cephalothorax and the length of the dorsal stylets and *K. triakos* by the shape of the cephalothorax and the shape of the terminal part of the dorsal stylets. Thus, these *Kroyeria* specimens required a detailed morphological description illustrated by drawings.

3.4.1. Description of *Kroyeria* sp.

Host species: *Galeorhinus galeus* (Linnaeus, 1758).

Geographical distribution: West coast of South Africa (Atlantic Ocean).

Female description (Fig. 1 & 2).

Total length in dorsal view about 5.2 mm. Body elongated, with cephalothorax, thorax consisting of three free segments, elongate, tubular genital complex and a three-segmented abdomen (Fig. 1a). Cephalothorax (Fig. 1a) wide and sub-quadrangular in shape, bearing ventrally antennules, antennae, mandibles, maxillules, maxillae, maxillipeds and the first pair of swimming legs. Dorsally, with sclerotized anterolateral sutures which unite posteromedially, dividing the dorsal shield into two lateral regions and a frontal region which extends into the rostellum. Dorsal stylets (Fig. 1a, 1b) originate from the posterolateral sinuses extending to almost half of the second free thoracic segment, slightly curving inwardly with a cuticular distolateral flange. First thoracic segment fused with the cephalon to form the cephalothorax. Following three thoracic segments (Fig. 1a) free and have non-overlapping terga dorsally, as well as a medial suture and equal widths. Third free segment slightly longer than previous two. All thoracic segments with pair of unmodified, biramous, trimerite, swimming legs. Genital complex (Fig. 1a) tubular, elongate, comprising about 69% of total body length. Abdomen (Fig. 1a) small, tapered, indistinctly three-segmented. Caudal ramus (Fig. 1a, 1c) lamelliform, longer than wide, with medial fringe of setules, bearing six terminal setae with distal four pinnate decreasing in size from medial to lateral and two slender, naked setae, one distolaterally and the other distomedially.

Antennule (Fig. 1d) indistinctly seven- or eight segmented, armature (base to apex) as follows: 8, 5, 3, 1, 1, 1, 7+1 aesthete. Antenna (Fig. 1e) chelate, prehensile and probably four segmented. Fourth segment bearing a proximal slender seta and forms a robust claw with a tip that fits into the receptacle of the third segment, forming main corpus of the chela. Maxilla (Fig. 1f) branchiform; branchium bearing two patches of fine denticles and long setules near base of claw-like calamus. Calamus with convex membranous surface. Maxilliped (Fig. 1g) subchelate; corpus probably two-segmented, bearing distolateral flange; subchela not divided into shaft and claw, bearing a slender seta distally.

The armature of rami (Arabic numerals represent fully pinnate setae and Roman numerals represents deviations from that state).

Leg 1	Exopod I-1 0-1 II, 4	Endopod 0-1 0-0 6
Leg 2	Exopod I-1 0-1 II, 4	Endopod 0-1 0-0 6
Leg 3	Exopod I-1 I-1 III, 4	Endopod 0-1 0-0 4
Leg 4	Exopod I-1 0-1 II, 4	Endopod 0-1 0-1 I, 2

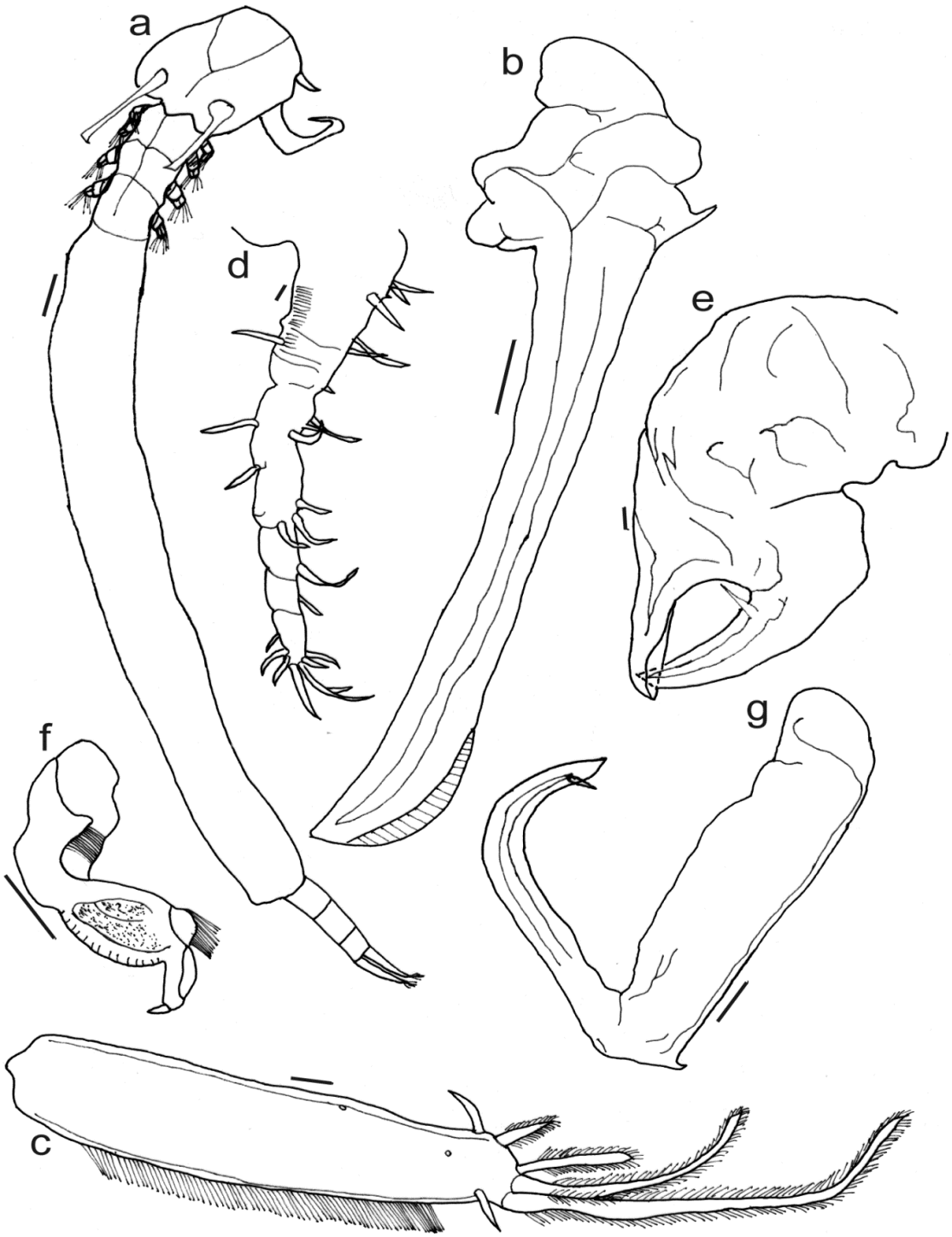

Figure 1 Adult female *Kroyeria* sp.

a, General habitus; b, Dorsal stylet; c, Caudal ramus; d, Antennule; e, Antenna; f, Maxilla; g, Maxilliped. Scale bars: a = 2 mm; b-e = 10 μm; f = 50 μm; g = 10 μm.

Leg 1 (Fig. 2a) biramous, trimerite, basis bearing a short lateral pinnate seta and a short medial pinnate seta. Exopod with pectinate lateral membrane, first segment with short distolateral spine and long pinnate medial seta; second segment with long pinnate medial seta; third segment with four long pinnate terminal setae, lateral semi-pinnate seta and short distolateral spine. Endopod segments with lateral pectinate membrane; first segment with long medial pinnate seta; second segment with seven endopodal denticulations and setules along the lateral margin; third segment with six long terminal pinnate setae.

Leg 2 (Fig. 2b) biramous, trimerite, basis bearing a short lateral naked seta. Exopod with pectinate lateral membrane, first segment with short distolateral spine and long pinnate medial seta, second segment with long pinnate medial seta; third segment with four long pinnate terminal setae, lateral semi-pinnate seta with a lateral membrane and a short distolateral spine. Endopod, first segment with setules on the lateral margin and long medial pinnate seta; second segment with setules on the lateral margin (not visible on the diagram) and eight endopodal denticulations; third segment with six long terminal pinnate setae.

Leg 3 (Fig. 2c) biramous, trimerite. Exopod, first segment with short distolateral spine and long medial pinnate seta; second segment with short distolateral spine and long medial pinnate seta; third segment with four long pinnate setae, short lateral semi-pinnate seta and two short lateral spines. Endopod, first segment with a long medial pinnate seta; second segment with seven endopodal denticulations and setules on the lateral margin; third segment with four long terminal pinnate setae.

Leg 4 (Fig. 2d) biramous, trimerite, basis bearing a short lateral naked seta. Exopod, first segment with medial setules, short distolateral spine and long medial pinnate seta; second segment with pectinate lateral membrane and long medial pinnate seta; third segment with pectinate lateral membrane, four long pinnate setae, lateral semi-pinnate seta and a short distolateral spine. Endopod, first segment with long medial pinnate seta; second segment with nine endopodal denticulations, setules on the lateral margin and long medial pinnate seta; third segment with two long terminal pinnate setae and a short stout naked seta.

Figure 2 Adult female *Kroyeria* sp.

a, Leg 1; b, Leg 2; c, Leg 3; d, Leg 4. Scale bars: a-d = 50 *μ*m.

3.4.2. Host-parasite relationships

Eleven different *Kroyeria* species were collected from 10 different elasmobranch hosts in this study (Table 3.2). In order to estimate the host-parasite relationships, numbers of collected copepods include those collected from both the left and right gills. In cases where only the left or right gills were examined, the numbers were doubled to estimate the total number of copepods per host individual.

Kroyeria sp. recorded from *G. galeus* and *K. dispar* had very high prevalence values (Fig. 3.1), 95.7% and 94.1% respectively. The majority of the other *Kroyeria* species had relatively lower prevalence values, with the exception of *K. papillipes* (68.6%). *Kroyeria procerobscena* collected from *C. leucas* had the lowest prevalence value (6.3%); in fact, lower than that of the same species collected from *C. amboinensis* (33.3%) while *K. sphyrnae* from *S. lewini* had a higher prevalence value (40%) than that of *K. sphyrnae* from *S. zygaena* (22%).

Kroyeria dispar had the highest mean abundance value (69 individuals per examined host) of all the collected *Kroyeria* species (Fig. 3.2) whereas *K. procerobscena* from *C. leucas* had the lowest mean abundance value (0 individual per examined host) and lower than that of *K. procerobscena* from *C. amboinensis (*1 individual per examined host). Similarly, the mean abundance value of *K. sphyrnae* from *S. zygaena* was slightly lower (2 individuals per examined host) than that of *K. sphyrnae* from *S. lewini* (3 individuals per examined host). *Kroyeria dispar* exhibited the highest mean intensity value of 74 individuals per examined host (Fig. 3.3).

Even though the mean intensity values were mostly relatively low, the lowest mean intensity value was exhibited by *K. deetsi* (4 individuals per infected host). In contrast to the prevalence and mean abundance values, the mean intensity value for *K. procerobscena* from *C. leucas* (6 individuals per infected host) was slightly higher than that of the same species on *C. amboinensis* (4 individuals per infected host) and the mean intensity value for *S. zygaena* (13 individuals per infected host) was slightly higher than that of *S. lewini* (9 individuals per infected host).

Distribution results of *Kroyeria* species suggest that most *Kroyeria* species display an aggregated pattern of distribution on their hosts ($s^2 > \bar{x}$), with *K. carchariaeglauci* being an exception by displaying a random distribution pattern ($s^2 < \bar{x}$) (Table 3.2).

Table 3.2 The collected *Kroyeria* species from different elasmobranch hosts, the number of collected copepods, number of infected hosts and total number of hosts examined for infection, calculated prevalence (%), mean abundance (individuals per examined host), mean intensity (individuals per infected host) and distribution ($s^2/\bar{x}$) values for *Kroyeria* species on their hosts.

Kroyeria species	Host species	No of parasites	No of infected hosts	Total no of hosts	Prevalence %	Mean abundance	Mean intensity	Dispersion pattern
K. carchariaeglauci	*C. leucas*	50	7	16	43.8	3.1	7.1	$s^2 < \bar{x}$ Random
K. decepta	*C. obscurus*	328	17	92	18.4	3.6	19.3	$s^2 > \bar{x}$ Aggregated
K. deetsi	*C. brevipinna*	55	14	36	38.9	1.5	3.9	$s^2 > \bar{x}$ Aggregated
K. dispar	*G. cuvier*	3521	48	51	94.1	69	73.4	$s^2 > \bar{x}$ Aggregated
K. elongata	*R. acutus*	9	1	8	12.5	1.1	9	Insufficient samples
K. lineata	*M. palumbes*	107	14	45	31.1	2.4	7.6	$s^2 > \bar{x}$ Aggregated
K. longicauda	*C. limbatus*	291	10	29	34.5	10	29.1	$s^2 > \bar{x}$ Aggregated
K. papillipes	*G. cuvier*	1153	35	51	68.6	22.6	33	$s^2 > \bar{x}$ Aggregated
K. procerobscena	*C. leucas*	6	1	16	6.3	0.4	6	Insufficient samples
K. procerobscena	*C. amboinensis*	4	1	3	33.3	1.3	4	$s^2 > \bar{x}$ Aggregated
Kroyeria sp.	*G. galeus*	1589	67	70	95.7	22.7	23.7	$s^2 > \bar{x}$ Aggregated

K. sphyrnae	*S. zygaena*	162	13	59	22	2.7	12.5	$s^2 > \bar{x}$ Aggregated
K sphyrnae	*S. lewini*	92	10	25	40	3.7	9.2	$s^2 > \bar{x}$ Aggregated

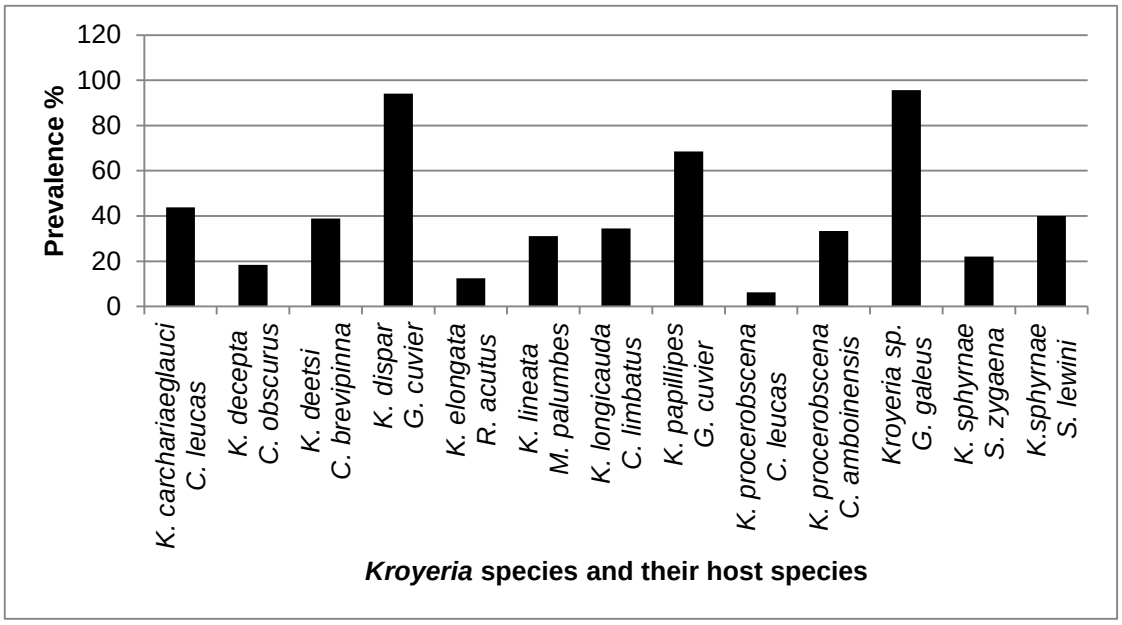

Figure 3.1 The prevalence (%) of *K. decepta* Deets, 1994; *K. deetsi* Dippenaar, Benz & Olivier, 2000; *K. dispar* Wilson, 1935; *K. elongata* Pillai, 1967; *K. lineata* van Beneden, 1853; *K. longicauda* Cressey,1970; *K. papillipes* Wilson, 1932; *K. procerobscena* Deets, 1994; *Kroyeria* sp.; *K. sphyrnae* Rangnekar, 1957 collected from 10 elasmobranch hosts off the coasts of South Africa.

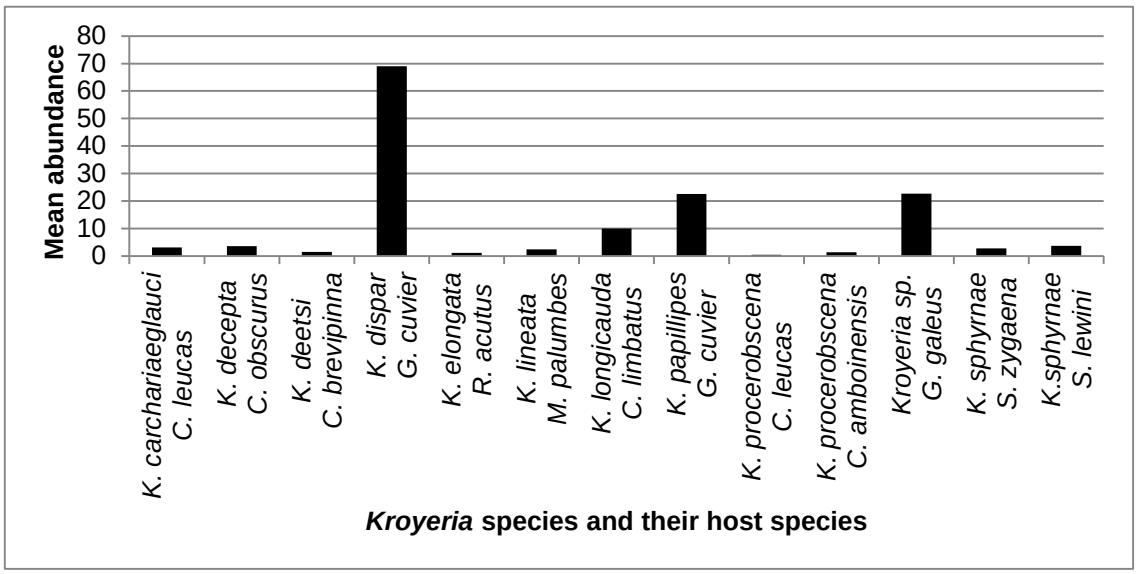

Figure 3.2 The mean abundance (individuals per examined host) of *K. decepta* Deets, 1994; *K. deetsi* Dippenaar, Benz & Olivier, 2000; *K. dispar* Wilson, 1935; *K. elongata* Pillai, 1967; *K. lineata* van Beneden, 1853; *K. longicauda* Cressey, 1970; *K. papillipes* Wilson, 1932; *K. procerobscena* Deets, 1994; *Kroyeria* sp.; *K. sphyrnae* Rangnekar, 1957 collected from 10 elasmobranch hosts off the coasts of South Africa.

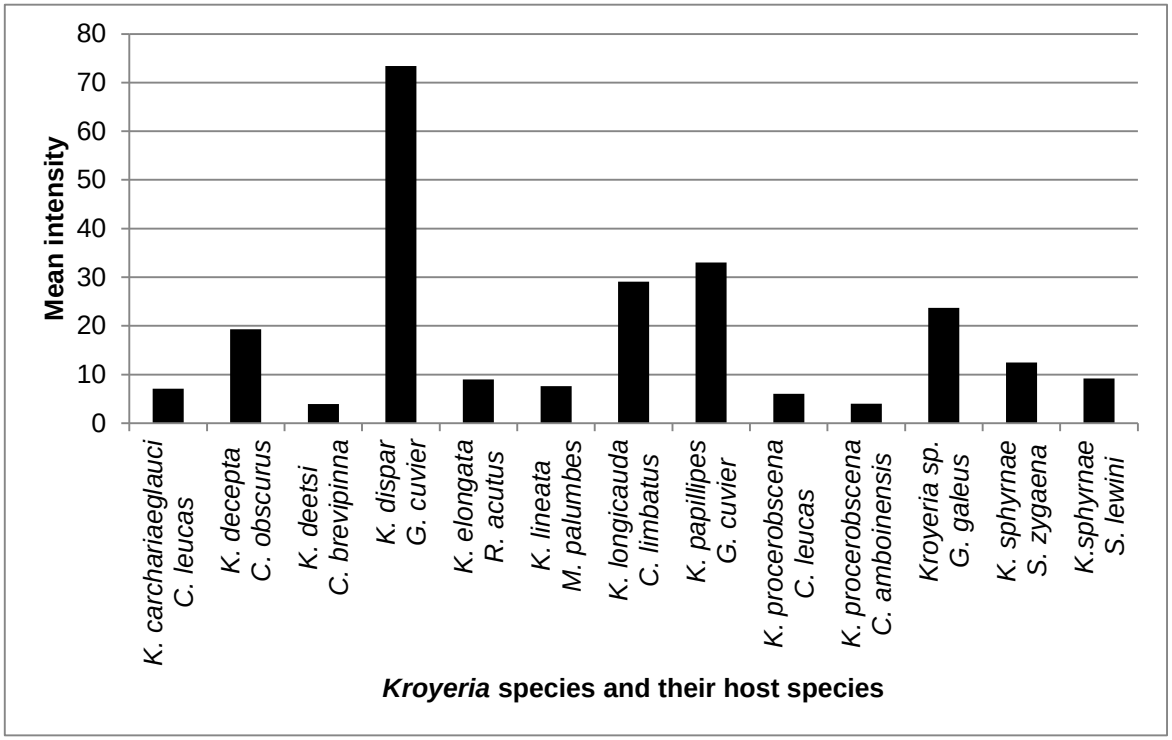

Figure 3.3 The mean intensity (individuals per infected host) of *K. decepta* Deets, 1994; *K. deetsi* Dippenaar, Benz & Olivier, 2000; *K. dispar* Wilson, 1935; *K. elongata* Pillai, 1967; *K. lineata* van Beneden, 1853; *K. longicauda* Cressey, 1970; *K. papillipes* Wilson, 1932; *K. procerobscena* Deets, 1994; *Kroyeria* sp.; *K. sphyrnae* Rangnekar, 1957 collected from 10 elasmobranch hosts off the coasts of South Africa.

3.5. Discussion

Of the known 21 nominal *Kroyeria* species, 11 have been collected of which nine have previously been reported from elasmobranchs off the coasts of South Africa. This is the first record of *K. lineata* being reported from the south coast of South Africa as well as a new host record, *Mustelus palumbes*. An unknown *Kroyeria* species was also collected from the gills of *Galeorhinus galeus*. *Kroyeria* species individuals that were previously reported from hosts that were examined in this study, but were not found include *K. brasiliense* from *G. galeus*, *K. echinata* from *S. zygaena*, *K. minuta* from *R. acutus*, *K. rhophemophaga* from *G. galeus, K. spatulata* from *C. limbatus, R. acutus,* and *C. leucas*.

3.5.1. Morphological comparison of *Kroyeria* sp. from *G. galeus* with other reported species

3.5.1.1. Comparison of *Kroyeria* sp. with other *Kroyeria* species reported from *G. galeus* (i.e. *K. brasiliense*, *K. lineata* and *K. rhophemophaga*)

There are three *Kroyeria* species that have been reported from the host species *G. galeus*, namely *K. brasiliense, K. lineata* and *K. rhophemophaga*. From the morphological description and drawings (Fig. 1 & 2) of the *Kroyeria* sp., it is evident that this *Kroyeria* sp. is not *K. lineata* as the endopods of *K. lineata* are devoid of endopodal denticulations (Deets 1994, see Fig. 92), which are however, present on the second endopodal segments of all the legs on the *Kroyeria* sp. (Fig. 2). Additionally, *Kroyeria* sp. is not *K. brasiliense* due to the fact that it has three abdominal segments (Fig. 1a) whereas *K. brasiliense* has only two (Thatcher & Júnior 2006). The last species reported from *G. galeus* is *K. rhophemophaga* which is similar to *K. branchiocetes*, *K. lineata*, *K. cresseyi* and *K. triakos* (Deets 1994).

3.5.1.2. Comparison of *Kroyeria* sp. with other most similar *Kroyeria* species (i.e. *K. rhophemophaga*, *K. branchiocetes*, *K. cresseyi* and *K. triakos*)

Kroyeria sp. individuals are distinguishable from *K. branchiocetes* which has endopodal denticulations on the second and third segments of endopods of all the legs (Deets 1994, see Fig. 72) as well as a distal membranous expansion and two proximal slender setae (Deets 1994, see Fig. 71E) on the fourth segment of the antenna, while the current species has endopodal denticulations only on the second segment of endopods of all the legs (Fig. 2) and possesses one slender seta and no membranous expansion on the fourth segment of the antenna (Fig. 1e). Furthermore, the sub-quadrangular cephalothorax of the *Kroyeria* sp. (Fig. 1a) is different from the orbicular head of *K. cresseyi* (Deets 1994, see Fig. 79A) and *K. cresseyi* has dorsal stylets with a bifid terminal end (Deets 1994, see Fig. 79B), while the dorsal stylets of the *Kroyeria* sp. terminates in a cuticular distolateral flange (Fig. 1b), similar to that observed in *K. branchiocetes* (Deets 1994, see Fig. 71B) and *K. elongata* (Deets 1994, see Fig. 87C). However, *K elongata* has a dorsal stylet reaching the anterior part of the third free thoracic somite (Deets 1994, see Fig. 87C) differing from that of the *Kroyeria* sp. which only reaches the middle of the second free thoracic somite (Fig. 1a). The fourth segment of the antenna bears three slender setae and forms a robust claw with a distal cuticular membranous expansion in *K.*

elongata (Deets 1994, see Fig. 87E) but has only a single slender seta and lacks a membranous expansion in the *Kroyeria* sp. (Fig. 1e) (as previously mentioned).

Specimens of *Kroyeria* sp. strongly resemble *K. rhophemophaga* and *K. triakos* in the shape of the cephalothorax, length of the dorsal stylets (to half of second free thoracic somite), three-segmented abdomen and shape of the genital complex (Table 3.3). Firstly, the three species differ in size, with *K. rhophemophaga* being the largest (8.1 mm), (Deets 1994, see Fig.100A, Table 3.3) followed by the *Kroyeria* sp. (5.2 mm) (Fig. 1a, Table 3.3) and lastly *K. triakos* (4.6 mm) (Deets 1994, see Fig.107A, Table 3.3). The dorsal stylets of the three species differ in the way they terminate, with the dorsal stylets of *K. rhophemophaga* having acute terminal ends (Deets 1994, see Fig. 100C), and those of *K. triakos* curving slightly inwardly with a narrow distolateral flange (Deets 1994, see Fig.107B, Table 3.3), while those of the *Kroyeria* sp. are curving slightly inwardly with a cuticular distolateral flange (Fig. 1b). Of the three species, *Kroyeria* sp. has a larger genital complex, occupying 69% of the entire body length, whereas it occupies 67% of the entire body length in *K. rhophemophaga* and 66% in *K. triakos* (Table 3.3). The caudal rami of the *Kroyeria* sp. have four pinnate setae and two slender naked setae (Fig. 1c, Table 3.3) instead of four pinnate setae (two elongate and two slender) and two stout semi-pinnate setae as in *K. rhophemophaga* (Deets 1994, see Fig. 100D) and *K. triakos* (Deets 1994, see Fig. 107C). The four segmented antennae of the *Kroyeria* sp. specimens have only one proximal slender seta (Fig. 1e, Table 3.3) instead of two as seen in *K. rhophemophaga* (Deets 1994, see Fig. 100G) and *K. triakos* (Deets 1994, see Fig. 107E). When considering the legs of the three species, they are mostly similar with the following differences: the third segment of the exopod of leg 1 of *K. rhophemophaga* has a lateral slender seta with a membrane along the lateral edge (Deets 1994, see Fig. 101B), *K. triakos* has a slender, lateral naked seta (Deets 1994, see Fig. 108A), while the *Kroyeria* sp. has a lateral slender, semi-pinnate seta with no visible membrane (Fig. 2a, Table 3.3). The third segment of the exopod of leg 2 has two slender lateral setae with membranes along the lateral edges in *K. rhophemophaga* (Deets 1994, Fig. 101C), a slender naked lateral seta in *K. triakos* (Deets 1994, see Fig. 108B), with only a lateral semi-pinnate seta with a lateral membrane along the edge is observed in *Kroyeria* sp. (Fig. 2b, Table 3.3). The third segment of the exopod of leg 3 distinguishes *K. triakos* (Deets 1994, see Fig. 108D),

from all its congeners. *Kroyeria triakos* has five elongate pinnate setae on the exopod of the third segment of leg 3 (Deets 1994, see Fig. 108D) whereas only four are noted in the *Kroyeria* sp. specimens (Fig. 2c) and in *K. rhophemophaga* (Deets 1994, see Fig. 101D). Furthermore, the third segment of the exopod of leg 3 of *K. rhophemophaga* is armed with a semi-pinnate seta and a short slender lateral seta (both with membranes along the lateral edges) as well as a short distolateral spine (Deets 1994, see Fig. 101D) while that of the *Kroyeria* sp. has a short semi-pinnate seta and two short lateral spines (Fig. 2c, Table 3.3). Finally, the third exopodal segment of leg 4 contains a semi-pinnate seta with a membrane along the lateral edge and two short lateral spines in *K. rhophemophaga* (Deets 1994, Fig. 101E), a semi-pinnate seta with a serrated membrane, a naked lateral seta and a short distolateral spine in *K. triakos* (Deets 1994, see Fig. 108F), in contrast to a lateral semi-pinnate seta with no visible membrane and a short distolateral spine in *Kroyeria* sp. (Fig. 2d, Table 3.3). Thus, the last segments of the exopods of legs 1–4 of *Kroyeria* sp. have different chaetotaxy from that of *K. rhophemophaga* and *K. triakos*. The number of setae and spines on the terminal segments of exopods 1–4 respectively in *K. rhophemophaga* is 6,7,7,7 (Deets 1994), 6,7,6,7 in *K. triakos* and 6,6,7,6 in the *Kroyeria* sp. Thus the most important distinguishing feature between *Kroyeria* sp. and *K. triakos* is the third segment of the exopod of leg 3 whereas the main distinguishing feature between *Kroyeria* sp. and *K. rhophemophaga* is the difference in the chaetotaxy of the legs.

Izawa (2008) regarded *K. sublineata* as a separate species from *K. lineata* based on the differences in the chaetotaxy of their legs. Other differences between *K. rhophemophaga*, *K. triakos* and the *Kroyeria* sp. can be seen in the number of endopodal denticulations on the second segment of the endopod of each leg (see Table 3.3). Thus, considering all the morphological differences between the known *Kroyeria* species, especially the most similar *K. rhophemophaga*, *K. triakos* and *Kroyeria* sp., it seems like *Kroyeria sp*. is a new species.

Table 3.3 Comparison of detailed morphological features in morphologically similar species: *Kroyeria rhophemophaga* Deets, 1994; *Kroyeria triakos* Fukui, 1965 and *Kroyeria* species.

Morphological	*K. rhophemophaga*	*K. triakos*	*Kroyeria*. sp.
Size of specimen	8.1 mm	4.6 mm	5.2 mm
Dorsal stylet	Extends posteriorly to about the middle of the second thoracic somite and curves slightly inwardly with an acute terminal end.	Extends to posterior margin of second thoracic somite and curves slightly inwardly with a narrow distolateral flange.	Extends posteriorly to terminate almost in line with the centre of the second thoracic somite, slightly curving inwardly with a cuticular distolateral flange.
Thoracic somites	3 free somites with non-overlapping terga.	3 free somites with slightly overlapping terga.	3 free somites with non-overlapping terga.
Genital complex	Cylindrical and forming about 67% of the entire body length.	Cylindrical and forming about 66% of the entire body length.	Cylindrical and forming about 69% of total body length.
Abdomen	Indistinctly three-segmented.	Indistinctly three-segmented.	Indistinctly three-segmented.
Caudal ramus	Lamelliform, longer than wide bearing the typical medial fringe of setules, two elongate pinnate setae, two shorter, stout semi-pinnate setae and two slender setae one laterally and the other medially.	Lamelliform, longer than wide bearing the typical medial fringe of setules, two elongate pinnate setae, two shorter, stout semi-pinnate setae and two slender pinnate setae distally, one laterally and the other medially.	Lamelliform, longer than wide, with typical medial fringe of setules, bearing six terminal setae as follows: two elongate pinnate, two shorter, stout pinnate setae and two slender naked setae, one laterally and the other medially.
Antennule	Indistinctly seven- or eight-segmented; Armature: 11, 5, 1, 3, 1, 1, 13+1 aesthete.	Indistinctly seven- or eight-segmented; Armature: 9, 1, 5, 3, 1, 1, 13+1 aesthete.	indistinctly seven- or eight-segmented; Armature 8, 5, 3, 1, 1, 1, 7+1 aesthete.

Antenna	Four-segmented, chelate and prehensile; fourth segment bearing one elongate, slender seta and one proximal slender seta.	Four-segmented, chelate and prehensile; fourth segment bearing one elongate, slender seta and one proximal slender seta.	Four-segmented, chelate and prehensile; fourth segment bearing only one proximal slender seta.
Leg 1	Third segment of exopod bearing four long pinnate setae, a long, slender, lateral seta with membrane along lateral edges and a short distolateral spine. Second segment of endopod with five to six endopodal denticulations.	Third segment of exopod bearing four long pinnate setae, a slender, lateral naked seta and a short distolateral spine. Second segment of endopod with seven endopodal denticulations.	Third segment of exopod bearing four long pinnate setae, a lateral semi-pinnate seta and a short distolateral spine. Second segment of endopod with seven endopodal denticulations.
Leg 2	Third segment of exopod bearing four long pinnate setae, two slender lateral setae with membranes along the lateral edges and a short distolateral spine. Second segment of endopod with five to seven endopodal denticulations.	Third segment of exopod bearing four long pinnate setae, a semi-pinnate seta, a slender naked lateral seta and a short distolateral spine. Second segment of endopod with six to eight endopodal denticulations.	Third segment of exopod bearing four long pinnate setae, a lateral semi-pinnate seta with a lateral membrane along edge and a short distolateral spine. Second segment of endopod with eight endopodal denticulations.
Leg 3	Third segment of the exopod bearing four long pinnate setae, a semi-pinnate seta and a lateral short slender setae (both with membranes along the lateral edges) and a short distolateral spine.	Third segment of the exopod bearing five long pinnate setae and a naked lateral seta. Second segment of endopod with seven to ten endopodal denticulations.	Third segment of exopod bearing four long pinnate setae, a short semi-pinnate seta and two short lateral spines. Second segment of endopod with seven endopodal denticulations.

	Second segment of endopod with three to eight endopodal denticulations.		
Leg 4	Third segment of the exopod bearing four long pinnate setae, a semi-pinnate seta with membrane along the lateral edge, and two short lateral spines. Second segment of endopod with nine endopodal denticulations.	Third segment of the exopod bearing four long pinnate setae, a semi-pinnate seta with a serrated membrane, a naked lateral seta and a short distolateral spine. Second segment of endopod devoid of endopodal denticulations.	Third segment of the exopod bearing four long pinnate setae, a lateral semi-pinnate seta and a short distolateral spine. Second segment of endopod with nine endopodal denticulations.

3.5.2. Host-parasite relationships

The prevalence for *K. dispar* (94.1%) on *G*. *cuvier* in this study differed from the 100% found previously (Dippenaar *et al*. 2009) while the mean intensity of 73 individuals per infected host was the same in both studies. Similarly, the prevalence for *K. papillipes* (68.6.1%) on *G*. *cuvier* in this study differed from the 78.6% found previously (Dippenaar *et al*. 2009) while the mean intensity of 33 individuals per host was the same in both studies. The difference in the prevalences of the two studies resulted from the different number of hosts examined during the two studies with 14 hosts examined previously (Dippenaar *et al*. 2009) whereas 51 hosts were examined in this study. However, the evidence strongly supports a mean infection of 73 and 33 individuals of *K. dispar* and *K. papillipes* per infected host, respectively. The higher mean intensity reported for *K. dispar* vs *K. papillipes* is still unexplainable since there is no inter-specific competition between the two *Kroyeria* species on *G. cuvier*, even though they occupy the same niche (Dippenaar *et al*. 2009).

According to Deets (1994), *K. sphyrnae* mostly prefers *S. zygaena* to *S*. *lewini* as a host. However, this study indicates that *K. sphyrnae* has a higher prevalence on *S. lewini* (40%) than *on S. zygaena* (22%), with mean intensities of 9 and 13 individuals per host on *S. lewini* and *S. zygaena* respectively. These findings corroborate those

of a previous study that *K. sphyrnae* had a higher prevalence on *S. lewini* (46.7%) than on *S. zygaena* (33%), with mean intensities of 18 and 5 individuals per host on *S. lewini* and *S. zygaena* respectively (Dippenaar *et al*. 2001). However, the decrease in prevalence and mean intensity of *K. sphyrnae* on both host species in this study compared to the previous study (Dippenaar *et al*. 2001) could be, as stated before, due to the fact that the number of hosts examined in this study is higher (Table 3.2).

It seems that *Kroyeria* species have in general low parasite loads (with the exception of *K. dispar* (Table 3.2.)) compared to other siphonostomatoid species, for instance as many as 74 individuals of *Nemesis lamna* have been reported per infected host with prevalences of 100% on *Carcharodon carcharias* (Linnaeus, 1758) (Dippenaar *et al*. 2008).

The pattern of dispersion on the host displayed by *Kroyeria* species is aggregated (Table 3.2) indicating that individuals have social interactions. This is similar to previous findings (Deets 1994; Dippenaar *et al*. 2009) for *Kroyeria* species. Additionally an aggregated pattern is most common among parasites (Rohde *et al*. 1995; Bush *et al*. 2001) and has also been observed in other siphonostomatoid copepods (Benz 1994; Deets 1994; Dippenaar *et al*. 2008; Dippenaar *et al*. 2009). An aggregated pattern of dispersion can be due to social interactions such as mutual defence, cooperative feeding, mating purposes or the availability of suitable resources (Bush *et al*. 2001). However, in *Kroyeria* species it is suspected to be due to purposes related to mating and the availability of suitable resources rather than cooperative feeding and mutual defence (Dippenaar *et al*. 2009).

3.6. Conclusion

Even though *Kroyeria* species are sometimes difficult to identify based on their morphological features, it is still possible if a combination of characteristics is considered. Due to all the morphological differences amongst the unknown *Kroyeria* species and the known *Kroyeria* species the *Kroyeria* sp. collected from *G. galeus* is considered to be a new species. Additionally, this is the first record for *K. lineata* found in South African waters on a new host, *M*. *palumbes*.

Kroyeria species differ in their prevalences, mean abundances and mean intensities on their elasmobranch hosts. However, in general, they display a very low parasite

load compared to other siphonostomatoid species. Additionally, species infecting the same host species display different parasite host relationships. All *Kroyeria* species display an aggregated or clustered dispersion pattern similar to most parasitic species. This is probably due to mating purposes or the availability of suitable resources. Furthermore, this study confirms previous suggestions that *Kroyeria* species are generally host specific, with only a few species found on multiple hosts.

CHAPTER 4

THE DISTINCTION AND PHYLOGENETIC RELATIONSHIPS AMONG *KROYERIA* SPECIES

4.1. Introduction

The difficulty and problems encountered when distinguishing *Kroyeria* species on the basis of morphological characteristics (see Chapter 3) have also been encountered in free-living copepods e.g. calanoid copepods (Bucklin *et al*. 2003; Thum 2004), cyclopoid copepods e.g. *Mesocyclops* Sars, 1914 (Wyngaard *et al*. 2010) and other symbiotic siphonostomatoid copepods e.g. genera and species in the family Caligidae ("sea lice") Burmeister, 1835 (Dojiri & Ho 2013) and *Nemesis* species (Hewitt 1969; Kabata 1979). Rajthilak *et al*. (2010) recommended the use of molecular techniques in the identification and classification of marine copepods. Thus it became necessary in this study to assess the possible use and efficiency of molecular techniques in an attempt to distinguish among the different species of *Kroyeria*.

A number of molecular techniques have been utilised in the past to distinguish small invertebrates. Among these are PCR based techniques such as allele-specific PCR amplification (Bucklin *et al*. 1998), competitive, multiplexed, species-specific PCR (Bucklin *et al*. 1999; Hill *et al*. 2001; Bucklin *et al*. 2003; Grabbert *et al*. 2010) and real-time PCR (McBeath *et al*. 2006; Pan *et al*. 2008). McBeath *et al*. (2006) distinguished two caligid copepods, *Lepeophtheirus salmonis* and *Caligus elongatus* larvae whereas Pan *et al*. (2008) distinguished decapod crustaceans i.e. *Liocarcinus depurator* (Linnaeus, 1758) larvae, from unsorted marine plankton. Both studies used species-specific primers and Taqman® -MGB probes.

The phylogenetic relationships of metazoans at different taxonomic levels have been reconstructed by using molecular data (Murphy *et al*. 2007). The use of molecular data in studying phylogenetic relationships implies that genetic markers should be employed successfully. However, very few mitochondrial and nuclear genetic markers have been used successfully to resolve phylogenetic relationships in the phylum Copepoda (Wyngaard *et al*. 2010). Reports of successful studies in certain copepod groups include those of species in the family Euchaetidae Philippi, 1843 (Calanoida) (Braga *et al*. 1999), species of *Calanus* Leach, 1816 (Calanoida) (Hill *et*

al. 2001), calanoid species in the genera *Clausocalanus* Giesbretcht, 1888, *Neocalanus* Sars, 1925 and *Pseudocalanus,* Boeck 1872 (Bucklin *et al*. 2003) and very few selected families in the Siphonostomatoida (Dippenaar 2009). The unsuccessful application of certain molecular markers in the study of copepods may be due to the fact that some copepods have faster evolving mitochondrial genes than other arthropods (Shao and Barker 2007). This makes mitochondrial genes markers of choice in studying phylogenetic relationships of copepods at species level (Folmer *et al*. 1994; Bucklin *et al*. 2003: Machida *et al*. 2004; Thum 2004; Minxiao *et al*. 2011).

The mitochondrial gene, Cytochrome Oxidase I (COI), has been successfully employed as a molecular marker for copepods mostly in the order Calanoida (Grabbert *et al*. 2010; Figueroa 2011; Minxiao *et al*. 2011) for instance, the estimation of the phylogenetic relationships of 34 calanoid species belonging to 10 genera representing the families Calanidae Dana, 1849 and Clausocalanidae Giesbretcht, 1893 (Bucklin *et al*. 2003). In the Siphonostomatoida, COI has been used as a marker to recognize different cryptic species (Dippenaar *et al*. 2010) and to distinguish different species in *Nemesis* (Mangena *et al*. in press).

The 18S rDNA gene has been used to resolve the phylogeny of copepods among the North American calanoid fresh water copepods of the genus *Diaptomus* Westwood, 1836 (Thum 2004). However, this gene is highly conserved, i.e. it has a slow evolutionary rate, and thus in most cases it cannot be used alone to determine interspecies phylogenetic relationships (Gonzalez & Schmickel 1986; Thum 2004; Hejazi *et al*. 2010). Therefore, in most studies, including those of copepods, the combined effect of both mitochondrial and nuclear genes as genetic markers is used to resolve phylogenetic relationships (Braga *et al*. 1999; Machida *et al*. 2004; Dippenaar 2009; Wyngaard *et al.* 2010).

Additionally, partial sequences of the mitochondrial gene 16S rDNA and the nuclear gene 28S rDNA were used to determine the phylogenetic relationships of copepods within the calanoid family, Euchaetidae (Braga *et al*. 1999). Similarly, the molecular phylogenetic relationships of six siphonostomatoid families, including the family Kroyeriidae, were estimated by using the combined sequences of parts of the mitochondrial genes, 16S rDNA and COI and the complete nuclear gene, 18S rDNA

(Dippenaar 2009). Additionally, the small subunit (SSU) rDNA sequences have been able to demonstrate host switching of the Monstrilloida (symbiotic Copepoda) from a vertebrate to an invertebrate host (Huys *et al*. 2007).

In this study, an attempt was made to estimate the phylogenetic relationships of some *Kroyeria* species by employing molecular data obtained from sequences of the mtDNA COI and the nuclear gene, 18S rDNA. The estimated phylogeny can then be compared with the existing phylogeny for *Kroyeria* species based on morphological data (Deets 1994). Additionally, real-time PCR (qPCR) was employed by utilizing universal crustacean primers and melt curve analysis as an attempt to distinguish among the different species of *Kroyeria*.

4.2. Aim and objectives

4.2.1. Aim: To estimate phylogenetic relationships among *Kroyeria* species and distinguish among them using molecular data.

4.2.2. Objectives:

- To estimate phylogenetic relationships among different *Kroyeria* species using a fragment of the COI and the complete 18S rDNA genes.
- To distinguish among different *Kroyeria* species using their sequence divergences.
- To try and distinguish among different *Kroyeria* species based on their different melt temperatures of a fragment of the COI gene.

4.3. Material & methods

Material and methods are as described in Chapter 2.

4.4. Results

4.4.1. DNA quantification

The measured concentrations of the extracted DNA were mostly below the ideal concentration of 50 ng/μl (Table 4.1). Additionally, the 260/280 ratio, which is an assessment for the purity of nucleic acids, of most samples was below the required range of 1.8–2.0, indicating contamination by the presence of residual components like phenol and proteins from the DNA extraction process or very low DNA concentration. Other samples had a 260/280 ratio above 2.0, indicating the presence

of RNA (Wilhelm *et al*. 2003). Only a few samples had the desired ratio between 1.8 and 2.0 (Table 4.1). All the samples had 260/230 ratios below the expected range of 2.0–2.2, confirming contamination by phenol residuals from the extraction process as well as guanine residuals which are common in column based kits.

Table 4.1 *Kroyeria* species DNA sample concentrations measured with the nanospectrophotometer indicating the concentration (ng/μl), UV absorption at 260 nm (A260), UV absorption at 280 nm (A280) as well as the 260/280 and 260/230 ratios. Samples marked with * were selected for whole genome amplification (WGA).

Species name	Sample ID	Conc. (ng/ul)	A260	A280	260/280	260/230
K. lineata	A1AF/13/1/5a2	110.6	2.212	1.733	1.28	0.6
K. lineata	A1AF/13/1/5b2	90.3	1.807	1.199	1.51	0.58
K. lineata	A1AF/13/1/5a	5	0.099	0.027	3.66	0.07
K. lineata	A1AF/13/1/5b	2.9	0.059	0.018	3.27	0.07
K. lineata	A1AF/21/1/3a2	270.8	5.416	4.012	1.35	0.62
K. lineata	A1AF/21/1/3b2	425.1	8.502	6.154	1.38	0.65
K. lineata	*A1AF/21/1/3a	1.9	0.037	0.009	3.97	0.06
K. lineata	A1AF/21/1/3b	2.3	0.046	0.016	2.89	0.19
K. lineata	*A2AF/3/5/2a	2.3	0.046	0.004	12.24	0.12
K. lineata	A2AF/3/5/2 2	67.1	1.342	0.917	1.46	0.58
K. lineata	A1AF/27/1/7c	62.7	1.253	0.824	1.52	0.57
K. lineata	*A1AF/27/1/7b2	8.1	0.162	0.094	1.73	0.18
K. lineata	A2AF/2/5/1a2	25.1	0.502	0.338	1.48	0.53
K. lineata	A2AF/2/5/1b2	22	0.441	0.299	1.47	0.57
K. lineata	A1AF/27/1/7a	33.1	0.661	0.43	1.54	0.35
K. lineata	*A1AF/27/1/7b	9.3	0.186	0.09	2.05	0.11
K. lineata	*A2AF/2/5/1a	15.4	0.308	0.161	1.91	0.16
K. lineata	*A2AF/2/5/1b	22.2	0.444	0.219	2.03	0.12

K. dispar	B21N/25a	79.6	1.592	0.768	2.07	1.52
K. dispar	B21N/25b	16	0.32	0.181	1.77	0.45
K. dispar	B4N/1b	22.4	0.448	0.225	1.99	0.15
K. dispar	B4N/1a	40.5	0.809	0.467	1.73	0.26
K. dispar	B14N/4a	54.8	1.097	0.723	1.52	0.78
K. dispar	B14N/4b	13.9	0.279	0.153	1.83	0.62
K. dispar	BAMA 06023a	17.8	0.357	0.206	1.73	0.17
K. dispar	B21N/25a2	130.4	2.609	1.821	1.43	0.66
K. dispar	B21N/25b2	34.8	0.697	0.481	1.45	0.64
K. dispar	B4N/1a2	62.5	1.25	0.835	1.5	0.45
K. dispar	B4N/1b2	28.5	0.57	0.368	1.55	0.35
K. dispar	B14N/4a2	22.9	0.458	0.287	1.6	0.31
K. dispar	B14N/4b2	31.9	0.638	0.411	1.55	0.47
K. dispar	*BAMA06023b	6.1	0.122	0.05	2.42	0.1
K. dispar	B23N/48a2	30.8	0.617	0.435	1.42	1.38
K. dispar	B23N/48b	32.9	0.657	0.447	1.47	1.01
K. dispar	B23N/48b2	67.1	1.342	0.902	1.49	0.78
K. dispar	B23N/52b2	57.9	1.157	0.808	1.43	0.93
K. dispar	B23N/52a	246.6	4.932	3.719	1.33	0.74
K. dispar	B23N/52a2	33.3	0.666	0.438	1.52	1.03
K. decepta	*C21N/36b2	5.1	0.103	0.057	1.82	0.1
K. decepta	C6N/8a2	21.6	0.433	0.29	1.49	0.3
K. decepta	*C6N/8b2	7.5	0.151	0.075	2.01	0.12
K. decepta	C6N/8La	80.5	1.61	0.96	1.68	0.79
K. decepta	C21N/16a	19.2	0.383	0.23	1.67	0.66
K. decepta	*C7N/1a	4.5	0.089	0.011	8.08	0.07

K. decepta	C7N/1b2	24	0.48	0.4	1.2	0.41
K. decepta	C7N/19b	11.1	0.222	0.147	1.51	0.25
K. decepta	*C9RSB/3a	4.7	0.094	0.034	2.75	0.13
K. decepta	*C9RSB/3b	2.7	0.054	0.026	2.1	0.16
K. decepta	C9RSB/3b2	38.9	0.778	0.533	1.46	0.61
K. decepta	C7N/1a2	107.1	2.143	1.438	1.49	0.62
K. decepta	C21N/36a	42.1	0.843	0.413	2.04	0.59
K. decepta	*C21N/36b	6.6	0.132	0.058	2.26	0.12
K. decepta	*C6N/8a	5.2	0.103	0.054	1.9	0.13
K. decepta	C6N/8b	21.7	0.434	0.308	1.41	0.4
K. decepta	C21N/36a2	36.5	0.73	0.469	1.56	0.38
K. decepta	C9RSB/3a2	20.7	0.414	0.256	1.62	0.56
K. decepta	C7N/19b2	75.9	1.518	1.013	1.5	0.6
K. papillipes	DBAL06a2	5.2	0.104	0.055	1.91	0.38
K. papillipes	*DBAL06b2	7	0.14	0.085	1.65	0.33
K. papillipes	D16N/7a	20.1	0.403	0.238	1.69	0.18
K. papillipes	D16N/7a2	67.4	1.348	0.913	1.48	0.62
K. papillipes	D16N/7b	33.9	0.678	0.432	1.57	0.36
K. papillipes	D16N/7b2	22.1	0.442	0.336	1.32	0.67
K. papillipes	D4N/1RGa	45.7	0.913	0.615	1.48	0.43
K. papillipes	D4N/1RGa2	16.2	0.323	0.205	1.58	0.52
K. papillipes	D4N/1RGb	25.4	0.508	0.32	1.59	0.33
K. papillipes	D4N/1RGb2	76.8	1.537	1.045	1.47	0.6
K. longicauda	E6N/2a2	34.8	0.696	0.435	1.6	0.31
K. longicauda	E6N/2b2	27.5	0.55	0.353	1.56	0.3
K. longicauda	*E6N/2a	4.5	0.09	0.04	2.23	0.11

K. longicauda	*E6N/2b	4	0.08	0.026	3.12	0.1
K. longicauda	*E6N/2LGa	6.7	0.135	0.061	2.22	0.12
K. longicauda	E6N/2LGa2	234.4	4.689	3.492	1.34	0.64
K. longicauda	*E6N/2LGb2	9.5	0.19	0.08	2.36	0.15
K. longicauda	E6N/2LGc2	46.3	0.926	0.632	1.47	0.61
K. longicauda	E6N/2LGd	18.6	0.372	0.206	1.81	0.13
K. longicauda	E6N/2LGd2	74.9	1.497	1.002	1.49	0.59
K. longicauda	E6N/2LGa	6.7	0.135	0.061	2.22	0.12
K. sphyrnae	*F12N/2a	0.1	0.003	-0	-1.59	0.02
K. sphyrnae	F12N/2a2	14.3	0.286	0.139	2.06	0.12
K. sphyrnae	F12N/2b	15.7	0.315	0.166	1.9	0.12
K. sphyrnae	F18N/12	21.3	0.427	0.281	1.52	0.49
K. sphyrnae	F18N/12 2	46.7	0.934	0.606	1.54	0.57
K. sphyrnae	F14N/1a	12.5	0.249	0.148	1.68	0.41
K. sphyrnae	F14N/1a2	22.4	0.448	0.287	1.56	0.51
K. sphyrnae	F14N/1b2	147.5	2.95	2.057	1.43	0.65
K. sphyrnae	F9RSB/4a	78.1	1.562	1.036	1.51	0.5
K. sphyrnae	F9RSB/4a	60.2	1.204	0.784	1.54	0.57
K. sphyrnae	F9RSB/4b2	157.1	3.143	2.338	1.34	0.73
K. sphyrnae	F12N/2a2	15.6	0.313	0.197	1.59	0.27
K. sphyrnae	*F12N/2b2	8.7	0.175	0.095	1.84	0.15
K. elongate	G15N/15c2	47.6	0.953	0.658	1.45	0.62
K. elongate	*G16N/15c	7.6	0.152	0.1	1.51	0.29
K. deetsi	I18N/14 2	18.6	0.371	0.239	1.55	0.53
K. deetsi	I21N/3	6.5	0.13	0.085	1.53	0.17
K. deetsi	I21N/3 2	132.6	2.653	1.806	1.47	0.62

K. deetsi	I18N/14	11.9	0.238	0.133	1.8	0.15
K. deetsi	I23N/16	225	4.501	3.279	1.37	0.52
K. carchariaglauci	J20N/16 2	84	1.68	1.13	1.49	0.61
K. carchariaglauci	*J23N/51	2.7	0.054	0.012	4.58	0.16
K. carchariaglauci	J23N/51 2	37.7	0.754	0.502	1.5	0.57
K. procerobscena	6N/3	16.9	0.337	0.214	1.58	0.15
K. procerobscena	6N/3 2	13.9	0.278	0.17	1.64	0.23
Kroyeria sp.	22GNB/30a	56.2	1.124	0.836	1.34	0.29
Kroyeria sp.	22GNB/30b	23.7	0.474	0.255	1.85	0.21
Kroyeria sp.	*22GNB/30a2	9.2	0.185	0.091	2.03	0.14
Kroyeria sp.	22GNB/30b2	37.1	0.742	0.49	1.52	0.39

4.4.2. Whole genome amplification (WGA)

Due to the low DNA concentrations of most samples (Table 4.1), 24 DNA samples (A1AF/27/1/7b, A1AF/27/1/7b2, A2AF/2/5/1a, A2AF/2/5/1b, C6N/8a, C6N/8b2, BAMA 06023b, E6N/2a, E6N/2b, C21N/36b, C21N/36b2, 22GNB/30a2, F12N/2a, F12N/2b2, A/1AF21/1/3a, G16N/15c, J23N/51, DBAL 06b2, C7N/1a, C9RSB/3a, C9RSB/3b, E6N/2LGa, E6N/2LGb2 and A2AF/3/5/2a) with DNA concentrations of < 10 ng/*u*l were selected to amplify the whole genome in order to increase the concentration. The concentration values of these samples seemed to have increased indicative of successful amplification of the whole genome (Table 4.2). However, according to the manufacturers, the concentration values obtained using a nanospectrophotometer after using the kit are not accurate. Since very high concentrations are known to inhibit normal PCR reactions, it was suggested that the concentrations should be reduced by making serial dilutions (1:5, 1:10, 1:100, 1:1000 and 1:10000) of the DNA samples before attempting any PCR reactions (C. Wairuri, pers. comm.). However when the whole genome amplified DNA and the serial dilutions of each sample were electrophorised, only those samples that were not diluted produced very faint bands (Fig. 4.1). All the samples (including the serial dilutions) were used in the attempted amplification of the selected gene regions via

PCR following the methods described in Chapter 2. None of these resulted in successful amplifications.

Table 4.2 DNA sample concentrations of 24 selected *Kroyeria* species samples measured with the nanospectrophotometer before and after they were amplified using whole genome amplification REPLI-g® mini kit (QIAGEN), indicating the concentration (ng/μl) as well as the 260/280 and 260/230 ratios.

Species name	Sample ID	Conc. (ng/μl) before	260/280	260/230	Conc. (ng/μl) After	260/280	260/230
K. lineata	A1AF/27/1/7b	9.3	2.05	0.11	1263.8	1.83	2.39
K. lineata	A1AF/27/1/7b2	8.1	1.73	0.18	386.5	1.01	1.11
K. lineata	A2AF/2/5/1a	5	3.66	0.07	463.7	1.95	2.41
K. lineata	A2AF/2/5/1b	2.9	3.27	0.07	391.5	1.99	2.68
K. decepta	C6N/8a	5.2	1.9	0.13	398.4	1.98	2.6
K. decepta	C6N/8b2	7.5	2.01	0.12	393.8	1.86	2.56
K. dispar	BAMA06023b	6.1	2.42	0.1	480.9	1.88	2.43
K. longicauda	E6N/2a	4.5	2.23	0.11	149.9	189.35	16.36
K. longicauda	E6N/2b	4	3.12	0.1	404.5	0.85	0.63
K. decepta	C21N/36b	6.6	2.26	0.12	375.9	1.73	2.36
K. decepta	C21N/36b2	5.1	1.82	0.1	373.6	1.83	2.5
Kroyeria sp.	22GNB/30a2	9.2	2.03	0.14	334	0.85	1.09
K. sphyrnae	F12N/2a	0.1	-1.59	0.02	351.4	1.27	1.24
K. sphyrnae	F12N/2b2	8.7	1.84	0.15	446.8	2.03	2.62
K. lineata	A/1AF21/1/3a	1.9	3.97	0.06	351.2	0.71	0.68
K. elongata	G16N/15c	7.6	1.51	0.29	290.9	1.94	2.18
K. carchariaglauci	J23N/51	2.7	4.58	0.16	370.2	1.98	2.19
K. papillipes	DBAL06b2	7	1.65	0.33	280.7	2	2.2
K. decepta	C7N/1a	4.5	8.08	0.07	328.7	2.03	2.21
K. decepta	C9RSB/3a	4.7	2.75	0.13	330.6	1.84	2.08

K. decepta	C9RSB/3b	2.7	2.1	0.16	262.6	1.81	2.09
K. longicauda	E6N/2LGa	6.7	2.22	0.12	224.8	1.88	2.03
K. longicauda	E6N/2LGb2	9.5	2.36	0.15	298.6	1.99	2.05
K. lineata	A2AF/3/5/2a	2.3	12.24	0.12	134	2.28	2.47

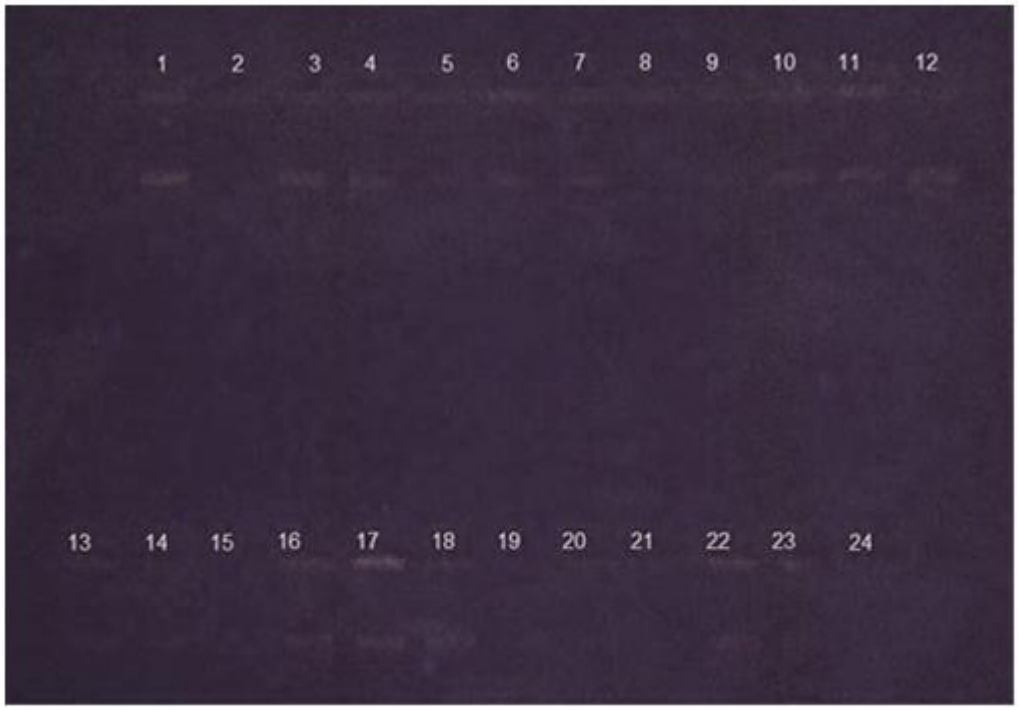

Figure 4.1 Gel electrophoresis (1.5% agarose) of the whole genome amplified PCR products using the REPLI-g® mini kit (QIAGEN) of the 24 undiluted samples (1 = A 1AF/27/1/7b, 2 = A1AF/27/1/7b2, 3 = A2AF/2/5/1a, 4 = A2AF/2/5/1b, 5 = C6N/8a, 6 = C6N/8b2, 7 = BAMA06023b, 8 = E6N/2a, 9 = E6N/2b, 10 = C21N/36b, 11 = C21N/36b2, 12 = 22GNB/30a2, 13 = F12N/2a, 14 = F12N/2b2, 15 = A/1AF21/1/3a, 16 = G16N/15c, 17 = J23N/51, 18 = DBAL06b2, 19 = C7N/1a, 20 = C9RSB/3a, 21 = C9RSB/3b, 22 = E6N/2LGa, 23 = E6N/2LGb2 and 24 = A2AF/3/5/2a (see Table 4.2)).

4.4.3. Gradient annealing temperature determination for COI

From the annealing temperatures (T_A) that were tested (45–55°C), the best T_A for COI universal primers HCO 1490 and LCO 2198 during the PCR gradient reaction was 45.7°C. Amplification was the highest at this T_A during the exponential phase of the amplification process (Fig. 4.2). Therefore, the initial T_A used in the COI amplification reactions using HCO 1490 and LCO 2198 was 45.7°C.

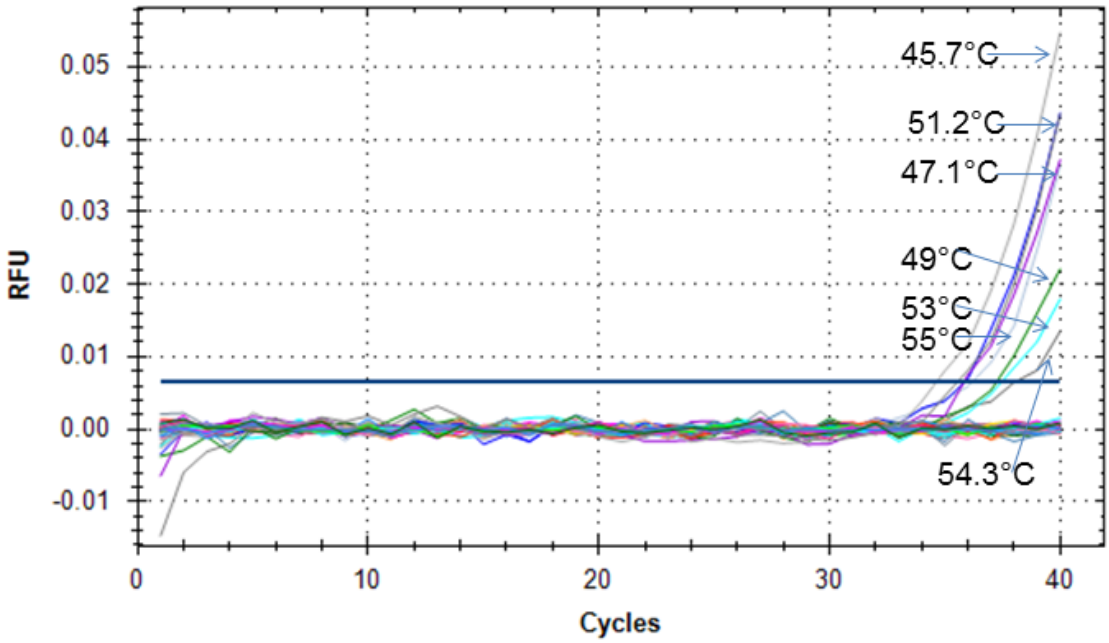

Figure 4.2 The amplification graph of the COI gene fragment of *Nemesis lamna* Risso, 1826, amplified with universal primers HCO 1490 and LCO 2198 using a gradient of annealing temperatures varying from 45 to 55°C.

4.4.4. PCR and sequencing

4.4.4.1. COI

The complete COI data set included 17 newly generated sequences, five sequences downloaded from GenBank (*K. decepta*, *K. dispar*, *K. longicauda, K. papillipes*, and *K. sphyrnae*) and two newly generated *Kroeyerina elongata* sequences forming the outgroup. The sequences were 674 bp long (with the exception of *K. deetsi* and *K. procerobscena* that were 500 bp long), with 373 characters being constant, 60 variable characters being parsimony-uninformative and 241 characters being parsimony-informative. In addition, there were 176

synonymous changes and 79 nonsynonymous changes.

The sequences for *K*. *deetsi* and *K*. *procerobscena* were excluded from the data set as they poorly aligned with the other sequences and were of poor quality in comparison with the sequences of the other *Kroyeria* species. After the data set was trimmed, these sequences were only 309 bp long, with 193 characters being constant, 15 variable characters being parsimony-uninformative and 101 characters being parsimony-informative.

4.4.4.2. 18S rDNA

The data set of the 18S rDNA gene consisted of four newly generated sequences, three sequences from *K. dispar* (B14N4a, B14N4b and B21N25b), one from *K. decepta* (C6N8La) as well as five sequences downloaded from GenBank (*K. dispar*, *K. longicauda, K. papillipes*, *K. sphyrnae* and *Kroyeria* sp.). The sequences were 1668 bp long, with 1619 characters being constant, 22 variable characters being parsimony-uninformative and 27 characters being parsimony-informative.

4.4.5. Phylogenetic analyses

4.4.5.1. COI

The NJ tree for COI (Fig. 4.3), which is based on pair-wise sequence divergence, reveals there are two main monophyletic groups, with the first group consisting of two sister groupings. The first sister grouping consists of three GenBank species (*K*. *sphyrnae*, *K*. *longicauda* and *K*. *decepta*) and *K*. *papillipes* individuals. The second sister grouping is composed of only *K*. *dispar* individuals. The second monophyletic group is comprised of *K*. *lineata*, *K*. *sphyrnae* and the new *Kroyeria* species. These two monophyletic groupings are firmly supported by high bootstrap values (100%).

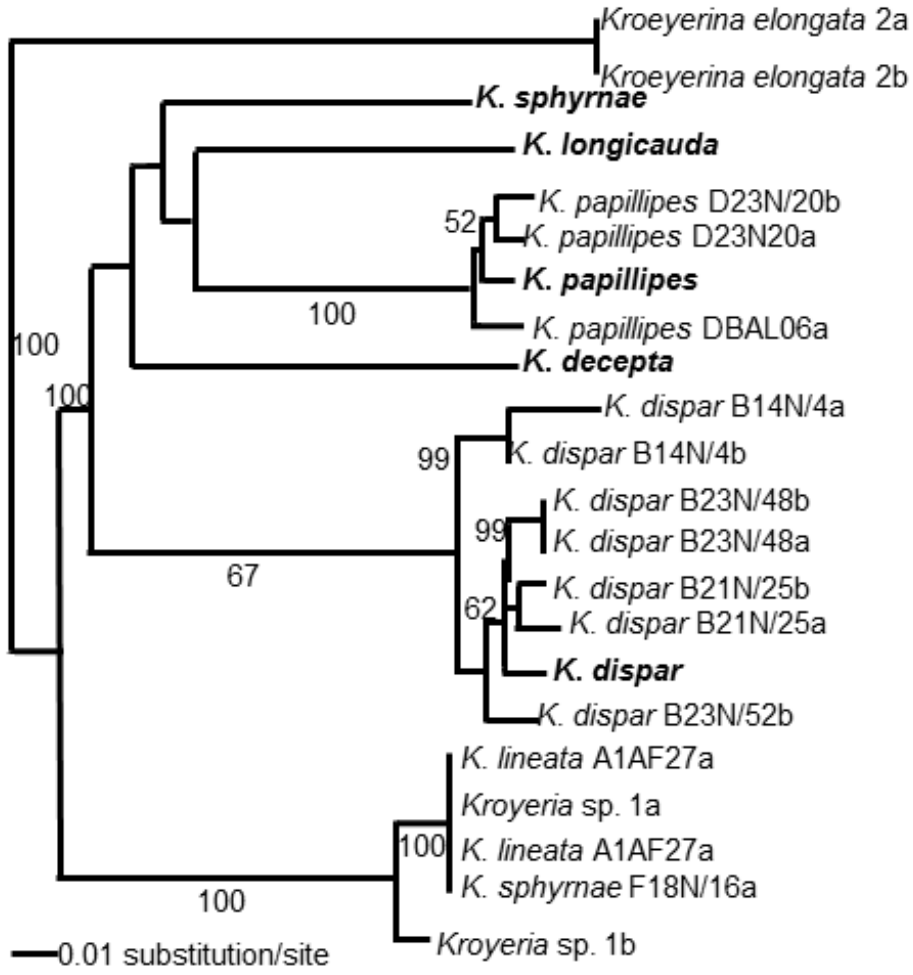

Figure 4.3 Neighbor-joining (NJ) tree of cytochrome oxidase I (COI) sequences, constructed using the general time reversible (GTR) model of evolution, displaying the phylogenetic relationships among seven *Kroyeria* species (species downloaded from GenBank, *K. decepta*, accession no. FJ447365.1; *K. dispar*, accession no. FJ447361.1; *K. longicauda*, accession no. FJ447364.1; *K. papillipes*, accession no. FJ447362.1 and *K. sphyrnae*, accession no. FJ447363.1 indicated in bold) with *Kroeyerina elongata* forming the outgroup and bootstrap values (%) indicated on the branches.

A parsimony branch and bound search yielded 44 most parsimonious trees with a tree length (TL) of 255 steps, consistency index (CI) of 0.659, retention index (RI) of 0.858, re-scaled consistency index (RC) of 0.565 and a homoplasy index (HI) of 0.341. As in NJ topology, the 50% majority rule tree of the 44 most parsimonious trees also consists of two monophyletic groups (Fig. 4.4), with *K*. *dispar* in the one and all the other species in the other. As in NJ topology, the two monophyletic groupings are firmly supported with high bootstrap values (100%).

For maximum likelihood (ML) analysis of the COI sequences, the general time reversible model (GTR) plus estimates of gamma distribution shape parameter (G = 0.500) and assumed proportions of invariable sites (I = 0.406) rate heterogeneity (Rodriguez *et al*. 1990) fitted the data best, with the following nucleotide base frequencies: A = 25%, C = 11%, G = 22% and T = 42%; transition rates were (A-G) 15.300 and (C-T) 9.493, transversion rates were (A-C) 0.974, (A-T) 2.597, (C-G) 1.494 e-10 and (G-T) 1.000. Several polyphyletic groupings were estimated and thus the ML tree (-In L = 1472.214) (Fig. 4.5) provides little resolutionof relationships among different *Kroyeria* species.

The mitochondrial COI sequence divergence ranges from 16.2 to 22.4% between *Kroyeria* species and the outgroup species, *Kroeyerina elongata*. The sequence divergence between *K. dispar* and *K. papillipes* found on *G. cuvier* ranges from 13.7 to 16.1%. *Kroyeria dispar* differs from *K*. *decepta* by 14.9–16.2%, from *K*. *sphyrnae* by 12.6–14.5%, from *K*. *longicauda* by 14.5–16.8%, from *K*. *lineata* by 14.6-17.2% and from *Kroyeria* species by 14.0–17.2%. Additionally, *K*. *sphyrnae* sequence from GenBank differs from the newly generated *K*. *sphyrnae* sequence by 14.0% whereas the new *Kroyeria* sp. from *G. galeus* has a sequence divergence similar to that of *K. lineata* or varies from it by 1.2%. With the exception of *K*. *sphyrnae*, the intra-specific variation among *Kroyeria* species individuals ranges from 0 to 3.9%.

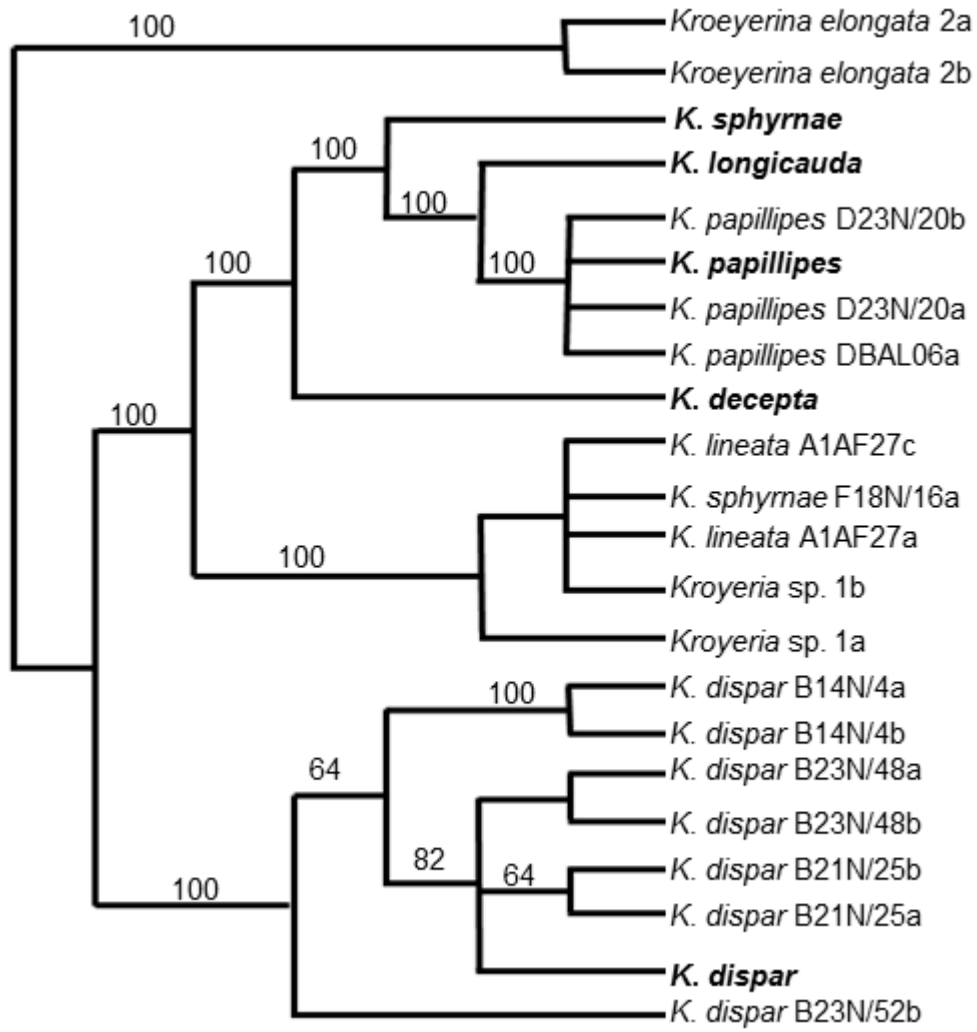

Figure 4.4 50% majority rule consensus tree (MP) (TL = 255, CI = 0.659, RI = 0.858, RC = 0.565, HI = 0.341) with bootstrap (%) values displaying phylogenetic relationships among seven *Kroyeria* species (species downloaded from GenBank, *K. decepta*, accession no. FJ447365.1; *K. dispar*, accession no. FJ447361.1; *K. longicauda*, accession no. FJ447364.1; *K. papillipes*, accession no. FJ447362.1 and *K. sphyrnae*, accession no. FJ447363.1, indicated in bold) with *Kroeyerina elongata* forming the outgroup.

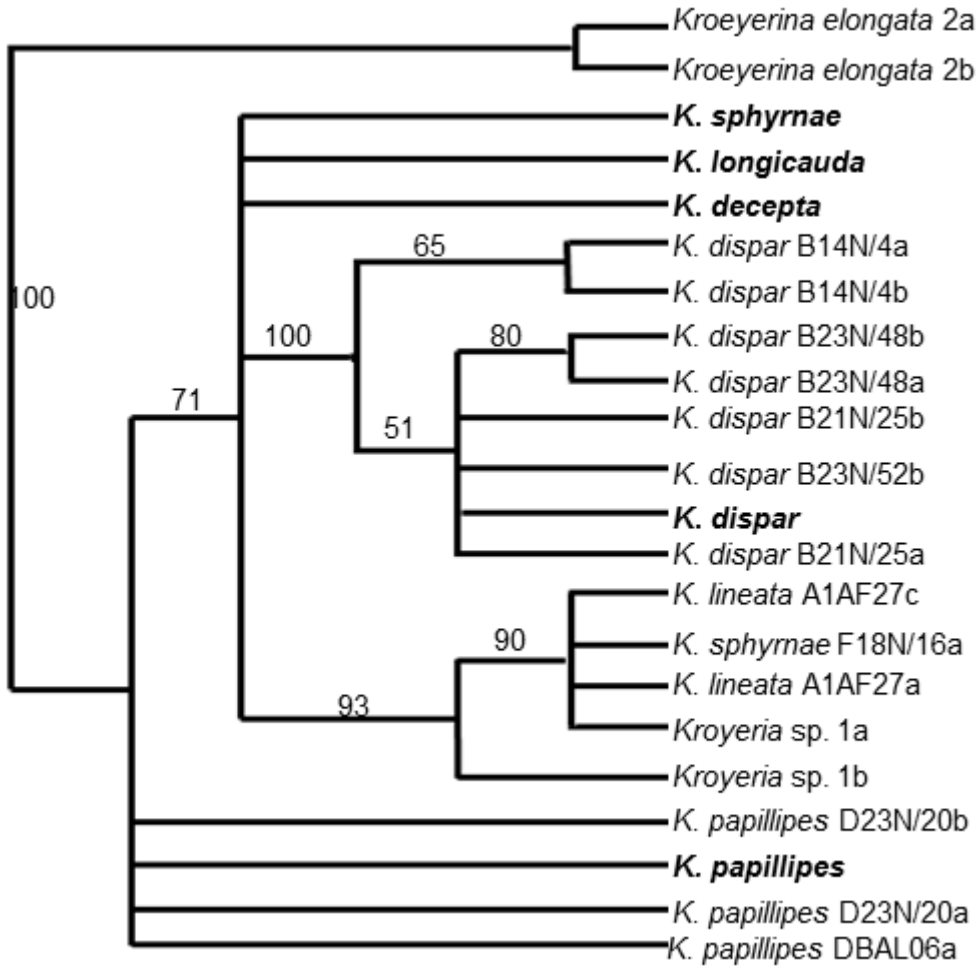

Figure 4.5 Maximum likelihood (ML) tree (-In L = 1472.214) with bootstrap (%) values displaying phylogenetic relationships among seven *Kroyeria* species (species downloaded from GenBank, *K. decepta*, accession no. FJ447365.1; *K. dispar*, accession no. FJ447361.1; *K. longicauda*, accession no. FJ447364.1; *K. papillipes*, accession no. FJ447362.1 and *K. sphyrnae*, accession no. FJ447363.1, indicated in bold) with *Kroeyerina elongata* forming the outgroup.

Table 4.3. Comparison of uncorrected pairwise COI sequence divergence among individuals of *K. decepta* (*K. dec*), *K. dispar* (B14N4a, B14N4b, B21N25a, B21N/25b, B23N/48a, B23N/48b, B23N/52b and *K. dis*), *K. longicauda* (*K. lon*), *K. lineata* (A1AF27a and A1AF27c), *K. papillipes* (DBAL06a, D23N/20a, DBAL20b and *K. pap*), *K. sphyrnae* (F18N/16a and *K. sph*) and *Kroyeria* sp. from *Galeorhinus galeus* (sp.1a and sp.1b) with *Kroeyerina elongata* (2G and 3G) forming the outgroup species.

	1	2	3	4	5	6	7	8	9	10	11	12	13	14	15	16	17	18	19	20	21	22
1 2G																						
2 3G	0.000																					
3 *K . sph*	0.203	0.203																				
4 *K . lon*	0.192	0.192	0.102																			
5 *K . dec*	0.197	0.197	0.124	0.120																		
6 D23N/20b	0.168	0.168	0.121	0.100	0.130																	
7 *K . pap*	0.168	0.168	0.121	0.103	0.127	0.007																
8 D23N/20a	0.162	0.162	0.127	0.105	0.136	0.005	0.012															
9 DBAL06a	0.176	0.176	0.126	0.105	0.130	0.009	0.012	0.014														
10 B14N/4a	0.224	0.224	0.145	0.168	0.162	0.158	0.156	0.161	0.155													
11 B14N/4b	0.202	0.202	0.132	0.154	0.149	0.151	0.149	0.155	0.148	0.014												
12B23N/48b	0.205	0.205	0.135	0.150	0.155	0.155	0.152	0.152	0.151	0.034	0.019											
13 B48N/48a	0.205	0.205	0.135	0.150	0.155	0.155	0.152	0.152	0.151	0.034	0.019	0.000										
14 B21N/25b	0.205	0.205	0.135	0.145	0.149	0.149	0.146	0.146	0.145	0.039	0.024	0.009	0.009									
15 B23N/52b	0.198	0.198	0.137	0.148	0.155	0.140	0.137	0.137	0.137	0.036	0.021	0.017	0.017	0.017								
16 *K . dis*	0.205	0.205	0.141	0.154	0.159	0.152	0.153	0.149	0.149	0.037	0.021	0.012	0.012	0.012	0.014							
17 B21N/25a	0.205	0.205	0.129	0.145	0.161	0.152	0.149	0.149	0.152	0.039	0.024	0.014	0.014	0.009	0.017	0.012						
18 A1AF27c	0.177	0.177	0.140	0.133	0.159	0.159	0.165	0.153	0.162	0.172	0.152	0.152	0.152	0.155	0.146	0.146	0.152					
19 F18N/16a	0.177	0.177	0.140	0.133	0.159	0.159	0.165	0.153	0.162	0.172	0.152	0.152	0.152	0.155	0.146	0.146	0.152	0.000				
20 A1AF27a	0.177	0.177	0.140	0.133	0.159	0.159	0.165	0.153	0.162	0.172	0.152	0.152	0.152	0.155	0.146	0.146	0.152	0.000	0.000			
21 sp. 1a	0.184	0.184	0.135	0.133	0.153	0.153	0.159	0.153	0.156	0.160	0.140	0.146	0.146	0.149	0.146	0.141	0.146	0.012	0.012	0.012		
22 sp. 1b	0.177	0.177	0.140	0.133	0.159	0.159	0.165	0.153	0.162	0.172	0.152	0.152	0.152	0.155	0.146	0.146	0.152	0.000	0.000	0.000	0.012	

4.4.5.2. 18S rDNA

Partition homogeneity test (ILD) yielded a non-significant p-value, which indicated that the different 18S sequences were homogenous and thus can be midpoint rooted.

The nine complete 18S rDNA sequences of six different *Kroyeria* species (i.e. *K. dispar*, *K. papillipes*, *K. decepta*, *K. longicauda*, *K. sphyrnae* and *Kroyeria* sp. from *Negaprion acutidens* (Rüppell, 1837)) were analysed using NJ, MP and ML and midpoint rooted (MPR) (Farris 1972). Midpoint rooting is a rooting method that is independent of the outgroup as it places the root on the midpoint between the two most divergent ingroup taxa (calculating the sum of the branch lengths between them) on a tree (Hess & De Moraes Russo 2007). The NJ tree for 18S rDNA (Fig. 4.6), which is based on pair-wise sequence divergence contained two sister groupings, the first grouping is formed by a polytomy consisting of four *K. dispar*

individuals with *Kroyeria* sp. from *N. acutidens* basal and being their closest relative, whereas the second grouping is formed by *K. papillipes*, *K. sphyrnae*, *K. longicauda* and *K. decepta*. *Kroyeria papillipes* and *K. sphyrnae* are sister taxa whereas *K. decepta and K. longicauda* are also sister taxa and form a sister group to *K. papillipes* and *K. sphyrnae*.

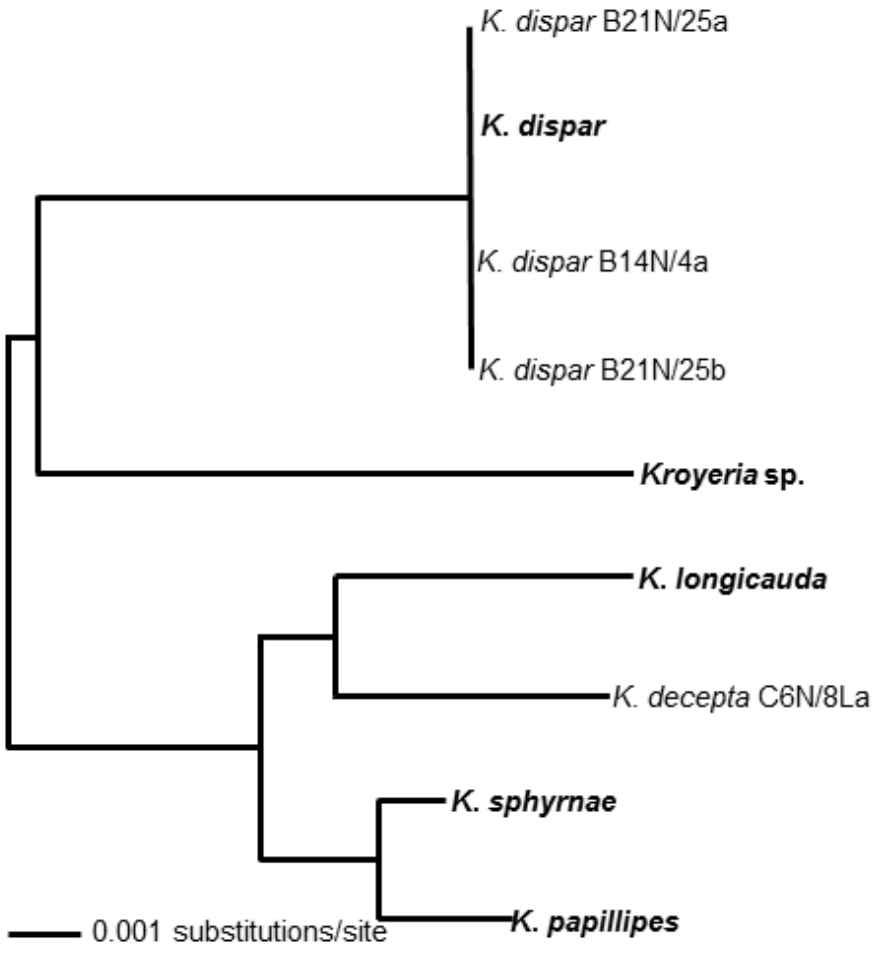

Figure 4.6. Midpoint rooted neighbor-joining (NJ) tree, constructed using the general time reversible (GTR) model of evolution, displaying the phylogenetic relationships among *K. dispar*, *Kroyeria* sp. (from *N. acutidens*), *K. decepta*, *K. longicauda*, *K. sphyrnae* and *K. papillipes* (species downloaded from GenBank, *K. decepta*, accession no. FJ447365.1; *K. dispar*, accession no. FJ447361.1; *K. longicauda*, accession no. FJ447364.1; *K. papillipes*, accession no. FJ447362.1 and *K. sphyrnae*, accession no. FJ447363.1; *Kroyeria* sp., accession no. DQ538499, indicated in bold letters).

A parsimony exhaustive search yielded a single parsimonious tree with a tree length (TL) of 59 steps, consistency index (CI) of 0.881, retention index (RI) of 0.895, re-scaled consistency index (RC) of 0.787 and a homoplasy index (HI) of 0.122 (Fig.

4.7). As in the NJ tree (Fig 4.6), there are two groupings but with *K*. *dispar* samples forming an unresolved polytomy (Fig. 4.7).

For maximum likelihood (ML) of 18S rDNA sequences, the general time reversible model (GTR) plus estimates of gamma distribution shape parameter (G = 1.429) and assumed proportions of invariable sites (I = 0.916) rate heterogeneity (Rodriguez *et al*. 1990) fitted the data best, with the following nucleotide base frequencies: A = 25%, C = 21%, G = 27% and T = 27%; transition rates were (A-G) 6.494 and (C-T) 6.940, transversion rates were (A-C) 3.247, (A-T) 1.126, (C-G) 0.670 and (G-T) 1.000. Maximum likelihood tree (-In L = 3560.874) (Fig. 4.7) had the same topology as that of the MP tree (Fig. 4.7).

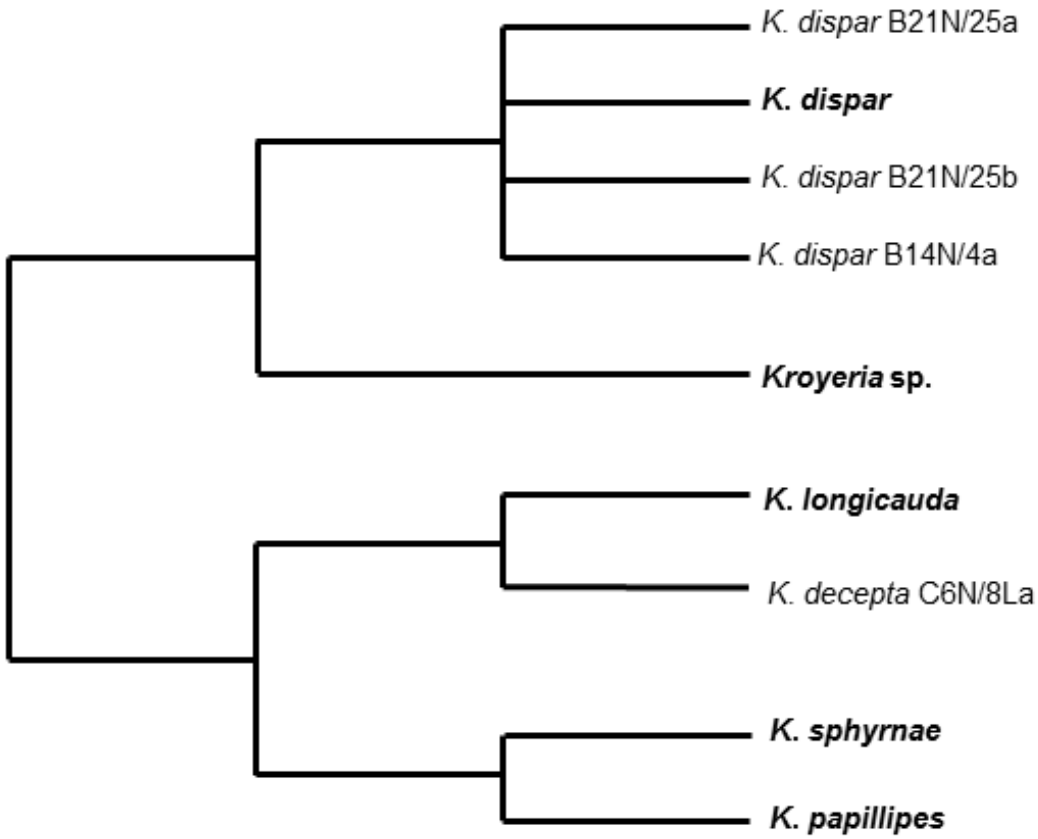

Figure 4.7. Midpoint rooted parsimony (MP) (TL = 59, CI = 0.881, RI = 0.895, RC = 0.787, HI = 0.122) and maximum likelihood (ML) (-In L = 3560.874) trees displaying 18S relationships among *K. dispar*, *Kroyeria* sp. (from *Negaprion acutidens)*, *K. decepta*, *K. longicauda*, *K. sphyrnae* and *K. papillipes* (species downloaded from GenBank, *K. decepta*, accession no. FJ447365.1; *K. dispar*, accession no. FJ447361.1; *K. longicauda*, accession no. FJ447364.1; *K. papillipes*, accession no. FJ447362.1 and *K. sphyrnae*, accession no. FJ447363.1; *Kroyeria* sp. from *N. acutidens*, accession no. DQ538499, indicated in bold letters).

The nuclear sequence divergence ranges from 0.0 to 2.0% (Table 4.4). *Kroyeria dispar* has an intra-specific variation of 0.0% and an inter-specific variation of 1.0% with *K. decepta*, *K. longicauda* and *K. papillipes,* but has an inter-specific variation of 2.0% with *K. longicauda* and the *Kroyeria* sp. from *N. acutidens*.

Table 4.4. Comparison of uncorrected pairwise 18S rDNA sequence divergence among individuals of *K. decepta* (C6N/8La), *K. dispar* (B14N/4a, B21N25a, B21N/25b and *K. dis*), *K. longicauda* (*K. lon*), *K. papillipes* (*K. pap*), *K. sphyrnae* (*K. sph*) and *Kroyeria* sp. (*Kroyeria*) (from *Negaprion acutidens*).

	1	2	3	4	5	6	7	8	9
1 B21N/25a	-								
2 *K. lon*	0.020	-							
3 *K. dis*	0.000	0.020	-						
4 *K. sph*	0.010	0.010	0.010	-					
5 *Kroyeria*	0.020	0.020	0.020	0.020	-				
6 B14N/4a	0.000	0.020	0.000	0.010	0.020	-			
7 *K. pap*	0.010	0.010	0.010	0.000	0.020	0.010	-		
8 C6N/8La	0.010	0.010	0.010	0.010	0.020	0.000	0.010	-	
9 B21N/25b	0.000	0.020	0.000	0.010	0.020	0.000	0.010	0.010	-

4.4.6. Haplotype analyses

4.4.6.1. COI

In the construction of the COI haplotype network, some of the sequences downloaded from GenBank were excluded because they included nucleotide ambiquities which could not be recognized by the programs used. The estimated median joining network (Templeton *et al*. 1995) resulted in14 haplotypes (H1–H14) (Fig. 4.8). Only one (H1) of the 14 haplotypes is shared while the remaining 13 (H2-H14) are rare and represented by single individuals. Haplotype H1 is represented by four individuals representing three species, namely one *K. sphyrnae* individual, two *K. lineata* individuals and one *Kroyeria* sp. individual collected from *G. galeus*. Haplotypes H2, H4, H5, H11, H12, H13 and H14 are represented by single *K. dispar* individuals; H3 is represented by a single individual of the *Kroyeria* sp. while H6, H7, H8 and H9 are represented by single individuals of *K. papillipes* and H10 is

represented by a single *K*. *decepta* individual. There are many haplotypes that are not sampled which are represented by the missing variables (mv) (Fig. 4.8). There are 47 mutational steps between mv17 and mv21, 48 mutational steps between H4 and mv9 (Fig. 4.8), thus dividing the network into three distinct groupings, similar to what is observed in NJ and MP (Fig. 4.3, Fig. 4.4).

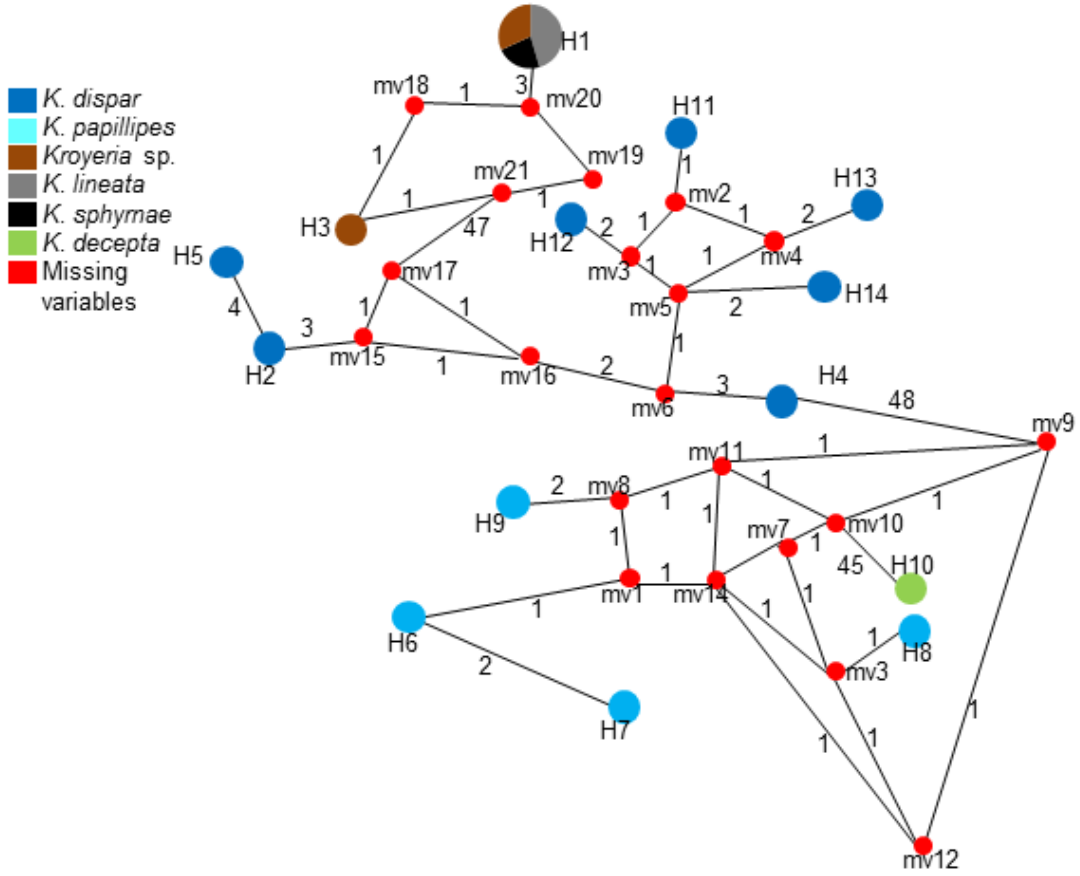

Figure 4.8. Haplotype network of COI sequences of different *Kroyeria* species, with the numbered red nodes representing missing variables, the terminal circles representing the different haplotypes with their diameters and pie wedges proportional to the number of individuals sharing that particular haplotype. The lines and numbers between the haplotypes and the nodes represent mutational steps.

4.4.6.2. 18S rDNA

In the construction of 18S rDNA networks, all sequences were included. The estimated median joining network (Templeton *et al*. 1995) resulted in six haplotypes (H1–H6) (Fig. 4.9). Of the six haplotypes, only H1 is commonly shared while the remaining five (H2, H3, H4, H5 and H6) are rare and only represented by single

individuals. Haplotype H1 is represented by four *K. dispar* individuals, H2 by *K. longicauda*, H3 by *K. sphyrnae*, H4 by *Kroyeria* sp. collected from *N. acutidens*, H5 by *K. papilipes* and H6 by *K. decepta*. According to the coalescent theory, H1 is the hypothesized ancestral haplotype since it is the most commonly represented haplotype, however, H1, H3 and H4 may be descended from individuals represented by the missing variable, mv5 (Fig. 4.9). There are known cases where an internal node is the oldest, thus becoming the ancestral haplotype with younger haplotypes radiating from it (Castelloe & Templeton 1994). There are 11, 14 and 11 mutational steps between mv5 and H1, H4 and H3 respectively, thus dividing the network into three distinct, closely related (due to the low number of mutational differences) groupings, the *K. dispar* group (represented by H1), the *Kroyeria* sp. group (represented by H4) and the second grouping (represented by H3 and H5), the third grouping (represented by H2 and H6). The groupings are similar to those estimated in the NJ, MP and ML topologies (Fig. 4.6, Fig. 4.7).

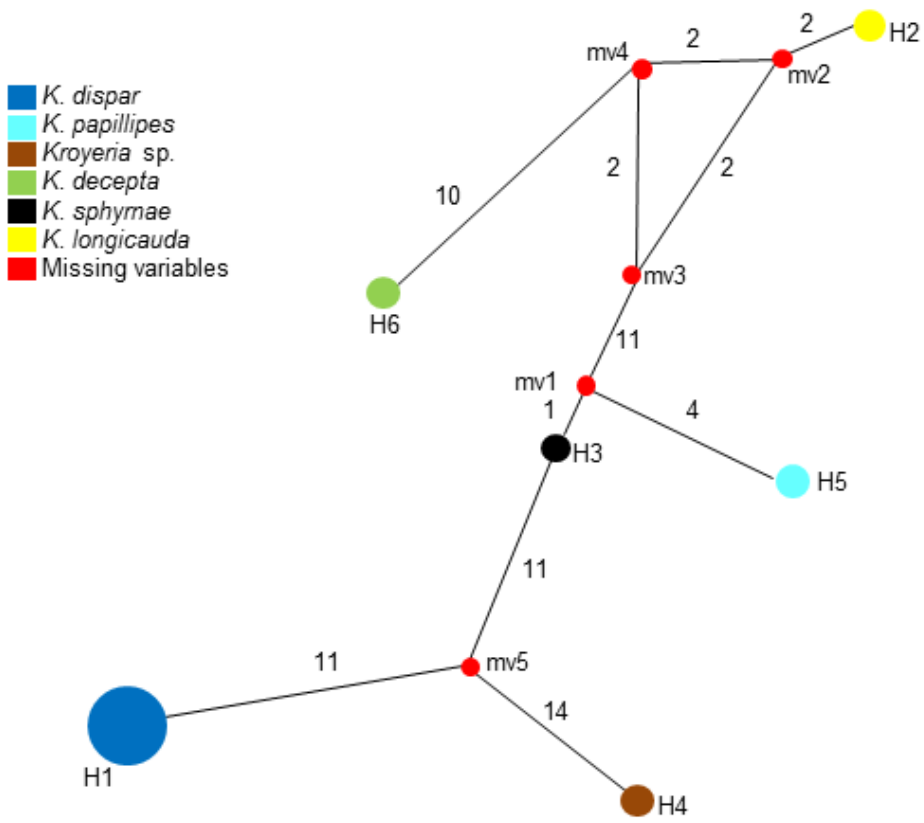

Figure 4.9. Haplotype network of 18S rDNA sequences of different *Kroyeria* species, with the numbered red nodes representing missing variables, the circles representing the different haplotypes with their diameters proportional to the number of individuals sharing that particular haplotype. The lines and numbers between the haplotypes and the nodes represent mutational steps.

4.4.7. Distinction of *Kroyeria* species using real-time PCR and melt curve analysis

Real-time PCR (qPCR) of the partial mtDNA gene COI using universal primers LCO 1490 and HCO 2198 (see Chapter 2, Table 2.2) and melt curve analysis were able to distinguish three samples of *K. papillipes*. The three samples, namely D23N/20a, D23N/20b and DBAL06a had the same T_m of 80°C on multiple occasions (Fig. 4.10). However, both D23N/20a and DBAL06a also had a T_m of 79.5°C in two and three other separate reactions respectively, with DBAL06a having an additional T_m of 80.5°C in one other separate reaction (Table 4.5). These samples that were amplified successfully had quantification cycle (Cq) values ranging from 21.07, e.g. D23N/20a (80°C), to 28.97, e.g. DBAL06a (79.5°C) (Table 4.5). The Cq value is based on the threshold cycle (CT) value which indicates the cycle number at which the generated fluorescence within the PCR reaction rises above the threshold. This value is inversely proportional to the amount of the starting material in the reaction, i.e. a higher Cq value is indicative of low initial DNA concentration in the sample and *vice versa* (D'haene *et al*. 2010). All the amplified products for the three samples had the same size which was estimated by gel electrophoreses to be between 500 and 750 bp (expected size 670 bp) (Fig. 4.11).

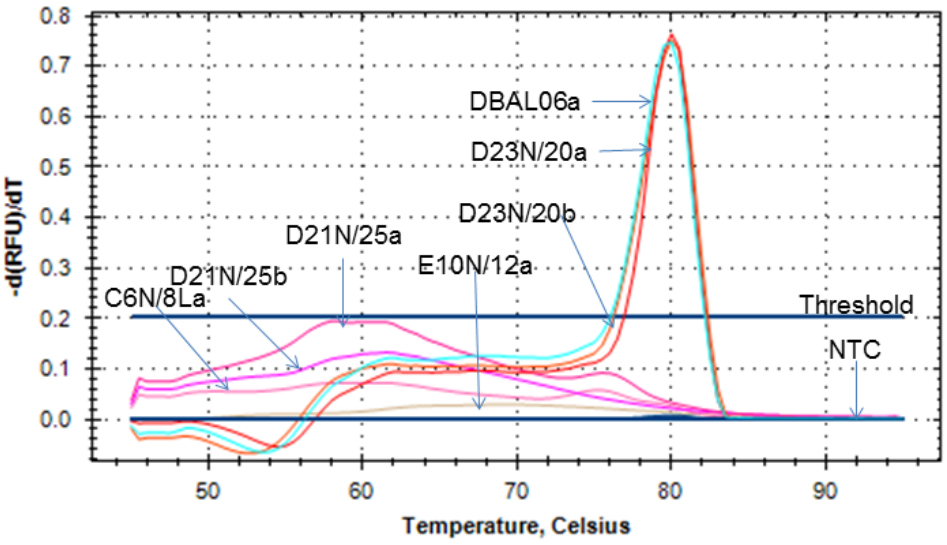

Figure 4.10. The melt peak results for the partial COI gene for *Kroyeria* samples. Clear melt peaks are observed for *K. papillipes* (D23N/20a, D23N/20b and DBAL06a) samples which have T_m of 80°C. Unsuccessfully amplified *K. decepta* (C6N/8La), *K. longicauda* (E10N/12a) and *K. papillipes* (D21N/25a and D21N/25b) samples as well as the non-template control (NTC) can be observed

below the threshold.

Table 4.5. The melt temperature (T_m) and quantitative cycle (Cq) results for three *Kroyeria papillipes* samples (D23N/20a, D23N/20b and DBAL06a) obtained when amplifying partial COI mitochondrial gene.

D23N/20a		D23N/20b		DBAL06a	
Tm °C	Cq	Tm °C	Cq	Tm °C	Cq
80	21.22	80	21.14	80	24.35
80	22.56	80	21.46	79.5	25.3
80	26.61	80	23.38	79.5	26.41
80	21.07	80	20.34	80	26.39
80	23.26	80	20.8	80.5	24.68
80	23.4	80	21.92	79.5	28.97
80	23.3	80	22.28		
80	21.58	80	21.66		
80	22.46	80	23.43		
		79.5	24.26		
		79.5	28.8		

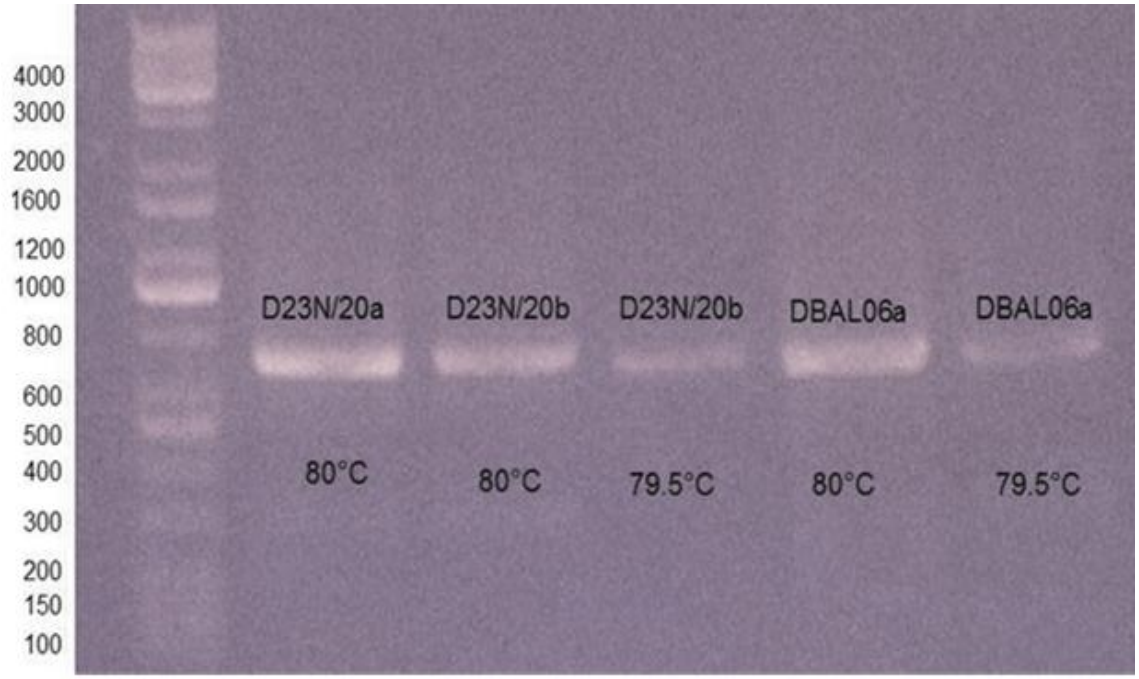

Figure 4.11. Gel electrophoresis (1.5% agarose) of the real-time PCR (qPCR) products for the partial fragment of the COI gene for selected *K. papillipes* samples, D23N/20a (T_m = 80°C), D23N/20b (T_m = 80°C), D23N/20b (T_m = 79.5°C), DBAL06a (T_m = 80°C) and DBAL06a (T_m = 79.5°C).

The remaining *Kroyeria* species (*K. carchariaeglauci*, *K. decepta*, *K. dispar*, *K. deetsi*, *K. elongata*, *K. lineata*, *K. longicauda*, *K. papillipes* and *K. sphyrnae*) samples seemed to have been successfully amplified (Table 4.6), but had overlapping T_m values and generally very high Cq values. However, when the samples were electrophorised, there were no bands but only primer dimers (Fig. 4.12).

Table 4.6. The melt temperature (T_m) and quantitave cycle (Cq) results for *K. carchariaeglauci, K. decepta, K. dispar, K. deetsi, K. elongata, K. lineata, K. longicauda, K. papillipes* and *K. sphyrnae* samples which apparently amplified successfully using universal primers HCO and LCO.

Species name	Sample ID	Tm °C	Cq	Tm °C	Cq	Tm °C	Cq	Tm °C	Cq
K. lineata	A/1AF 27a	75.5	36.41	75.5	35.35				
K. lineata	A/1AF 27b	76	40.14	76	39.24	75.5	37.04		
K. lineata	A/1AF21/1/3a	69.5	38.95	76.5	33.99				
K. lineata	A/1AF21/1/3b	75.5	37.78						

K. dispar	B19N/2b	76	36.42	75.5	36.24				
K. dispar	B10N/3a	77.5	36.59	75.5	34.55				
K. dispar	B10N/3b	74.5	29.71	75	35.86	76	37.18	76	37.4
K. dispar	B23N/52a	74.5	30.03						
K. dispar	B23N/52b	75	34.46	75	36.83	76.5	36.88		
K. decepta	C9RSB/3b	77	39.09						
K. decepta	C7N/1a	74	37.12						
K. decepta	C7N/1b	77	37	76	35.77	78	35.68		
K. papillipes	D16N/7a	74	36.31						
K. papillipes	D16N/7b	74.5	36.49						
K. papillipes	4N/1RGa	75	36.3	74.5	33.01				
K. papillipes	4N/1RGb	75	36.5	74.5	36.58				
K. longicauda	E6N/2LGa	76.5	34.75	69.5/76.5	39.48	77	36.89	76	36.8
K. longicauda	E6N/2LGc	77	36.93	76	37.13				
K. longicauda	E6N/2LGd	76.5	42.13						
K. sphyrnae	F15N/22	75.5	34.06	75.5	35.82				
K. sphyrnae	F9RSB/4a	75	37.94						
K. sphyrnae	F9RSB/4b	77.5	33.09	77.5	31.91	77	31.83	77	35.3
K. sphyrnae	F14N/1a	77.5	32.13	77	36.73	77.5	30.95	77	33.7
K. elongata	G16N/15c	75.5	37.84						
K. deetsi	I21N/3	76.5	37.51	69.5/76	37.31	76.5	35.83		
K. deetsi	I18N/14	69.5/75	38.47	69.5	37.33	70/75.5	37.39		
K. carchariaeglauci	J20N/16	76	33.13						
K. carchariaeglauci	J23N/51	77	35.85	77.5	34.35	77.5	34.08	77.5	33.2

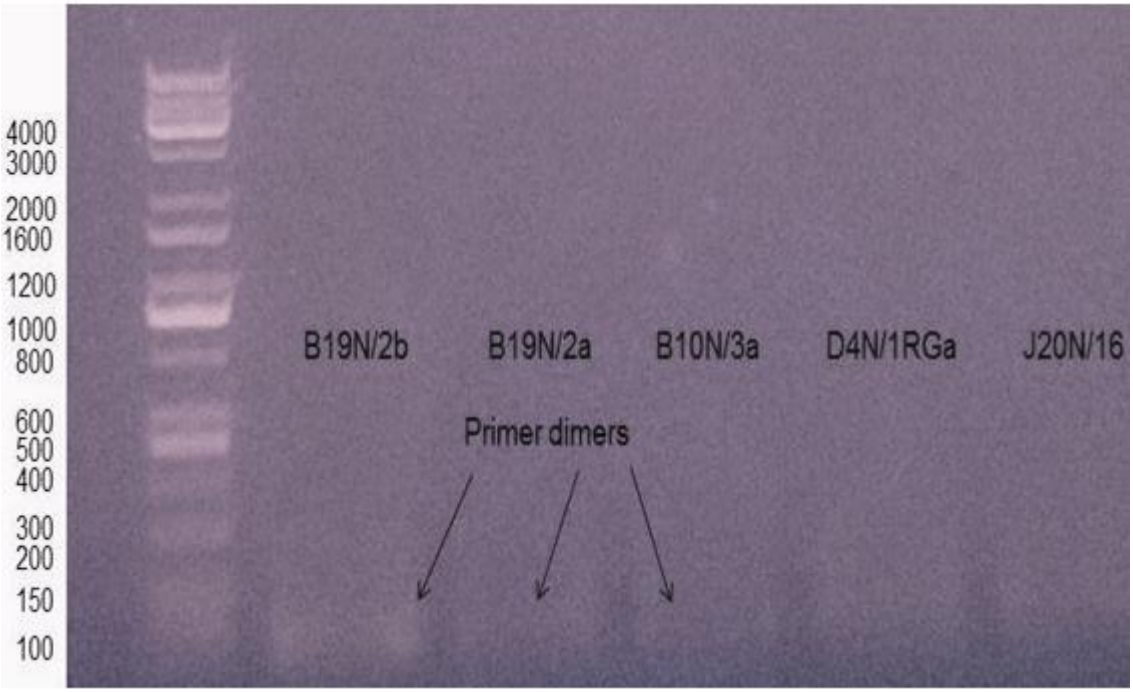

Figure 4.12. Gel electrophoresis (1.5% agarose) of the real-time PCR (qPCR) products for the partial fragment of the COI gene for selected samples, *K. dispar* (B19N/2b, B19N/2a and B10N/3a), *K. papillipes* (D4N/1RGa) and *K. carchariaeglauci* (J20N/16).

4.5. Discussion

4.5.1. DNA quantification

The low 260/280 ratios (the normal ratio ranges between 1.8 and 2) and the very low 260/230 ratios (normal ratio ranges between 2.0 and 2.2) (see Table 4.1), suggest the presence of protein or phenol contamination as well as the presence of guanine (common in column kit based extractions) which could be from the residues in the extraction process. The presence of these residual substances is known to inhibit maximum enzyme activities in PCR (Wilhelm *et al*. 2003). Another challenge which could have led to difficulties in extracting DNA and obtaining successful amplifications is the defrosting of frozen hosts from which the majority of the samples were obtained (see Chapter 2). Similar challenges were also experienced in a study by Dippenaar *et al*. (2010), which suggests that the freezing and defrosting of hosts could have led to degeneration in copepod DNA. Additionally, failure in amplification of certain samples led Bucklin *et al*. (2003) to combine 5 to

20 copepods to improve results. Similarly, Dippenaar (2009) combined several copepods of the same species taken from the same host to increase DNA yield during extraction. However, in this study DNA extraction was extracted from individual copepods. Øines and Schram (2008) also had difficulties in the amplification of some copepod species, which they eventually abandoned. Finally, Machida *et al*. (2004) reported the difficulties experienced in their experiments and provided details concerning lack of successful amplifications in certain calanoid species, which eventually led to designing species specific primers that also produced no positive results despite repeated attempts with experimental conditions.

4.5.2. Whole genome amplification

The 24 DNA samples that were amplified by using REPLI-g® mini kit (QIAGEN) did not produce any bands on gel electrophoresis after PCR amplification of the COI gene. In contrast, a previous study has demonstrated that DNA amplified by using REPLI-g® kits can be used in high throughput techniques like qPCR (Han *et al*. 2012). The failure in getting positive results when employing PCR using WGA DNA in this study could be due to the fact that the concentrations were still not sufficient or high enough, even though the unreliable or erroneous nanospectrophotometer readings were very high.

4.5.3. Phylogenetic analyses

In the present study, the monophyletic grouping formed by *K*. *dispar* is basal in the MP topology and is highly supported (bootstrap value of 100%). The basal position of *K*. *dispar* is similar to what was estimated by Deets (1994), who used morphological characteristics of 16 *Kroyeria* species to construct a cladogram showing the relationships among the species. On the contrary, the polyphyly formed by *K*. *papillipes* individuals is basal in the ML topology. In Deets' (1994) study, *K*. *dispar* and *K*. *papillipes* which infect *G. cuvier* are closely related forming the basis of the cladogram. In this study, the two species are not closely related, for instance, in the MP topology, *K*. *papillipes* forms a polytomy in the first monophyletic group and is closely related to the three GenBank species namely, *K*. *longicauda* which in turn is closely related to *K*. *sphyrnae*, with *K*. *decepta* being basal to that

monophyletic grouping. In the ML topology *K*. *dispar* forms a large part of a monophyletic group and is closely related to the polyphyly formed by the three GenBank species. *K*royeria *dispar* and *K*. *papillipes* have similar morphological characters (Deets 1994) but have a mitochondrial COI sequence divergence of 13.7–16.1% between them (Table 4.3).

In the present study, *K. sphyrnae* (except for the one downloaded from Genbank) forms a polytomy with *K. lineata* and the new *Kroyeria* sp. from *G. galeus* in both MP and ML topologies. In Deets' (1994) study *K. sphyrnae* is outside the monophyletic grouping consisting of *K. lineata*, *K. rhophemophaga, K*. *cresseyi* and *K*. *triakos* which are sister taxa. In the current study *K. lineata* is closely related to the new *Kroyeria* sp. (having a sequence divergenc of ≤ 1.2%), which is morphologically similar to *K. rhophemophaga* (see Chapter 3) and all three of them are found on the same host species, *G. galeus.* Furthermore, *K. rhophemophaga* and the new *Kroyeria* sp. share many morphological characters (see Chapter 3).

With the exception of *K*. *sphyrnae*, the present intra-specific variation (0.0–3.9%) is within the range of what was reported previously (1–4%) by Bucklin *et al*. (2003) in calanoid species in the genera *Clausocalanus*, *Neocalanus* and *Pseudocalanus*. The sequence divergence of the newly generated *K. sphyrnae* species differs from that of the same species downloaded from GenBank by 14%. Even though high intra-specific variations like these are uncommon, they have been reported in a previous study (Burton 1998), where two populations of *Tigriopus californicus* (Baker, 1912) from separate locations had sequence divergence of 22%. However, this is difficult to explain in the case of *Kroyeria* as the newly generated *K. sphyrnae* sequences and that downloaded from GenBank all came from samples collected from the east coast of South Africa and from the same host species.

Excluding *K*. *lineata*, *K*. *sphyrnae* and the new *Kroyeria* sp. from *G*. *galeus*, *Kroyeria* species have an inter-specific variation of 13.7–16.8% between them (Table 4.3), which is different from what was reported previously (7–25%) (Bucklin *et al*. 1999, Hill *et al*. 2001; Bucklin *et al*. 2003). Previous studies have reported that sequence divergence can be used as a tool to differentiate species (Hill *et al*. 2001; Bucklin *et al*. 2003, Rajthilak *et al*. 2010). However, in the present study only four of the seven *Kroyeria* species (*K. decepta*, *K. dispar*, *K*. *longicauda* and *K. papillipes*) could be

distinguished using COI sequence divergence. *Kroyeria lineata, K. sphyrnae* and the new *Kroyeria* sp. found on *G. galeus* could not be differentiated using sequence divergence (Table 4.3). However, these three species have clear morphological differences (see Chapter 3). Therefore it is advisable to use both morphology and molecular data to distinguish among *Kroyeria* species.

The 18S rDNA gene did not make any significant changes in the estimated relationships of the topology, except that the grouping containing the GenBank sequences was resolved into two sister groups (Fig. 4.7). Thus 18S, with low inter-specific variation (≤ 2%), is of little value in estimating relationships at species of *Kroyeria*, (Table 4.4). These results are similar to to those of Øines and Schram (2008) who found insignificant differences in the 18S rDNA sequence divergence of two *Caligus elongatus* genotypes. In addition, Bucklin *et al*. (2003) also reported that the 18S rDNA sequences had no variations that could be used to distinguish among species of the same genus, but were useful in distinguishing different genera. The very low genetic variation displayed by *Kroyeria* species when using 18S rDNA as a genetic marker, as with other copepods, reveals that the gene is unsuitable for differentiating among species in this genus. This is because 18S rDNA has a low mutation rate when compared to other genes like COI and16S rDNA (Thum 2004; Øines & Schram 2008). 18S rDNA evolves slowly in most animals with the sequence divergence between human and mouse genes over a period of 80 million years since mammalian radiation only 0.1% (Gonzalez & Schmickel 1986). Therefore, for future studies, it is recommended that COI should be combined with other fast evolving molecular markers like cytochrome b (Cyt b), 16S rDNA and ITS 2 (internal transcribed spacer 2) to provide resolution among taxa in the phylogenetic trees. It is also recommended that for future studies, more taxa should be used in the reconstruction of *Kroyeria* phylogenies to have more reliable and accurate relationships among the species.

4.5.4. Haplotype analyses

Haplotype analyses are commonly used to show haplotype distributions in populations. In this study they were used to compare the distribution of different haplotypes among the different *Kroyeria* species. Haplotype sharing does occur between species e.g. for COI, H1 is shared by *K. sphyrnae*, *K. lineata* and *Kroyeria*

sp. This haplotype sharing by different species is unexpected and could be due to specimen misidentification before DNA extraction. Specimen misidentification is common for *Kroyeria* species because some of them are not easy to identify due to homogeneity in morphological characteristics (see Chapter 3). However, the haplotype network results in this study confirm the relationships shown by the phylogenetic trees, dividing *Kroyeria* species into different groupings. More sequences from different *Kroyeria* species need to be amplified to reach an acceptable conclusion.

4.5.5. Species identification by real-time PCR

Only three *K. papillipes* samples seemed to have amplified successfully during qPCR and had the same T_m of 80°C on multiple occasions (Fig. 4.9). However, the wide range of melt temperatures (79.5–80.5°C), i.e. 1°C difference for the same species, *K. papillipes* (Table 4.5), is high in comparison to those of other non-vertebrate studies. For instance, in *Candida* Berkh, 1923 species the variation in T_m was ≤ 0.25°C (Hays *et al*. 2011) and ≤ 0.24°C in weevil and tick species (Winder *et al*. 2011). Even though the T_m, was not constant, the results for these three samples seemed to be reproducible and thus can possibly distinguish these samples from the rest. More samples would have to be tested in future to confirm the 1°C difference for *K. papillipes*. Furthermore, even though the samples had lower Cq values than those of other *Kroyeria* species samples (in general all the samples had high Cq values ranging from 21.07 to 42.13) suggesting that the extracted DNA had a higher starting concentration and was of better quality. The –d(RFU)/dT values of all melt peaks were very low (not reaching 0.8). The –d(RFU)/dT values of all melt peaks of other studies have values above 2.5 (Morgan *et al*. 2011), reaching 6 (Khan *et al*. 2009), ranging from 2.5 to 10 (Nicolas *et al*. 2002) and above 10 (Hays *et al*. 2011). Another factor that should be noted is that the sequences had the same length (except for *K. deetsi* and *K. procerobscena*) and all had a 40% GC content when calculated using uMelt^{SM} (Dwight 2011) (see Chapter 2). Since all the samples that were successfully amplified via PCR had the same GC content in their sequences, it is expected that they would also have T_m values that are very close (GC content is one of the determining factors for T_m), with slight differences in T_m between different *Kroyeria* species.

It is recommended that primers which amplify a fragment that ranges in size from 80 to 150 bp (Thornton & Basu 2011) or a fragment that less than 300 bp (Gene Target Solutions 2014) should be used for qPCR as amplification efficiency (especially primer annealing) and sensitivity are significantly reduced with an increase in amplicon size. In this study a 670 bp fragment was amplified, this could have influenced the success of qPCR. Additionally, the use of universal primers may also have had an effect on the success of qPCR as it is noted that successful studies in the past have used species-specific primers (McBeath *et al*. 2006; Pan *et al*. 2008; Khan *et al*. 2009). It is stated that the designing of optimal primer pairs is a prerequisite for success in qPCR amplifications (QIAGEN 2009). Fluorescent dyes are advantageous in minimizing costs but are also known to cause product inhibition, enzyme instability and a decrease of reaction components in time (Ramakers *et al*. 2002).

4.6. Conclusion

The difficulties experienced in the identification and distinction of *Kroyeria* species based on morphological characteristics led to using molecular techniques as an attempt to solve these problems. DNA based phylogeny can provide a more accurate record of the relationship among the known *Kroyeria* species. Similarly, the rapid distinction of different *Kroyeria* species based on differences in their melt temperatures as employed in real-time PCR could be of great importance and can provide an easy solution to the time consuming, tedious, labour expensive process when trying to distinguish them morphologically. This can also prevent the misidentification and erroneous synonymising of species common in the genus *Kroyeria* (see Chapter 3). However, these molecular techniques depend not only on the quality of the DNA used, e.g. DNA concentration, but also on the molecular markers employed.

This study presents an initial attempt to reconstruct *Kroyeria* phylogeny based on molecular data as well as to distinguish *Kroyeria* species using melt temperatures. Even tough morphological variation seems to be higher than genetic variation, this is not the case since species were probably misidentified before DNA extrcation due to lack of morphological variation. Challenges experienced include low DNA concentrations and contamination by residual components from DNA extraction,

unsuccessful amplifications, unresolved polytomies and indistinct melt temperatures. Thus it is recommended that the elution volume should be decreased from 100 μl to a much smaller volume during the DNA extraction. It is also recommended that nucleic acid purification kits like QIAprep® should be utilised to remove impurities from the extraction process that interfere with fluorescence detection in real-time PCR. Recommendations are also made to combine COI with other fast evolving molecular markers like Cyt b, 16S rDNA and ITS 2 to provide the necessary resolution in the phylogenies. Additionally, it is also recommended that species-specific primers that can amplify a fragment that ranges from 80 bp to 300 bp should be designed and used in real-time PCR instead of universal primers, LCO 1490 and HCO 2198 that amplify a fragment that is 670 bp long, to obtain better amplification results. Finally, it is recommended that in case of *Kroyeria* species, both morphological and molecular data should be used to complement each other in the identification, distinction and reconstruction of phylogenies.

CHAPTER 5

GENERAL DISCUSSION AND CONCLUSION

There are currently 21 nominal species in the genus *Kroyeria* (Deets 1994; Dippenaar *et al*. 2000; Thatcher & Júnior 2006; Izawa 2008), of which 11 were collected from the gill filaments of elasmobranchs belonging to the families Carcharhinidae, Sphyrnidae and Triakidae off the coast of South Africa (Table 2.1, Table 3.2). These include *K*. *carchariaeglauci* from *C. leucas*; *K*. *decepta* from *C*. *obscurus*; *K*. *deetsi* from *C*. *brevipinna*; *K*. *dispar* from *G. cuvier; K*. *elongata* from *R. acutus*; *K*. *lineata* from *M. palumbes*; *K*. *longicauda* from *C*. *limbatus*; *K*. *papillipes* from *G*. *cuvier*; *K*. *procerobscena* from both *C*. *leucas* and *C*. *amboinensis*; *K. sphyrnae* from both *Sphyna lewini* and *S*. *zygaena* and *a* new *Kroyeria* sp. from *G. galeus*. This is the first record of *K. lineata* from the south coast of South Africa and is also a new host record for *M*. *palumbes*. Three *Kroyeria* species have previously been reported from *G. galeus*, namely *K. brasiliense, K. lineata* and *K. rhophemophaga*. The new *Kroyeria* sp. is most similar to *K*. *rhophemophaga* which in turn shares morphological features with *K. triakos*. However, the *Kroyeria* sp. can be distinguished from both *K. rhophemophaga* and *K. triakos* in the armature or chaetotaxy of the legs (Table 3.3).

Most *Kroyeria* species are relatively host specific, infecting a single host or related group of host species. During this study two species, *K. dispar* and *K. papillipes* were collected from *G. cuvier*, while *K. procerobscena* was collected from *C*. *leucas* and *C*. *amboinensis* and *K. sphyrnae* from *S*. *lewini* and *S*. *zygaena*.

Kroyeria sp. and *K. dispar* displayed very high prevalence values (Fig. 3.1), 95.7% and 94.1% respectively, in contrast to the other *Kroyeria* species which have lower values (6.3–68.6%). Additionally, when compared to other siphonostomatoid species such as *N. lamna*, *Kroyeria* species have relatively low prevalence values. *Kroyeria* species generally have low parasite loads (between 4 and 33 copepods per infected host), except for *K. dispar* which has a high mean intensity of 74 copepods per infected host (Fig. 3.3). The mean abundance

of *Kroyeria* species is also generally low (between 0 and 23 per examined host), with *K. dispar* (69 individuals per examined host) being an exception. Furthermore *Kroyeria* species generally display an aggregative pattern of distribution (Table 3.2) which is common in most copepod species indicating that individuals have social interactions.

A preliminary estimation of the phylogenetic relationships among seven *Kroyeria* species was done using molecular techniques. Relationships displayed by neighbor joining (NJ), parsimony (MP) and maximum likelihood (ML), when using a part of the COI gene, revealed topologies with polytomies (Fig. 4.3, Fig. 4.4, Fig. 4.5). The 18S rDNA gene did not make any significant contribution to the topology, except that it produced very minimal resolution in one of the groupings (Fig. 4.7). Therefore, COI is found to be the gene of choice that can be used in estimating molecular phylogenies and determining the population genetics of siphonostomatoids as it provides detectable sequence divergence within individuals of the same species as well as among congeneric species (Table 4.3) due to its fast evolving rate. This is similar to findings in free-living copepods (Bucklin *et al*. 2003). However, in this study, single species did not form monophyletic groupings.

The 18S rDNA gene is found to be very conservative, providing no sequence divergence within individuals of the same species and very little divergence among conspecifics (Table 4.4), due to its low mutation rate and is therefore more useful at genus and family levels (Thum 2004; Øines & Schram 2008).

Due to the estimated polytomies among different species, haplotype networks were used to compare the distribution of different haplotypes among the different species. Haplotype sharing did occur between species e.g. for the amplified part of the COI gene haplotypes, H1 is shared by *Kroyeria* sp., *K. lineata* and *K. sphyrnae*. This haplotype sharing by different species is unexpected and could be due to specimen misidentification before DNA extraction, as it was mentioned previously that specimen misidentification is common for *Kroyeria* species due to the homogeneity in morphological characteristics, making it difficult to easily identify some species. The haplotype network results confirmed the relationships shown by the phylogenetic trees, thus dividing *Kroyeria* species into three

different groupings.

Real-time PCR and melt curve analysis have the potential to distinguish among *Kroyeria* species. However, the quality of the extracted DNA is an important factor in producing successful amplifications and determining the T_m. Therefore it is necessary to ensure that the extracted DNA has the ideal concentration of 50 ng/μl and is free of Taq polymerase inhibitors such as phenol, RNA and guanine residuals from the extraction process. Additionally, PCR amplification of 80–300 bp may be more appropriate than the current 670 bp, since amplification efficiency (especially primer annealing) and sensitivity are significantly reduced with an increase in amplicon size.

Identification of species by the use of classical, unsophisticated techniques like microscopy is an essential skill to acquire for every biological scientist. Molecular techniques are essential in complementing these classical taxonomic techniques, by using sequences that are generated via PCR and specific, distinct melt temperatures produced by combining real-time PCR with melt curve analysis. The differences in the generated sequences or sequence divergence can then be used as a tool that distinguishes certain species from each other depending on the genetic marker used, for instance, genetic markers like COI are fast evolving producing significant species divergence whereas others are like 18S rDNA are highly conserved, slowly evolving and do not provide significant divergence at species level. However, these techniques are not always successful as evidenced by much of the molecular work in this study as well as a few available publications where these techniques have been successful in few species. Even in the few successful studies, most researchers describe the setbacks encountered when using these techniques. Thus the sophisticated molecular techniques are not always a solution to the simple basic task, low-tech sciences like identification by microscopy.

Future efforts in improving the success of these molecular techniques should include reducing the elution volume during DNA extraction process, utilising nucleic acid purification kits to remove impurities from the extraction process that interfere with fluorescence detection in real-time PCR, combinining COI with other fast evolving molecular markers like Cyt b, 16S rDNA and ITS 2 to provide

the necessary resolution on the phylogenies as well as designing species-specific primers that would amplify an amplicon of 80–300 bp long in real-time PCR.

REFERENCES

BENZ, G.W. 1994. Evolutionary Biology of Siphonostomatoida (Copepoda) Parasitic on Vertebrates. PhD thesis, University of British Columbia.

BENZ, G.W., BORUCINSKA, J.D. & GREENWALD, A. 2002. First descriptions of early- and middle-stage copepodids of *Anthosoma crassum* (Dichelesthiidae: Siphonostomatoida) and lesions on shortfin makos (*Isurus oxyrinchus*) infected with *A. crassum*. *Journal of Parasitology* **88**: 241–244.

BIMI, L. 2007. Potential vector species of Guinea worm (*Dracunculus medinensis*) in Northern Ghana. *Vector Borne Zoonotic Diseases* **7**: 324–329.

BOXSHALL, G.A. 2014. World of Copepods database. Available online at http://www.marinespecies.org/copepeoda/aphia (Accessed on 12 February 2014).

BOXSHALL, G.A. & DEFAYE, D. 2008. Global diversity of copepods (Crustacea: Copepoda). *Hydrobiologia* **595**: 195–207.

BOXSHALL, G.A. & HALSEY, S.H. 2004. *An Introduction to Copepod Diversity.* The Ray Society, London.

BOXSHALL, G.A. & JAUME, D. 2000. Making waves: the repeated colonization of fresh water copepod crustaceans. *Advances in Ecological Research* **31**: 61–79.

BRAGA, E., ZARDOYA, R., MEYER, A. & YEN, J. 1999. Mitochondrial and nuclear rRNA based copepod phylogeny with emphasis on the Euchaetidae (Calanoida). *Marine Biology* **133**: 79–90.

BRON, J.E., FRISCH, D., GOETZE, E., JOHNSON, S.C., LEE, C.E. & WYNGAARD, G.A. 2011. Observing copepods through a genomic lens. *Frontiers in Zoology* **8**: 22.

BUCKLIN, A., BENTLEY, A.M. & FRAZEN, S.P. 1998. Distribution and relative abundance of *Pseudocalanus moultoni* and *P. newmani* (Copepoda: Calanoida) on Georges Bank using molecular identification of sibling species. *Marine Biology* **132**: 97–106.

BUCKLIN, A., FROST, B.W., BRADFORD-GRIEVE, J., ALLEN, L.D. & COPLEY, N.J. 2003. Molecular systematics and phylogenetic assessment of 34 calanoid species of the Calanidae and Clausocalanidae. *Marine Biology* **142**: 333–343.

BUCKLIN, A., GUARNIERI, M., HILL, R.S., BENTLEY, A.M. & KAARTVEDT, S. 1999. Taxonomic and systematic assessment of planktonic copepods using mitochondrial COI sequence variation and competitive, species-specific PCR. *Hydrobiologia* **401**: 239–254.

BURTON, S.D. 1998. Intraspecific phylogeography across the point conception biogeographic boundary. *Evolution* **52**: 734–745.

BUSH, A.O., FERNANDEZ, J.C., ESCH, G.W. & SEED, J.R. 2001. *Parasitism*: *The Diversity and Ecology of Animal Parasites*. Cambridge University Press, UK.

BUSH, A.O., LAFFERTY, K.D., LOTZ, J.M. & SHOSTAK, A.W. 1997. Parasitology meets ecology on its own terms: Margolis *et al*. revisited. *Journal of Parasitology* **83**: 575–583.

CAMIN, J.H. & SOKAL, R.R. 1965. A method for deducing branching sequences in phylogeny. *Evolution* **19**: 311–326.

CASTELLOE, J. & TEMPLETON, A.R. 1994. Root probabilities for intraspecific gene trees under neutral coalescent theory. *Molecular Phylogenetic Evolution* **3**: 102–113.

COMPAGNO, L.J.V. 1999. An overview of Chondrichthyan systematics and biodiversity in southern Africa. *Transactions of the Royal Society of South Africa* **54**: 75–120.

COMPAGNO, L., DANDO, M. & FOWLER, S. 2005. *Sharks of the World*. Princeton University Press, USA.

COSTELLO, M. 2009. The global economic cost of sea lice to the salmonid farming industry. *Journal of Fish Diseases* **32**: 115–118.

DEETS, G.B. 1987. Phylogenetic analysis and revisison of *Kroeyerina* Wilson, 1932 (Siphonostomatoida: Kroyeriidae), copepod parasitic on chondichthyans, with

description of four new species and the erection of a new genus, *Prokroyeria*. *Canadian Journal of Zoology* **65**: 2121–2148.

DEETS, G.B. 1994. Copepod-Chondrichthyan Coevolution: A Cladistics Consideration. PhD thesis, University of British Columbia.

DEETS, G.B. & HO, J.S. 1988. Phylogenetic analysis of the Eudactylinidae (Crustacea: Copepoda: Siphonostomatoida), with descriptions of two new genera. *Proceedings of the Biological Society of Washington* **101**: 317–339.

D'HAENE, B., VANDESOMPELE, J. & HELLEMANS, J. 2010. Accurate and objective copy number profiling using real-time quantitative PCR. *Methods* **50**: 262–270.

DIEBAKATE, C., RAIBAUT, A. & KABATA, Z. 1997. *Thamnocephalus cerebrinoxius* n. g., n. sp. (Copepoda: Sphyriidae), a parasite in the nasal capsules of *Leptocharias smithii* (Müller & Henle, 1839) (Pisces: Leptochariidae) off the coast of Senegal. *Systematic Parasitology* **38**: 231–235.

DIPPENAAR, S.M. 2005. Reported siphonostomatoid copepods parasitic on marine fishes of southern Africa. *Crustaceana* **77**:1281–1328.

DIPPENAAR, S.M. 2009. Estimated molecular phylogenetic relationships of six Siphonostomatoid families (copepoda) symbiotic on elasmobranchs. *Crustaceana* **82**: 1547–1567.

DIPPENAAR, S.M. & JORDAAN, B.P. 2007. New host and geographical records of siphonostomatoid copepods associated with elasmobranchs off the KwaZulu-Natal coast, South Africa. *Onderstepoort Journal of Veterinary Research* **74**: 169–175.

DIPPENAAR, S.M., MATHIBELA, R.B. & BLOOMER, P. 2010. Cytochrome oxidase I sequences reveal possible cryptic diversity in the cosmopolitan symbiotic copepod *Nesippus orientalis* Heller, 1868 (Pandaridae: Siphonostomatoida) on elasmobranch hosts from the KwaZulu-Natal coast of South Africa. *Experimental Parasitology* **125**: 42–50.

DIPPENAAR, S.M. & OLIVIER, P.A.S. 1999. New morphological information of the parasitic copepod *Kroyeria dispar* Wilson, 1935 (Copepoda: Kroyeriidae) from the east coast of South Africa. *South African Journal of Zoology* **34**: 125–129.

DIPPENAAR, S.M., OLIVIER, P.A.S. & BENZ, G.W. 2000. *Kroyeria deetsi* n.sp. (Kroyeriidae: Siphonostomatoida), a parasitic copepod infecting gills of spinner sharks, *Carcharhinus brevipinna* (Müller & Henle, 1839) in the Indian Ocean. *African Zoology* **35**: 185–192.

DIPPENAAR, S.M., OLIVIER, P.A.S. & BENZ, G.W. 2001. *Kroyeria sphyrnae* Rangnekar, 1957 (Copepoda, Siphonostomatoida, Kroyerridae): first description of the male, supplementary remarks on the female, a new geographic record for the species, and a key to *Kroyeria* males. *Crustaceana* **74**: 883–894.

DIPPENAAR, S.M., OLIVIER, P.A.S. & BENZ, G.W. 2004. *Schistobrachia jordaanae* n.sp. (Copepoda: Siphonostomatoida: Lernaeopodidae) from gill filaments of a diamond ray (*Gymnura natalensis*) captured in the Indian Ocean and a key to species of *Schistobrachia*, *Dendrapta*, and *Brianella*. *Journal of Parasitology* **90**: 481–484.

DIPPENAAR, S.M., VAN TONDER, R., WINTNER, S. & ZUNGU, P. 2008. Spatial distribution of *Nemesis lamna* Risso, 1826 (Copepoda: Siphonostomatoida: Eudactylinidae) on the gills of white sharks *Carcharodon carcharias* off KwaZulu-Natal, South Africa. *African Journal of Marine Science* **30**: 143–148.

DIPPENAAR, S.M., VAN TONDER, R.C. & WINTNER, S.P. 2009. Is there evidence of niche restriction in the spatial distribution of *Kroyeria dispar* Wilson, 1935, *K. papillipes* Wilson, 1932 and *Eudactylina pusilla* Cressey, 1967 (Copepoda: Siphonostomatoida) on the gill filaments of tiger sharks *Galeocerdo cuvier* off KwaZulu-Natal, South Africa? *Hydrobiologia* **619**: 89–101.

DOJIRI, M. & HO, J.S. 2013. *Systematics of the Caligidae, Copepods Parasitic on Marine Fisher*. Brill, Netherlands.

DWIGHT, Z., PALAIS, R. & WITTWER, C.T. 2011. uMelt: predictions of high-resolution melting curves and dynamic melting profiles of PCR products in a rich web application. *Bioinformatics* **27**: 1019–1020.

FARRIS, J.S. 1972. Estimating phylogenetic trees from distance matrices. *The American Naturalist* **106**: 645–668.

FELSENSTEIN, J. 1981. Evolutionary trees from DNA sequences: a maximum likelihood approach. *Journal of Molecular Evolution* **17**: 368–376.

FELSENSTEIN, J. 1985. Confidence limits on phylogenies: an approach using the bootstrap. *Evolution* **39**: 783–791.

FIGUEROA, D.F. 2011. Phylogenetic analysis of *Ridgewayia* (Copepoda: Calanoida) from the Galapagos and of a new species from Florida Keys with a reevaluation of the phylogeny of Calanoida. *Journal of Crustacean Biology* **31**: 153–165.

FLOYD, R.M., ROGERS, A.D., LAMBSHEAD, J.D. & SMITH, C.R. 2005. Nematode-specific PCR primers for the 18S small subunit rRNA gene. *Molecular Ecology Notes* **5**: 611–612.

FOLMER, O., BLACK, N., HOEH, W., LUZT, R. & VRIJENHOEK, R. 1994. DNA primers for amplification of mitochondrial cytochrome c oxidase subunit I from diverse metazoan invertebrates. *Molecular Marine Biology and Biotechnology* **3**: 294–299.

FREEMAN, S. & HERRON, J.C. 2007. *Evolutionary Analysis*. 4th edition. Pearson Education, Inc., London.

FRISCHER, M.E., HANSAN, A.S., WYLLIE, J.A., WIMBUSH, J., MURRAY, J. & NIERZWICKI-BAUER, S.A. 2002. Specific amplification of the 18S rRNA gene as a method to detect Zebra mussel (*Dreissener polymorpha*) larvae in planktonic samples. *Hydrobiologia* **487**: 33–34.

FROESE, R. & PAULY, D. 2014. FishBase. World Wide Web electronic publication. Available online at www.fishbase.org (Accessed on 04 February 2014).

Gene Target Solutions. 2014. Real-time PCR FAQS. Available online at http://www.genetargetsolutions.com (Accessed on 10 May 2014).

GIRIBET, G. 2010. A new dimension in combining data? The use of morphology and phylogenomic data in metazoan systematics. *Acta Zoologica* **91**: 11–19.

GONZALEZ, I.L. & SCHMICKEL, R.D. 1986. The human 18S ribosomal RNA gene: evolution and stability. *American Journal of Human Genetics* **38**: 419–427.

GRABBERT, S., RENZ, J., HIRCHE, H.J. & BUCKLIN, A. 2010. Species-specific PCR discrimination of species of the calanoid copepod *Pseudocalanus*, *P. acuspes* and *P. elongatus*, in the Baltic and North Seas. *Hydrobiologia* **652**: 289–297.

GUION, C.E., OCHOA, T.J., WALKER, C.M., BARLETTA, F. & CLEARY, T.G. 2008. Detection of diarrheagenic *Escherichia coli* by use of melting-curve analysis and real-time multiplex PCR. *Journal of Clinical Microbiology* **46**: 1752–1757.

HAJIBABAEI, M., SINGER, G.A.C., HEBERT, P.D.N. & HICKEY, D.A. 2007. DNA barcoding: how it complements taxonomy, molecular phylogenetics and population genetics. *Trends in Genetics* **23**: 4.

HALL, T.A. 1999. BioEdit: a user-friendly biological sequence alignment editor and analysis program for windows 95/98/NT. *Nucleic Acids Symposium Series* **41**: 92–94.

HAN, T., CHANG, C., KWEKEL, J.C., CHEN, Y., GE, Y., MARTINEZ-MURILLO, F., ROSCOE, D., TEŽAK, Ž., PHILIP, R., BIJWAARD, K. & FUSCOE, J.C. 2012. Characterization of whole genome amplified (WGA) DNA for use in genotyping assay development. *BMC Genomics* **13**: 217.

HAQUE, K.A., PFEIFFER, R.M., BEERMAN, M.B., STRUEWING, J.P., CHANOCK, S.J. & BERGEN, A.W. 2003. Performance of high throughput DNA quantification methods. *BMC Biotechnology* **3**: 20.

HARVEY, M.L., DADOUR, I.R. & GAUDIERE, S. 2003. Mitochondrial DNA cytochrome oxidase I gene: potential for distinction between immature stages

of some forensically important fly species (Diptera) in Western Australia. *Forensic Science International* **131**: 134–139.

HAYNES, G.D., GONGORA, J., NICHOLAS, F.W. & ZENGER, K.R. 2009. Rapid identification of maternal lineages in common carp (*Cyprinus carpio*) using real-time PCR and high resolution melt curve analysis. *Aquaculture* **287**: 59–66.

HAYS, C., DUHAMEL, C., CATTOIR, V. & BONHOMME, J. 2011. Rapid and accurate identification of species belonging to the *Candida parapsilosis* complex by real-time PCR and melting curve analysis. *Journal of Medical Microbiology* **60**: 477–480.

HEEMSTRA, P. & HEEMSTRA, E. 2004. *Coastal Fishes of Southern Africa*. NISC & SAIAB, South Africa.

HEJAZI, M.A., BARZEGARI, A., GHARAJEH, N.D. & HEJAZI, M.S. 2010. Introduction of a novel 18S rDNA gene arrangement along with distinct ITS region in the saline water microalga *Dunaliella*. *Saline Systems* **6**:4.

HESS, P.N. & DE MORAES RUSSO, C.A. 2007. An empirical test of the midpoint rooting method. *Biological Journal of the Linnean Society* **92**: 669–674.

HEWITT, G.C. 1969. Some New Zealand parasitic Copepoda of the Family Eudactylinidae. *Zoology publication from Victoria University of Wellington* **49**: 1–31.

HICKMAN, C.P.P., ROBERTS, L.S., KEEN, S.L., LARSON, A., l'ANSON, H. & EISENHOUR, D.J. 2008. *Integrated Principles of Zoology*. 14th edition. McGraw-Hill, London.

HILL, R.S., ALLEN, L.D. & BUCKLIN, A. 2001. Multiplexed species-specific PCR protocol to discriminate four N. Atlantic *Calanus* species, with an mtCOI gene tree for ten *Calanus* species. *Marine Biology* **139**: 279–287.

HO, J.S. 2001. Why do symbiotic copepods matter? *Hydrobiologia* **453/454**: 1–7.

HO, J.S. & ZHENG, G.X. 1994. *Ostrincola koe* (Copepoda, Myicolidae) and mass mortality of cultured hard clam (*Meretrix meretrix*) in China. *Hydrobiologia* **284**: 169–173.

HUMES, A.G. & GOODING, R.U. 1964. A method for studying the external anatomy of copepods. *Crustaceana* **6**: 238–240.

HURST, G.D.D. & JIGGINS, F.M. 2005. Problems with mitochondrial DNA as a marker in population, phylogeographic and phylogenetic studies: the effects of inherited symbionts. *Proceedings of Royal Society B* **272**: 1525–1534.

HUYS, R. & BOXSHALL, G.A. 1991. *Copepod Evolution*. The Ray Society, London.

HUYS, R., LLEWELLYN-HUGHES, J., CONROY-DALTON, S., OLSON, P.D., SPINKS, J.N. & JOHNSTON, D.A. 2007. Extraordinary host switching in siphonostomatoid copepods and the demise of the Monstrilloida: Integrating molecular data, ontogeny and antennulary morphology. *Molecular Phylogenetics and Evolution* **43**: 368–378.

IZAWA, K. 2008. Redescription of four species of *Kroyeria* and *Kroeyerina* (Copepoda, Siphonostomatoida, Kroyeriidae) infecting Japanese sharks. *Crustaceana* **81**: 695–724.

JITHENDRAN, K.P., NATARAJAN, M. & AZAD, I.S. 2008. Crustacean parasites and their management in brackish water finfish culture in freshwater. *Aquaculture Asia Magazine*, Jul-Sep.

JOHNSON, S.C., TREASURER, J.W., BRAVO, S., NAGASAWA, K. & KABATA, Z. 2004. A review of the impact of parasitic copepods on marine aquaculture. *Zoological Studies* **43**: 229–243.

KABATA, Z. 1979. *Parasitic Copepods of British Fishes*. The Ray Society, London.

KHAN, Z., MUSTAFA, A.S. & ALAM, F.F. 2009. Real-time LightCycler polymerase chain reaction and melting temperature analysis for identification of clinically important *Candida* spp. *Journal of Microbiology Immunology & Infection* **42**: 290–295.

KLEIN, D. 2002. Quantification using real-time PCR technology: applications and limitations. *Trends in Molecular Medicine* **8**: 6.

KNOWLTON, N. 2000. Molecular genetic analyses of species boundaries in the sea. *Hydrobiologia* **420**: 73–90.

LI, M., SENDA, M., KOMATSU, T., SUGA, H. & KAGEYAMA, K. 2010. Development of real-time PCR technique for the estimation of population density of *Pythium intermedium* in forest soils. *Microbiological Research* **165**: 695–705.

LIBRADO, P. & ROZAS, J. 2009. DnaSP v5: A software for comprehensive analysis of DNA polymorphism data. *Bioinformatics* **25**: 1451–1452.

LINDEQUE, P.K., HARRIS, R.P., JONES, M.B. & SMERDON, G.R. 2004. Distribution of *Calanus* spp. as determined using a genetic identification system. *Scientia Marina* **68**: 121–128.

LÖBL. I. 2014. Overestimation of molecular and modelling methods and underestimation of traditional taxonomy leads to real problems in assessing and handling of the world's biodiversity. *Zootaxa* **3768**: 497–500.

LUNT, D.H., ZHANG, D.X., SZYMURA, J.M. & HEWITT, G.M. 1996. The insect cytochrome oxidase I gene: evolutionary patterns and conserved primers for phylogenetic studies. *Insect Molecular Biology* **5**: 153–165.

MACHIDA, R.J., MIYA, M.U., NISHIDA, M. & NISHIDA, S. 2004. Large-scale gene rearrangements in the mitochondrial genomes of two Calanoid copepods *Eucalanus bungii* and *Neocalanus cristatus* (Crustacea), with notes on new versatile primers for the srRNA and COI genes. *Gene* **332**: 71–78.

MADDISON, D.R. & MADDISON, W.P. 2000. *MacClade 4: Analysis of phylogeny and character evolution*. Sinauer Associates, Sunderland, Massachusetts.

MADINABEITIA, I. & IWASAKI, S. 2013. A new species of *Procolobomatus* Castro Romero, 1994 (Copepoda: Philichthyidae) endoparasitic in a deepwater longtail red snapper (Actinopterygii: Lutjanidae) off Ishigaki Island, Japan, with records of philichthyid copepods reported from Asian waters. *Systematic Parasitology* **84**: 217–224.

MADINABEITIA, I., TANG, D. & NAGASAWA, K. 2013. Four new species of *Colobomatus* (Copepoda: Philichthyidae) parasitic in the lateral line system of marine finfishes captured off the Ryukyu Islands, Japan, with redescriptions of *Colobomatus collettei* Cressey, 1977 and *Colobomatus pupa* Izawa, 1974. *Journal of Natural History* **47**: 563–580.

MANGENA, T., JORDAAN, B.P. & DIPPENAAR, S.M. (in press). Phylogenetic relationships and genetic diversity of *Nemesis* Risso, 1826 species found on different elasmobranch host species off the KwaZulu-Natal coast, South Africa. *African Journal of Marine Science*.

MARTIN, J.W. & DAVIS, G.E. 2001. An updated classification of the recent Crustacea. Natural History Museum of Los Angeles County. *Contributions in Science* **39**: 1–123.

MCBEATH, A.J.A., PENSTON, M.J., SNOW, M., COOK, P.F., BRICKNELL, I.R. & CUNNINGHAM, C.O. 2006. Development and application of real-time PCR for specific detection of *Lepeophtheirus salmonis* and *Caligus elongatus* larvae in Scottish plankton samples. *Diseases of Aquatic Organisms* **73**: 141–150.

MESSING, J. 1983. New M13 vector for cloning. *Methods in Enzymology* **101**: 20–78.

MIESFELD, R.L. 1996. *Applied Molecular Genetics*. Wiley & Sons, Inc. Publication, New York.

MINXIAO, W., SONG, S. & XIN, S. 2011. Distinctive mitochondrial genome of Calanoid copepod *Calanus sinicus* with multiple large non-coding regions and reshuffled gene order: useful molecular markers for phylogenetic and population studies. *BMC Genomics* **12**: 73.

MORALES-RAMIREZ, A. & SUAREZ-MORALES, E. 2009. Marine Biodiversity of Costa Rica, Central America. I.S. Wehrtmann, J. Cortes (eds). University of Costa Rica Press, Mexico.

MORALES-SERNA, F.N., PINACHO-PINACHO, C.D., GÓMEZ, S. & PÉREZ-PONCE DE LEÓN, G. 2014. Diversity of sea lice (Copepoda: Caligidae) parasitic on marine fishes with commercial and aquaculture importance in

Chamela Bay, Pacific coast of Mexico by using morphology and DNA barcoding, with description of a new species of *Caligus*. *Parasitology International* **63**: 69–79.

MORGAN, J.A.T., WELCH, D.J., HARRY, A.V., STREET, R., BRODERICK, D. & OVENDEN, J.R. 2011. A mitochondrial species identification assay for Australian blacktip sharks (*Carcharhinus tilstoni*, *C. limbatus* and *C. amblyrhynchoides*) using real-time PCR and high-resolution melt analysis. *Molecular Ecology Resources* **11**: 813–819.

MURPHY, W.J., PRINGLE, T.H., CRINDER, T.A., SPRINGER, M.S., MILLER, W. 2007. Using genomic data to unravel the root of the placental mammal phylogeny. *Genome Research* **17**: 413–421.

MUSTAFA, A., RANKADUWA, W. & CAMPBELL, P. 2000. Estimating the cost of sea lice to salmon aquaculture in Eastern Canada. *Canadian Veterinary Journal* **41**: 54–56.

NAUMENKO, V.S., OSIPIVA, D.V., KOSTINA, E.V. & KULIKOV, A.V. 2008. Utilization of a two-standard system in real-time PCR for quantification of gene expression in the brain. *Journal of Neuroscience Methods* **170**: 197–203.

NEI, M. 1987. *Molecular Evolutionary Genetics*. Columbia University Press, New York.

NICOLAS, L., MILON, G. & PRINA, E. 2002. Rapid differentiation of old world *Leishmania* species by LightCycler polymerase chain reaction and melting curve analysis. *Journal of Microbiological Methods* **51**: 295–299.

ØINES, O. & SCHRAM, T. 2008. Intra- or inter-specific differences in genotypes of *Caligus elongatus* Nordmann 1832. *Acta Parasitologica* **53**: 93–105.

PAN, M., MCBEATH, A.J.A., HAY, S.J., PIERCE, G.J. & CUNNINGHAM, C.O. 2008. Real-time PCR assay for detection and relative quantification of *Liocarcinus depurator* larvae from plankton samples. *Marine Biology* **153**: 859–870.

PEARSON, D.L., HAMILTON, A.L. & ERWIN, T.L. 2011. Recovery plan for the endangered taxonomic profession. *BioScience* **61**: 1.

PEREIRA, F., CARNEIRO, J. & AMORIM, A. 2008. Identification of species with DNA based technology: current progress and challenges. *Recent Patents on DNA & Gene Sequences* **2**: 3.

PIASECKI, W., GOODWIN, A.E., EIRAS, J.C. & NOWAK, B.F. 2004. Importance of Copepoda in freshwater aquaculture. *Zoological Studies* **43**: 193–205.

PILLAI, N.K. 1967. Three species of dichelesthiid copepods parasitic on South Indian sharks. *Zoologische Anzeiger* **179**: 286–297.

PILLAI, N.K. 1985. *The Fauna of India: Copepod Parasites of Marine Fishes*. . Zoological survey of India, Calcutta.

POLZIN, T. & DANESCHMAND, S.V. 2003. On steiner trees and minimum spanning trees in hypergraphs. *Operations Research Letters* **31**: 12–20.

QIAGEN Real-time PCR brochure: Critical Factors for Successful Real-time PCR. 2009. Sample and Assay Technologies.

RAJTHILAK, C., PERUMAL, P., MURUGAN, A., JAYARAJ, S.S. & SANTHANAM, P. 2010. Study on molecular variations among marine copepods (*Acrocalanus gracilis* and *Euterpina acutifrons*) isolated from Vellar estuary-South East coast of India. *Global Journal of Molecular Sciences* **5**: 7–11.

RAMAKERS, C., RUIJTER, J.M., DEPREZ, R.H.L., & MOORMAN, A.F.M. 2002. Assumption-free analysis of quantitative real-time polymerase chain reaction (PCR) data. *Neuroscience Letters* **339**: 62–66.

RAVEN, H.R. & JOHNSON, G.B. 2002. *Biology*. 6th edition. McGrawHill, New York.

REBOUÇAS, E.L., COSTA, J.J.N., PASSOS, M.J., PASSOS, J.R.S., VAN DEN HURK, R. & SILVA, J.R.V. 2013. Real time PCR and importance of housekeepings genes for normalization and quantification of mRNA expression in different tissues. *Brazilian Archives of Biology and Technology* **56**: 143–154.

REID, J.W. 2001. A human challenge: discovering and understanding continental copepod habitats. *Hydrobiologia* **453/454**: 201–226.

RIRIE, K.M., RASMUSSEN, R.P. & WITTWER, C.T. 1996. Product differentiation by analysis of DNA melting curves during the Polymerase Chain Reaction. *Analytical Biochemistry* **245**: 154–160.

RODRIGUEZ, F., OLIVER, J.L., MARIN, A. & MEDINA, J.R. 1990. The general stochastic model of nucleotide substitution. *Journal of Theoretical Biology* **142**: 485–501.

ROHDE, K., HAYWARD, C. & HEAP, M. 1995. Aspects of the ecology of metazoan ectoparasites of marine fishes. *International Journal for Parasitology* **25**: 945–970.

SAIKI, R.K., GELFAND, D.H., STOFFEL, S., SCHARF, S.J., HIGUCHI, R., HORN, G.T., MULLIS, K.B. & ERLICH, H.A. 1988. Primer-directed enzymatic amplification of DNA with a thermostable DNA polymerase. *Science* **239**: 487–491.

SAITOU, N. & NEI, M. 1987. The neighbor-joining method: a new method for reconstructing phylogenetic trees. *Molecular Biology and Evolution* **4**: 406–425.

SHAO, R. & BARKER, S.C. 2007. Mitochondrial genomes of parasitic arthropods: implications for studies of population genetics and evolution. *Parasitology* **134**: 153–167.

SIVAGANESAN, M., HAUGHLAND, R.A., CHERN, E.C. & SHANKS. O.C. 2010. Improved strategies and optimization of calibration models for real-time PCR absolute quantification. *Water Research* **44**: 4726–4735.

ŠLAPETA, J. 2013. Ten simple rules for describing a new (parasite) species. *International Journal for Parasitology: Parasites and Wildlife* **2**: 152–154.

SMITH, M.M. & HEEMSTRA, P.C. 1986. *Smith's Sea Fishes*. J.B.L. Smith Institute of Ichthyology, Grahamstown.

SWOFFORD, D.L. 2002. PAUP* 4.0b10. Phylogenetic analysis using parsimony and other methods. Sinauer Associates, Sunderland, Massachusetts.

TAMURA, K., PETERSON, D., PETERSON, N., STECHER, G., NEI, M. & KUMAR, S. 2011. MEGA5: Molecular evolutionary genetics analysis using maximum likelihood, evolutionary distance and maximum parsimony methods. *Molecular Biology and Evolution* **28**: 2731–2739.

TAUTZ, D., ARCTANDER, P., MINELLI, A., THOMAS, R.H. & VOGLER, A.P. 2003. A plea for DNA taxonomy. *Trends in Ecology and Evolution* **18**: 2.

TEMPLETON, A.R., ROUTMAN, E. & PHILLIPS, C.A. 1995. Separating population structure from population history: a cladistics analysis of the geographical distribution of mitochondrial DNA haplotypes in the Tiger Salamander, *Ambystoma tigrinum*. Genetics **140**: 767–782.

THATCHER, V.E. & JÚNIOR, J.P. 2006. *Kroyeria brasiliense* sp.nov. (Copepoda, Kroyeriidae) a gill parasite of the shark, *Galeorhinus vitaminicus* de Buen, in Rio do Sul State, Brazil. *Revista Brasileira de Zoologia* **23**: 1185–1187.

THOMPSON, J.D., GIBSON, T.J., PLEWNIAK, F., JEANMOUGIN, F. & HIGGINS, D.G. 1997. The CLUSTAL_X windows interface: flexible strategies for multiple sequence alignment aided by quality analysis tools. *Nucleic Acids Research* **25**: 4876–4882.

THORTON, B. & BASU, C. 2011. Real-time PCR (qPCR) primer design using free online software. *Biochemistry and Molecular Biology Education* **39**: 145–154.

THUM, R.A. 2004. Using 18S rDNA to resolve diaptomid copepod (Copepoda: Calanoida: Diaptomidae) phylogeny: an example with North American genera. *Hydrobiologia* **519**: 135–141.

VAN HOOK, A.M. & PATEL, N.H. 2008. Crustaceans. *Current Biology* **18**: 13.

WALTER, T.C. & BOXSHALL, G.A. 2014. World of Copepods database. Available online at http://www.marinespecies.org/copepeoda/aphia (Accessed on 07 April 2014).

WILHELM, S.W., JEFFREY, W.H., DEAN, A.L., MEADOR, J., PAKULSKI, J.D. & MITCHELL, D.L. 2003. UV radiation induced DNA damage in marine viruses along a latitudinal gradient in the southeastern Pacific Ocean. *Aquatic Microbial Ecology* **31**:1–8.

WINDER, L., PHILLIPS, C., RICHARDS, N., OCHOA-CORONA, F., HARDWICK, S. VINK, C.J. & GOLDSON, S. 2011. Evaluation of DNA melting analysis as a tool for species identification. *Methods in Ecology and Evolution* **2**: 312–320.

WOO, P.C.Y., LEUNG, P.K.L., LEUNG, K.W. & YEUNG, K.Y. 2000. Identification by 16S ribosomal RNA gene sequencing of an Enterobacteriaceae species from a bone marrow transplant recipient. *Journal of Clinical Pathology* **53**: 211–215.

WoRMS Editorial Board. 2014. Available online at http://www.marinespecies.org at VLIZ (Accessed on 22 January 2014).

WYNGAARD, G.A., HOŁYŃSKA, M. & SCHULTER II, J.A. 2010. Phylogeny of the freshwater copepod Mesocyclops (Crustacea: Cyclopidae) based on combined molecular and morphological data, with notes on biogeography. *Molecular Phylogenetics and Evolution* **55**: 735–764.

YUAN, J.S., REED, A., CHEN, F. & STEWARD Jr, C.N. 2006. Statistical analysis of real-time PCR data. *BMC Bioinfomatics* **7**: 85.